TTMD

Turkish Society of HVAC & Sanitary Engineers

XVII TTMD INTERNATIONAL HVAC&R TECHNOLOGIES SYMPOSIUM

ARTIFICIAL INTELLIGENCE IN BUILDINGS

14-15 MAY 2026

Bağlarbaşı Convention and Cultural Center

Bağlarbaşı Kongre ve Kültür Merkezi



PROCEEDINGS

www.symposium.ttmd.org.tr

symposium@ttmd.org.tr

XVII TTMD
INTERNATIONAL HVAC&R
TECHNOLOGIES SYMPOSIUM

ARTIFICIAL INTELLIGENCE IN BUILDINGS

ISBN: 978-625-97915-3-1

© All rights reserved. This book or part of it cannot be printed or copied without the permission of the Turkish Society of HVAC and Sanitary Engineers.

www.symposium.ttmd.org.tr
symposium@ ttmd.org.tr

Contributors

Platinum Sponsor

KODSAN

Gold Sponsors

PAG AYDINGLOBAL

AYVAZ

ebitt FLUID TECHNOLOGIES

FORM 1965'ten beri

S&P

systemair

Lanyard Sponsor

TROX

Silver Sponsors

AGON Challenge for best solutions

DUYAR Since 1965

Halton

Johnson Controls

NORM TEKNİK Yangın Korunum Sistemleri

treemec more green solutions

Supported By

Organizing Committee

Gülsu Ulukavak Harputlugil (Chair)
Ahmet Arısoy
Ayşegül Tereci
Ece Kalaycıoğlu Özdemir
Kazım Beceren
Murat Çakan
Nermin Köroğlu Isın
Neşe Ganiç Sağlam
Pınar Kopuz
Sarven Çilingiroğlu
Seçil Kızanlık İskender
Simay Gökmenoğlu
Tuba Bingöl Altıok
Z.Haktan Karadeniz

Scientific Committee

Murat Çakan (Chair)
Ahmet Arısoy
Ayşegül Tereci
Ece Kalaycıoğlu Özdemir
Gülsu Ulukavak Harputlugil
Neşe Ganiç Sağlam
Z.Haktan Karadeniz
Ali Pınarbaşı
Derya Burcu Özkan
Gülfeza Karda
Halime Paksoy
Hasan Bedir
Hasan Heperkan
Macit Toksoy
Mehmet Bilgili
Ongun Berk Kazancı
Umut Orhan

Advisory Committee

Numan Şahin
Serdar Gürel
Ömer Kantaroğlu
Hüseyin Erdem
Abdullah Bilgin
Cafer Ünlü
Gürkan Arı
Bahri Türkmen
Sarven Çilingiroğlu
Birol Kılkış
Kemal Gani Bayraktar
Meriç Sapçı
Nermin Köroğlu Isın
Atalay Özdayı
Ekrem Erkut
Kazım Beceren
Murat Suiçmez
Tunç Korun
Turan Muşkara
Türkay Yıldırım

Preface

Distinguished Guests,
Esteemed Colleagues,

It is a great pleasure to welcome you to the XVII TTMD International HVAC&R Technologies Symposium, bringing together professionals, academics, researchers, and industry representatives from Türkiye and around the world. Over the years, this symposium has become an important international platform where knowledge is exchanged, new perspectives emerge, and the future of our industry is discussed collectively.

This year's theme, "Artificial Intelligence in Buildings," reflects one of the most significant transformations shaping not only the HVAC&R industry, but also the way we design, operate, and experience the built environment.

Today, digitalization is no longer simply a technological trend. It has become an essential part of how the world responds to some of its most pressing challenges. Rapid urbanization, increasing energy demand, climate change, resource scarcity, and the need to reduce carbon emissions require us to rethink conventional approaches. Digital technologies and artificial intelligence provide powerful tools to understand complex systems, optimize resources, improve energy performance, and make buildings more responsive to both people and the environment.

For the HVAC&R sector, this transformation carries particular importance. Heating, cooling, ventilation, and building systems represent a substantial part of global energy consumption. Through intelligent controls, data-driven optimization, predictive maintenance, digital twins, and AI-supported design and operation, we now have the opportunity to achieve levels of efficiency and performance that were previously difficult to imagine. The transition toward smarter buildings is therefore not only about technology; it is an important step toward a more efficient, resilient, and sustainable world.

This year's symposium also carries particular significance as it coincides with the year in which COP31 will be hosted by Türkiye. At a time when global attention will turn to our country to discuss climate action and a sustainable future, our focus on artificial intelligence and digitalization in buildings becomes even more relevant. The transformation of the built environment through smarter, more efficient, and data-driven solutions will undoubtedly be an important part of achieving our global climate goals.

However, technology alone cannot create this transformation. Its real value emerges when engineering knowledge, scientific research, industry experience, and human creativity come together. This is precisely where professional organizations and international platforms such as the TTMD Symposium have an important role to play. By bringing different disciplines and perspectives together, we can turn technological possibilities into practical and responsible solutions.

Throughout this symposium, we have had the opportunity to explore emerging technologies, exchange experiences, question established practices, and discuss how artificial intelligence will reshape our profession in the years ahead. I sincerely thank all our speakers, researchers, industry representatives, sponsors, and participants whose knowledge, experience, and contributions have enriched this international gathering.

Preface

I would also like to express my sincere appreciation to the Symposium Committee, composed of our esteemed academics who have generously supported TTMD and contributed to our work for many years, for their continued dedication and invaluable efforts in making this symposium possible.

As TTMD, we believe that our responsibility extends beyond following technological change. We must contribute to shaping it. We will continue to encourage knowledge sharing, international cooperation, research, education, and the responsible use of emerging technologies while supporting the development of our sector and the professionals who will lead its future.

I hope that the ideas and collaborations generated during the XVII TTMD International HVAC&R Technologies Symposium will extend far beyond these two days and contribute to smarter buildings, more efficient use of our resources, and a more sustainable future for generations to come.

Seçil İskender
Chair of the 17th TTMD International HVAC+R Technologies Symposium

Preface

It is my great pleasure, on behalf of the Organizing Committee, to welcome you to the Proceedings of the 17th International HVAC+R Technology Symposium, organized by the Turkish Society of HVAC and Sanitary Engineers (TTMD).

Founded in 1992, TTMD aims to advance professional and scientific knowledge in heating, refrigeration, ventilation, air-conditioning, plumbing, insulation, and building control systems. Over the years, the Society has evolved into a multidisciplinary platform that brings together designers, consultants, manufacturers, contractors, building operators, academics, researchers, and other stakeholders in pursuit of shared goals. Through its technical, educational, and scientific activities, TTMD continues to contribute to the development of the HVAC+R sector and the improvement of building performance and environmental quality.

The COVID-19 pandemic significantly affected the organization of scientific and professional events worldwide. The 14th TTMD Symposium, originally planned for 2020, was held online, and the 2022 and 2024 symposia also took place entirely through online platforms. The 17th Symposium therefore marked a particularly meaningful return to an in-person format, enabling our professional and academic community to meet face to face once again after a long interval. We were delighted to renew direct dialogue, exchange knowledge, and strengthen collaboration among the different stakeholders of the sector.

The main theme of the 17th International HVAC+R Technology Symposium was "Artificial Intelligence in Buildings and HVAC Applications." Artificial intelligence has entered our professional and everyday lives with remarkable momentum. Like many transformative innovations, it initially generated uncertainty and concern, followed by intense curiosity and exploration. We have now entered a period of broader acceptance, accompanied by an increasing awareness of both the opportunities offered by artificial intelligence and the technical, ethical, and professional challenges associated with its use.

For the building and HVAC+R sectors, artificial intelligence presents considerable potential across a wide range of applications, including building design, performance prediction, system optimization, fault detection and diagnosis, predictive maintenance, energy management, indoor environmental quality, and occupant-responsive control. At the same time, its effective integration requires reliable data, appropriate infrastructure, interdisciplinary expertise, transparency, and the development of new professional competencies. The central question addressed throughout the Symposium was therefore not simply whether artificial intelligence will transform our sector, but how this transformation can be guided to create meaningful, responsible, and lasting benefits.

The scientific and professional contributions presented during the Symposium examined these issues from multiple perspectives. Through invited lectures, technical presentations, discussions, and the panel entitled "The Future of Data Centers," distinguished experts explored both the direct applications of artificial intelligence in buildings and HVAC systems and the growing importance of data centers as one of the essential infrastructures supporting artificial intelligence. The papers included in this volume reflect the diversity of these discussions and provide valuable insights into current developments, emerging challenges, and future research and implementation priorities.

Preface

I sincerely hope that these proceedings will serve as a useful and enduring resource for academics, researchers, designers, engineers, manufacturers, practitioners, students, and decision-makers. I also hope that the knowledge and perspectives shared within this volume will encourage further research, interdisciplinary collaboration, and innovative applications in the building and HVAC+R sectors.

I would like to express my sincere gratitude to all invited speakers, panelists, authors, reviewers, session chairs, participants, sponsors, and supporting institutions whose contributions made this Symposium possible. I extend my heartfelt thanks, in particular, to all members of the Organizing Committee for their dedicated work, valuable contributions, and commitment throughout the preparation and implementation of the event.

On behalf of the Organizing Committee, I am pleased to present the Proceedings of the 17th International HVAC+R Technology Symposium to our professional and academic community.

Prof. Dr. Gülsu Ulukavak Harputlugil
Chair of the 17th TTMD International HVAC+R Technologies Symposium
Organizing Committee

Presenters Biographies



ANDREI CRISAN

Dr. Andrei Crişan is a lecturer at the Politehnica University Timişoara, within the Department of Steel Structures and Structural Mechanics, and Head of the Center for Innovation and Technological Transfer (CITT). A structural engineer by education, his academic and research activity combines steel structures with advanced numerical simulations and digital engineering methodologies.

His current work focuses on Building Information Modeling (BIM), Digital Twins, and structured information management across the entire lifecycle of built assets. He is particularly interested in the integration of simulation-driven approaches with BIM-enabled workflows, supporting performance-based design and decision-making.

With over a decade of experience bridging academia and industry, he contributes to applied research and international initiatives such as the BIM2in project, advancing training frameworks that connect BIM, Digital Twins, and simulation with real-world applications in Cultural Heritage, LCA and manufacturing.



CATALIN LUNGU

Mr. Lungu is Associate Professor at the Technical University of Civil Engineering (www.utcb.ro) and visiting professor at Ecole Nationale Superieure de l'Energie, l'Eau et l'Environment ENSE 3 (France). He is specialized in dynamic simulation of HVAC and RES systems, including EPB and NZEB assessment.
He represents AIIR (the Romanian Association of Building Services Engineers, www.aiiro.ro) as first vice president (since 2020), and REHVA as vice-president and treasurer since May 2017. In April 2021 he was elected as the next REHVA President for the mandate 2022-2025 (www.rehva.eu). Since 2013 he is the managing director of the Romanian Chamber of Energy Auditors (www.oaer.ro) and the main organizer of training and life-long learning courses for Romanian energy auditors.
Dr. Lungu was the organizing committee chair of the REHVA HVAC World Congress CLIMA 2019 (2016-2019). He is/was project director of 4 research projects and member in other 4, including the national project for recasting the national methodology for the calculation of the energy performance of buildings, according to the new set of EPB standards. He is also member of 6 standardization technical committees (5 ASRO and 1 ISO).
As main author or co-author, Dr. Lungu has been publishing 6 books and more than 50 scientific or technical articles.

Presenters Biographies



CHEOL-SOO PARK

Professor Cheol-Soo Park has shown his academic achievement in the area of building simulation through his extensive publication record and the mentoring of students who have achieved prestigious global and domestic recognition under his guidance. Professor Park's career spans impactful positions serving as an advisory council member for the President of Republic of Korea (ROK) on science & technology, the representative of IBPSA-Korea and the 15th president of the Korean Institute of Society of Architectural Sustainable Environment and Building Systems (KIAEBS). His recent research interests include MPC for real-life cases, physics-informed AI, federated learning model, causality-based model, model calibration, and occupant behavior.



GÜLSU ULUKAVAK-HARPUTLUGİL

Gülsu Ulukavak Harputlugil has been working as an academic researcher in the field of architecture since 1998. She completed her undergraduate, master's and doctoral studies at Gazi University. Since joining Çankaya University in 2014, she has continued her academic career there and currently serves as a full-time Professor at the Faculty of Architecture, where she is responsible for various undergraduate and graduate courses, including Architectural Design Studio, Building Physics and Construction Systems. Her academic interests include climate-responsive and energy-efficient building design, net-zero energy/carbon/water buildings, and performance-based design. Since 2010, her research has focused on comfort-driven occupant behaviour, retrofit strategies for the existing building stock, and climate change adaptation strategies for buildings and communities.

Her research has been funded by TÜBİTAK and the British Council Newton Fund, and she has taken part in several national and international research projects as a senior expert in the field.

In 2017, she established IBPSA-Turkey, the Turkish chapter of the International Building Performance Simulation Association, under the umbrella of TTMD, and served as its chair until 2024. She also served as a member of the 16th Term Board of Directors of TTMD. She currently represents the Republic of Türkiye as a member of the Executive Committee of the International Energy Agency Energy in Buildings and Communities Technology Collaboration Programme.



HALİME PAKSOY

Dr. Paksoy is currently a professor in the Chemistry Department, and the Director of the Center for Environmental Research at Çukurova University, Adana, Turkey.

She is a chemical engineer who has been concentrating on thermal energy storage technologies since 1992. She serves as the Turkish Delegate representing TTMD and was the former Chair of the Executive Committee of the International Energy Agency Energy Storage Technology Collaboration Program (IEA ES TCP).

Halime Paksoy leads the thermal energy storage research team at Çukurova University with main focus is on fundamental and applied energy storage studies, as well as on developing thermal energy storage materials and their applications on using renewable and alternative energy in buildings and industry. She is associate editor responsible for energy storage in the International Journal of Solar Energy Society.

Presenters Biographies



IOAN SILVIU DOBOȘI

Graduate in 1988 of the Faculty of Civil Engineering, Building Services Department, within the Traian Vuia Polytechnic Institute (currently Politehnica University of Timișoara) and PhD in Civil Engineering from Politehnica University of Timișoara since 2007.

In 1994, he founded SC Dosetimpex SRL, today one of the main competitors in the Romanian building services market. Since 1993, he has been an associate lecturer at the Faculty of Architecture of Politehnica University of Timișoara.

A member of AIIR since 1993, he served as Vice President (2007–2016), First Vice President (2016–2020), and President for two consecutive terms (2020–2024 and 2024–2028). He was also Vice President of REHVA (2007–2016), REHVA Ambassador for CLIMA 2019 (2016–2019), and is a REHVA Fellow.

An ASHRAE member since 2004 and ASHRAE Fellow, he served as Secretary of the ASHRAE Danube Chapter (2005–2019 and 2020–present) and President (2019–2020). He was ASHRAE Region XIV Europe Member Council Representative (2020–2023) and Regional Vice Chair for Government Affairs (2023–2026).

He is also a member of AICVF, France, and has served on the Board of Directors of ARACO since 2016.

He has designed and implemented major building services projects for large companies in Romania. Since 2013, Dosetimpex has also been active in the Belgian construction installations market.

He has extensive expertise in building services engineering, building energy performance, building sustainability, the use of solar energy, and achieving energy savings in buildings.

Presenters Biographies



İSMAİL CAN

İsmail Can completed his secondary education at Istanbul Erkek Lisesi. He graduated from Boğaziçi University with a degree in Computer Science in 1976 and Mechanical Engineering in 1980.

He began his career in 1980, working at Efes Pilsen and Boral Engineering until 1984, including as Design Team Leader for the mechanical systems of the Petlas Tire Factory projects. He relocated to Australia at the end of 1984.

Between 1985 and 1993, he worked on mechanical design projects for high-rise buildings in Australia and Singapore. Major projects included Suntec City (Singapore), Hobart Sheraton Hotel (Australia), Cairns Parkroyal Hotel (Cairns, Australia), Shangri-La International Hotel (Jakarta, Indonesia), War Memorial Museum (Canberra, Australia), GIO Computer Centre (Sydney, Australia), Charbon Collieries mine ventilation systems (Hunter Valley, Australia), University of New South Wales (Sydney, Australia), and Atomic Energy Centre (Sydney, Australia).

In 1993, he returned to Istanbul and founded Birikim Engineering Project Ltd., completing the mechanical system design of over 100 medium and large-scale projects between 1993 and 2013. Key projects included Istinye Park Shopping Mall and Residences, Trump Towers Shopping Mall and Residences, Kempinski Shopping Mall and Residences, MetroCity, Süzer Plaza (Gökkafes), Bomonti Hilton, and Sabancı University Campus and Nanotechnology Center (Istanbul); Moscow Tax Office and Interhotel Petrograd (Russia); Military Hospital and Theatre Buildings (Ashgabat); and Palm Jumeirah Village Centre (Dubai).

In 2013, he returned to Australia, specializing in the mechanical design of critical facilities, including cleanrooms, R&D centers, laboratories, data centers, and hospitals. Major projects between 2014 and 2022 included UA Pharmacological Sterile Cosmetics Factory, Sypharma Pharmaceuticals, and Mass Spectroscopy and Cryogenic Laboratories for Monash, Swinburne, and Melbourne Universities (Melbourne, Australia); Australian Antarctic Research Laboratories (Tasmania, Australia); Australian National University Semiconductor Development Centre (Canberra, Australia); and various hospital projects.
In 2022, he relocated to London and joined Arup Engineering Group as a Senior Consultant, focusing on decarbonization, energy efficiency, and large-scale data centers. Key projects between 2022 and 2024 included Francis Crick Institute (decarbonization, data center, and sustainable cooling water systems, London, UK), 1 Triton Square Research Institute (decarbonization and energy efficiency systems, London, UK), and Khorfakkan Research Institute (mechanical systems design, UAE).

He returned to Istanbul in mid-2024 and currently works as a Senior Consultant at Arup Engineering Turkey, focusing on large data centers and decarbonization projects.
Professional Memberships and Credentials: Engineers Australia – Chartered Professional Engineer; Registered Professional Engineer – NSW and Victoria, Australia; APEC – International Professional Engineer; ASHRAE (USA) – Life Member; CIBSE (UK) – Member.

He is fluent in English and German.

Presenters Biographies

- Various hospital projects

In 2022, he relocated to London and joined Arup Engineering Group as a Senior Consultant, focusing on decarbonization, energy efficiency, and large-scale data centers. Key projects between 2022 and 2024 include:

- Francis Crick Institute – decarbonization, data center, and sustainable cooling water systems – London, UK
- 1 Triton Square Research Institute – decarbonization and energy efficiency systems – London, UK
- Khorfakkan Research Institute – mechanical systems design – UAE

He returned to Istanbul in mid-2024 and is currently working as a Senior Consultant at Arup Engineering Turkey, focusing on large data centers and decarbonization projects.
Professional Memberships and Credentials:

- Engineers Australia – Chartered Professional Engineer
- Registered Professional Engineer – NSW and Victoria, Australia
- APEC – International Professional Engineer
- ASHRAE (USA) – Life Member
- CIBSE (UK) – Member

He is fluent in English and German.



KADİR İSA ISKAV

After almost 35 years of teaching in the field of HVACR at various vocational colleges and mechanical engineering departments, I retired in 2022. I am currently acting as a consultant.

I love music and I believe that “music makes us one”.



KIVANÇ ASLANTAŞ

Kıvanç Aslantaş is a Mechanical Engineer with over 25 years of experience in HVAC systems, spanning construction, project management, production, technical sales, and after-sales services.
He is a certified trainer for combustible gases and refrigeration cycles, including R744 (CO_2) refrigeration systems, registered in the European Union database. Since 2005, he has been actively involved in refrigeration systems using natural refrigerants, with a strong focus on the adoption and dissemination of CO_2-based solutions.

He has served as Project Coordinator for UNIDO demonstration and pilot activities promoting low Global Warming Potential (GWP) refrigerants in Türkiye, and continues to contribute as a national consultant for UNDP and UNIDO. He currently serves as Sales & Marketing Director at GVN Refrigeration.

In this seminar, he shares practical insights and field experience on sustainable refrigeration technologies and system applications.

Presenters Biographies



LIVIO MAZZARELLA

Livio Mazzarella graduated in Milan in Mechanical Engineering with a focus on Energy in 1982. Full Professor of Environmental Technical Physics since 2000, he has been teaching various disciplines in the field of environmental air conditioning and building physics at the Politecnico di Milano since 1990, and he is author of more than 200 publications in such sectors. Member of AICARR since 1979, he has held the position of member of the Board several times and represents AICARR in RHEVA, where he is the actual president for the term 2025-2028. He has been working in standardization since 1992 at CTI (Italian Standardization Committee for HVAC), where he is currently nominated Council Member by the Ministry of University and Research. He is also President of the Indoor Environmental Quality Global Alliance.



MERİÇ SAPÇI

Mr. Meriç Sapci is a mechanical engineer with over 30 years of experience in heating, ventilation, and air conditioning (HVAC), plumbing, and fire protection systems design. He has served as a lead designer and design coordinator for numerous high-profile projects across both domestic and international markets. He is the founder and principal of METTA Engineering.

He began his professional career by establishing GMD Engineering in 1995, where he successfully led a wide range of projects over a 14-year period. Since 2009, he has continued his work under METTA Engineering.

Mr. Sapci is a well-recognized expert in building mechanical systems and served as the 15th term President of the Turkish Society of HVAC & Sanitary Engineers. He has also been an active member of ASHRAE for more than 25 years. His expertise includes hydronic systems, water loop heat pump applications, and advanced HVAC design, with a strong focus on energy efficiency, sustainability, and performance-based engineering.

Presenters Biographies



SARVEN ÇİLİNGİROĞLU

Sarven Çilingiroğlu was born in Istanbul in 1963. He graduated from Getronagan High School in 1980 and from the Faculty of Mechanical Engineering at Istanbul Technical University (ITU) in 1984. In the same year, he began his master's studies at the ITU Institute of Science and Technology and completed his degree in 1987 in the Energy Program of the Mechanical Engineering Department, as a MSc Mechanical Engineer. During his graduate studies, he worked part-time for one year at Honeywell in the field of "Building Automation". In 1986, he completed a two-month internship at York International in the United Kingdom, where he conducted research for his master's thesis on heat pumps. He fulfilled his military service between 1987 and 1989.

He served as;
Board Member of the Turkish Society of HVAC and Sanitary Engineers (TTMD) during the 6th term (2003–2004) and the 10th term (2011–2012).
Chairman of the Board in the 12th term (2015–2016)
Vice Chairman in the 13th term (2017–2018).
Board Member of CLIMAMED, the Federation of Mediterranean HVAC Associations in 2017
Vice Chairman of the Board of ISKAV (Foundation for Research and Education in Heating, Cooling and Air Conditioning) during its 8th term (2018–2021).
He is currently serving as ISKAV Chairman of the Board for the 9th and 10th terms (2021–present).

He is the owner of Çilingiroğlu Engineering, a company providing mechanical installation design, supervision, and consultancy services.
He is married and has two children.



SİNAN ALKAŞ

Sinan Alkaş serves as a Principal Construction Project Manager at Turkcell and specializes in data center design and construction. He manages the entire project lifecycle end-to-end for advanced data center projects implemented in Turkey, from concept development to commissioning and international certification processes.

His work focuses particularly on mechanical systems and cooling infrastructure in data centers, developing strategies and implementations for managing high-density IT loads, energy efficiency, and sustainability. In this context, he actively contributes to ensuring that projects are developed in compliance with international quality standards such as EN 50600 and Uptime Institute criteria.

He also adopts a holistic approach to risk management, budget optimization, and operational continuity in critical infrastructure projects, supporting the long-term performance of data center investments through innovative and sustainable solutions.

Presenters Biographies



VOLKAN DODA

Volkan Doda is the Head of Design Technologies at Atelier Ten's US offices and the 2025 CIBSE Engineer of the Year. With a background in architecture, engineering science, and environmental design, he's spent his career at the overlap of disciplines where the spreadsheets meet the sketchbooks.

Since joining Atelier Ten in 2013, he's worked on a wide range of projects from resorts carved into desert mountains to unloved 1980s office blocks in need of a greener future. Along the way, he's led teams, mentored future designers, and set up knowledge-sharing networks that ensure no good new idea stays hidden for long.

Volkan is currently exploring how AI and data might change the way we design buildings, while reminding everyone that sound sustainable design remains a team sport regardless of which tools we adopt to deliver it.

Presenters Extended Summary

Andrei Crisan
Politehnica University Timişoara

Speech Title: Beyond 3D Models: BİM and Digital Twins in the Age of AI

Abstract:
The construction sector does not lack digital models, software platforms or data-generating technologies; its fundamental challenge is the absence of connected continuous and decision-oriented information. Within the BIM2in project (www.bim2in.eu), the consortium examines the transition from model-centred BIM practices towards integrated, lifecycle-oriented information ecosystems. It follows the evolution of information from early design and multidisciplinary coordination through construction verification and handover to asset operation, demonstrating how conventional and even BIM-based workflows may still generate fragmented datasets, disconnected documents and information silos. Such discontinuities frequently require asset operators to reconstruct essential knowledge after project completion. The main idea is to start considering BIM as a collaborative information management process through which objectives, responsibilities, requirements, exchanges and deliverables are coordinated to support reliable decision-making throughout the asset lifecycle. This perspective provides the basis for clarifying the practical relationship between the BIM framework, the Digital Twins use cases and Artificial Intelligence, used for decision making. Considering the entire project development process, information evolves continuously: during design, information primarily describes what is intended to be built; during construction, it records and verifies what has been delivered; and during operation, it is used to explain how interconnected asset systems perform. Within this operational space, Digital Twins aim to maintain meaningful relationships between physical assets, structured information models, IoT data, maintenance records, environmental conditions and performance indicators. Their value, however, cannot be derived from visual sophistication or technological integration alone. Incomplete, inconsistent or poorly governed information cannot provide a reliable foundation for monitoring, simulation, prediction or optimisation.

Building on the principle of "reliable information before intelligence", we introduced an ISO 19650-aligned pathway through which organisational objectives are translated into explicit information requirements, defined according to the Level of Information Need (according to ISO 7817) and delivered through controlled information exchanges. Information Delivery Manuals (defined according to ISO 29481) support the definition of processes and responsibilities, while Information Delivery Specifications (a standard developed by buildingSmart International) enable machine-readable requirements and automated verification. This structured pathway supports the transition from the Project Information Model used during delivery to the Asset Information Model required for operation, establishing the context, traceability and information quality needed by Digital Twins. Artificial intelligence can subsequently operate on this trusted foundation to identify patterns, forecast performance and support better decisions. AI is consequently positioned not as the starting point of digital transformation, but as the outcome of a mature information ecosystem supported by appropriate standards, processes, competencies and organisational change. The The conceptual basis of this proposal is further developed in the paper A BIM-Based Framework Proposal for Reliable Information Governance in Urban Digital Twins, where ISO-aligned processes are integrated into a traceable framework connecting organisational objectives, information requirements and Digital Twin applications.The conceptual basis of this proposal is further developed in the paper A BIM-Based Framework Proposal for Reliable Information Governance in Urban Digital Twins, where ISO-aligned processes are integrated into a traceable framework connecting organisational objectives, information requirements and Digital Twin applications.The conceptual basis of this proposal is further developed in the paper A BIM-Based Framework Proposal for Reliable Information Governance in Urban Digital Twins, where ISO-aligned processes are integrated into a traceable framework connecting organisational objectives, information requirements and Digital Twin applications.

Presenters Extended Summary

The conceptual basis of this proposal is further developed in the paper A BIM-Based Framework Proposal for Reliable Information Governance in Urban Digital Twins (Crisan, A.; Herban, S.; Pepe, M.; Karlshøj, J.; Baiocchi, V.; Runceanu, B. A BIM-Based Framework Proposal for Reliable Information Governance in Urban Digital Twins. Urban Sci. 2026, 10, 416. https://doi.org/10.3390/urbansci10070416), where ISO-aligned processes are integrated into a traceable framework connecting organisational objectives, information requirements and Digital Twin applications.

Presenters Extended Summary

Cheol-Soo Park
Seoul National University, South Korea

Speech Title: Real-life Examples and Future Challenges of AI-Assisted HVAC Operation

Abstract:
In this presentation, Professor Cheol Soo Park will address why the simulation model is so essential for effective HVAC operation of existing buildings. He will show several real-life examples of real-time implementation of AI for residential and commercial buildings in South Korea. It will be addressed that without resorting to passive or active building retrofits, AI-empowered control could save energy by 20% compared to existing controls. Subsequently, Prof. Park will address emerging challenges including physics-informed vs. AI-informed model, one-way vs. bi-directional AI, local vs. federated AI, and correlation vs. causality-based AI.

Presenters Extended Summary

Gülsu Ulukavak Harputlugil
Çankaya University

Speech Title: Artificial Intelligence in Buildings and HVAC: Opportunities, Risks, and the Changing Role of Engineers

Extended Abstract based on the AI interview presented at TTMD's 17th International HVAC+R Technology Symposium

Artificial intelligence (AI) is expanding the scope of building and HVAC applications beyond conventional automation toward systems that can learn, predict, generate alternatives, and support complex decisions. This extended abstract synthesizes a structured AI-mediated interview presented at TTMD's 17th International HVAC+R Technology Symposium. The interview addressed five interrelated themes: reinforcement learning for dynamic energy optimization; AI-integrated digital twins and predictive maintenance; the joint management of indoor air quality, energy use, and personalized comfort; generative design and the changing role of HVAC engineers; and the cybersecurity, privacy, and ethical challenges of connected buildings. Together, these themes describe a broader transformation in which buildings become adaptive cyber-physical systems. The central argument is that AI improves performance only when reliable data, appropriate infrastructure, human expertise, and accountable decision-making are integrated throughout design and operation.

The first theme concerned the limitations of traditional rule-based HVAC control. Conventional automation generally follows predefined thresholds and schedules. Although reliable and transparent, it responds imperfectly to changing weather, occupancy, internal gains, thermal inertia, and energy prices. Reinforcement learning instead allows a control agent to learn from the consequences of its actions. A reward function can seek to reduce energy use while maintaining comfort and indoor environmental quality, enabling control decisions to adapt as conditions evolve. The interview cited substantial energy-saving ranges under simulation and experimental conditions, but emphasized that real-building savings are generally more moderate and context-dependent. Performance varies with the baseline control strategy, building type, climate, equipment, occupancy, and commissioning quality; AI therefore cannot promise a universal efficiency rate. Its fundamental advantage is to treat a building as a changing, learnable system rather than a static collection of equipment.

The transition from simulation to operation remains a major challenge. An algorithm trained virtually may encounter sensor faults, unexpected occupant actions, unusual weather, or equipment behavior absent from its training data. This simulation-to-reality gap can produce unstable decisions if AI is deployed without safeguards. In hybrid control architectures, established engineering rules define safe boundaries while the learning algorithm adapts within them. High-resolution data on temperature, humidity, occupancy, air quality, equipment status, and weather are also needed. Yet data alone are insufficient: facility managers must understand the system, intervene when necessary, and evaluate recommendations that differ from established routines. Organizational readiness and change management are therefore as important as algorithmic performance.

The second theme explored AI-integrated digital twins. A digital twin is a continuously updated virtual representation of a physical building or HVAC system. Supplied with real-time temperature, flow, pressure, vibration, power, and equipment-status data, it can support anomaly detection and performance forecasting. AI-supported predictive maintenance identifies deviations before they become failures, allowing intervention at an appropriate time rather than only after breakdown or according to fixed replacement intervals.

Presenters Extended Summary

This can reduce emergency work, unnecessary service visits, downtime, and secondary damage, while extending equipment life by correcting small faults early. Because deteriorating equipment may consume excessive energy before complete failure, predictive maintenance can reduce both maintenance expenditure and operational energy use.

Indicative savings ranges for predictive maintenance and operating costs should not be generalized without considering abuilding's condition and maintenance regime. Buildings relying on reactive maintenance may offer greater potential than facilities with mature preventive programs and well-commissioned controls. More importantly, a digital twin creates no value merely by collecting or visualizing data. Savings occur when diagnostics inform maintenance planning, control, energy management, and operational procedures. This requires sustained investment: sensors must be calibrated, models synchronized with physical assets, data pipelines maintained, and facility teams trained. Without such integration, an expensive digital twin may remain only an advanced monitoring interface.

The third theme addressed indoor air quality (IAQ) and occupant comfort, which received greater attention after the COVID-19 pandemic. Ventilation creates a recurring trade-off: outdoor air reduces pollutant concentrations but must often be heated, cooled, humidified, or dehumidified. Traditional demand-controlled ventilation commonly reacts to a limited variable such as carbon dioxide, using fixed thresholds. AI can combine occupancy forecasts with real-time CO2, particulate matter, volatile organic compound, temperature, and humidity data to anticipate zone-level demand. Ventilation may be increased before a meeting and reduced in unoccupied areas, maintaining IAQ while avoiding unnecessary conditioning. The value of AI lies not simply in delivering more ventilation, but in determining when, where, and how much is required. Energy, health, and comfort can thus be optimized together.

The same approach supports personalized climate control. Conventional systems maintain a uniform setpoint for an average occupant, although thermal preferences vary. Feedback from mobile applications, environmental controls, or wearables could help AI learn preferences and coordinate central HVAC with personal fans, heaters, smart diffusers, or zonal units. This could provide localized comfort without conditioning an entire building to satisfy the most demanding request. However, user preferences must remain within energy and safety limits; additional sensors increase cost and maintenance; and physiological or occupancy data may reveal sensitive information. Personalized comfort is therefore most credible as a constrained, transparent optimization process rather than unlimited individual control.

The fourth theme considered generative design and the changing role of HVAC engineers. AI-enabled tools can generate and compare piping and ductwork configurations using criteria such as pressure loss, energy use, investment cost, coordination, fire safety, acoustics, hygiene, accessibility, and maintainability. This is valuable in complex buildings, where routes interact with structures, ceiling zones, shafts, fire compartments, architecture, and other services. The interview described a shift from engineer as drawing producer to curator of alternatives. Yet curatorship is not passive selection: the engineer must define the problem, set boundaries, select criteria, evaluate trade-offs, and judge whether a computationally optimal proposal is constructible and operationally sound. A shortest route may obstruct valve access, while an energy-efficient arrangement may conflict with fire protection. Practical knowledge remains indispensable.

Presenters Extended Summary

Reducing design error requires a human-in-the-loop process combining reliable BIM data, clear requirements, automated rule checks, simulation, interdisciplinary coordination, traceable assumptions, and professional review. AI can accelerate alternative generation, but poorly specified objectives produce misleading results: optimizing only energy may raise capital or maintenance costs, while minimizing first cost may weaken long-term performance. Future HVAC engineers will need both conventional competence and AI literacy - the ability to formulate questions, assess data quality, interpret outputs, identify constraints, and justify a selected solution. AI shifts professional activity from repetitive production toward strategic judgment without transferring responsibility to the algorithm.

The final theme concerned cybersecurity, privacy, and ethics. As HVAC and building management systems connect to cloud platforms, digital twins, analytics services, and external contractors, they become potential entry points for cyberattacks. Consequences may range from discomfort and energy waste to equipment damage, disruption of critical environments, or unauthorized access to organizational networks. Vulnerability increases with legacy controls, infrequent updates, weak credentials, and fragmented responsibility among mechanical, controls, IT, facility management, and service teams. Meanwhile, apparently harmless environmental and occupancy data can reveal work patterns, meeting schedules, health-related information, or individual behavior when combined over time.

The interview therefore advocated secure-by-design and privacy-by-design approaches. Measures include network segmentation; strong authentication and access management; encryption; regular updates; data minimization and anonymization; audit logs; anomaly detection; reviewable AI decisions; and clear allocation of responsibility. Human awareness remains critical because phishing, poor passwords, or disabling security functions can defeat technical safeguards. The ethical quality of an AI-enabled building depends not only on what can be measured and optimized, but also on whether data collection is proportionate, understandable, consensual, and governed throughout its life cycle.

In conclusion, AI can support lower energy use, better IAQ and comfort, longer equipment life, reduced operating costs, and more performance-oriented HVAC design. These outcomes are conditional, requiring reliable sensors and models, interoperable systems, carefully defined objectives, validated algorithms, skilled operators, professional oversight, and robust security governance. The appropriate perspective is accountable augmentation: buildings become adaptive systems in which human knowledge and machine intelligence complement one another. AI serves as an operational and design intelligence layer, while engineers retain responsibility for safety, feasibility, ethics, and long-term performance. The sustainable smart building of the future must therefore be not only efficient and comfortable, but also transparent, secure, privacy-conscious, and digitally resilient.

Keywords: Artificial intelligence; HVAC; reinforcement learning; digital twin; predictive maintenance; indoor air quality; generative design; cybersecurity

Presenters Extended Summary

Halime Paksoy
Çukurova University

Speech Title: GREENOLIVE Project for Decarbonization of Industry with Power to Heat Concept

Abstract:
Heat accounts for more than half of global energy consumption across power generation, industry, buildings, and transportation sectors. The associated greenhouse gas emissions continue to be a significant threat to the planet, making deep decarbonization an urgent priority to mitigate climate change. Among these sectors, industry—particularly processes requiring temperatures above 200 °C—remains one of the most challenging to decarbonize. Although renewable electricity generation from solar photovoltaic (PV) and wind is rapidly expanding, the intermittent nature of these resources and the continuous heat requirements of industrial processes create significant challenges for direct electrification. Power-to-Heat (PtH), particularly when coupled with thermal energy storage (TES), provides an attractive pathway for converting renewable electricity into reliable process heat while reducing dependence on fossil fuels.

The GREENOLIVE (Green Mediterranean through Solar Driven Decarbonization of Industries) project funded under the Interreg NEXT MED Programme 2021–2027 brings together six partners from Italy, Spain, France, Türkiye, Egypt, and Palestine and nine associated partners, with the aim of accelerating industrial decarbonization in the Mediterranean region. The project integrates a photovoltaic system, electrical heaters, and a sensible thermal energy storage system to provide process heat at the required temperature level for an industrial polymer production facility in Türkiye.

A pilot plant will be implemented at the ASCHEM polymer facility in Yumurtalık, Adana, Türkiye, to demonstrate the feasibility and benefits of the PtH approach. In this system, 600 kWe of renewable electricity generated by photovoltaics (PV) will be converted into process heat at approximately 300 °C using electric heaters. During periods of surplus PV generation, excess heat will be stored in a thermal energy storage (TES) system and utilized when renewable generation is insufficient. The pilot plant is expected to reduce natural gas consumption by 18–22%.
TES is a critical component of the proposed PtH system because it enables the temporal decoupling of renewable electricity generation from industrial heat demand. Sensible heat storage is employed in the GREENOLIVE pilot to store thermal energy generated when renewable electricity is available and subsequently deliver it when required by the industrial process.
A key innovation of the project is the valorization of waste materials available on-site, which will be used as storage media in a packed-bed TES system. The use of waste-based materials as packed-bed fillers additionally introduces a circular-economy dimension by valorizing locally available materials while potentially reducing the cost and environmental impacts associated with conventional TES materials.
The GREENOLIVE project demonstrates how the integration of renewable electricity, Power-to-Heat, thermal energy storage, waste-based materials, and intelligent control can provide a flexible pathway for industrial heat decarbonization. The combination of PtH and TES can address the temporal mismatch between variable renewable energy generation and continuous industrial heat demand, while AI-based control can further enhance renewable energy utilization and system flexibility. The results of the pilot are expected to provide valuable technical and operational knowledge for replicating this approach in other industrial sectors and temperature ranges, contributing to the transition toward more resilient, low-carbon industrial energy systems in the Mediterranean region.

Acknowledgements
This research has been carried out with the financial assistance of the European Union under the Interreg NEXT MED Programme (Grant Contract A-T_2.1_0213_GREENOLIVE)

Presenters Extended Summary

Ioan Silviu Dobosi
President AIIR - Romanian Association of Building Services Engineers

Title: The Smart Hospital of the Future

Subtitle:
Integration of BMS, BIM, and Artificial Intelligence in the Context of European Policies and ASHRAE Standards for Comfort, Indoor Air Quality, Energy Efficiency, and Decarbonization

Abstract:
In the context of climate change, digital transformation, and new requirements for indoor environment health, this paper proposes an integrated vision of the smart hospital of the future, where indoor comfort, air quality (IAQ), energy efficiency, and decarbonization are addressed through the integration of BMS, BIM, and Artificial Intelligence systems.
Healthcare buildings are characterized by a high level of complexity and strict performance requirements, which necessitates moving beyond traditional fragmented approaches and adopting integrated, data-driven models. The paper highlights the role of BMS as a real-time monitoring and control system, BIM as a data integration platform throughout the entire lifecycle, and Artificial Intelligence as a mechanism for predictive optimization and dynamic adaptation of hospital operations.
The approach is correlated both with European strategic directions on digitalization and decarbonization of the built environment, and with ASHRAE standards and priorities regarding indoor air quality, energy efficiency, and built environment safety.
Based on relevant case studies from Romania, the paper outlines an integrated BMS–BIM–AI model that paves the way for smart, autonomous, and sustainable hospitals, centered on the patient and indoor environment performance.

Presenters Extended Summary

Livio Mazzarella
REHVA, Federation of European Heating, Ventilation and Air Conditioning Associations

Speech Title: Artificial Intelligence in Building HVAC Systems: From Predictive Control to AI-Powered Digital Twin

Keywords
Artificial Intelligence, HVAC Systems, Building Automation, Digital Twin, Predictive Maintenance, Indoor Air Quality, IoT, Machine Learning

Abstract:
The building sector is undergoing a profound digital transformation driven by advances in Artificial Intelligence (AI), the Internet of Things (IoT), cloud computing, and Digital Twin technologies. Heating, Ventilation, and Air Conditioning (HVAC) systems, which account for a significant share of building energy consumption, represent one of the most promising application areas for AI-based solutions. This paper presents an overview of AI technologies and their application in building HVAC systems, highlighting current achievements, emerging trends, and existing limitations.

Artificial Intelligence can be defined as the capability of machines to emulate human cognitive functions such as learning, reasoning, planning, and creativity. The evolution of AI has progressed from traditional rule-based approaches to machine learning, deep learning, generative AI, and, most recently, autonomous AI agents capable of making decisions and performing complex tasks with limited human intervention. In the HVAC sector, these technologies enable systems to move beyond conventional control logic and towards predictive, adaptive, and self-optimizing operation.

Several AI paradigms contribute to HVAC management. Supervised machine learning models are widely applied to forecast thermal loads, energy demand, and equipment performance using historical operational data. Unsupervised learning techniques support anomaly detection and fault identification by recognizing hidden patterns within large datasets. More advanced approaches employ deep reinforcement learning (DRL), where AI agents learn optimal control strategies through continuous interaction with simulated environments, often implemented through Digital Twins. The agent receives performance-based feedback and progressively improves its ability to minimize energy consumption while maintaining indoor comfort.

The most mature AI applications in HVAC systems are predictive maintenance, dynamic optimization, and indoor air quality (IAQ) control. Predictive maintenance shifts maintenance strategies from fixed scheduling towards condition-based interventions. By continuously analysing sensor data such as vibration, temperature, pressure, electrical consumption, and flow rates, AI systems can identify early indicators of component degradation. Typical fault modes include compressor bearing wear, refrigerant leakage, fan motor overheating, pump failures, and variable frequency drive malfunctions. Early detection reduces downtime, lowers maintenance costs, and improves equipment reliability.

AI-based dynamic optimization enables real-time adjustment of HVAC operating parameters, including temperature setpoints, airflow rates, chilled water temperatures, pump operation, and compressor scheduling. These decisions are informed not only by current measurements but also by weather forecasts, occupancy conditions, electricity tariffs, renewable energy availability, and storage system status. Such predictive control strategies lead to significant energy savings while preserving occupant comfort.

Presenters Extended Summary

Indoor Air Quality management represents another important area of AI implementation. Continuous monitoring of CO_2 concentration, volatile organic compounds (VOCs), particulate matter, temperature, humidity, and occupancy allows intelligent ventilation control that responds dynamically to actual demand. AI-driven systems optimize outdoor air supply, avoiding both unnecessary ventilation energy consumption and inadequate indoor environmental conditions. Advanced solutions also monitor filter performance and predict replacement needs based on pressure-drop analysis.

The integration of AI with Digital Twin technology significantly expands HVAC capabilities. AI-powered Digital Twins combine Building Information Modelling (BIM), Building Energy Modelling (BEM), real-time sensor data, and advanced analytics into virtual representations of physical assets and systems. These models support predictive maintenance, scenario simulation, performance optimization, and operational decision-making. Furthermore, generative AI can create synthetic datasets to enhance model training and improve predictive accuracy when real operational data are limited.

The evolution of HVAC control systems can be described through several stages. HVAC 1.0 relied on manual operation and reactive maintenance. HVAC 2.0 introduced programmable electronic controls. HVAC 3.0 enabled digital automation through Building Automation Systems (BAS) using predefined control algorithms. Current HVAC 4.0 systems integrate AI, IoT, and Digital Twins to provide predictive and adaptive control. A future HVAC 5.0 paradigm is emerging, emphasizing human-centered collaboration, where AI acts as an intelligent co-pilot supporting operators while improving resilience and adaptability under changing conditions. Successful implementation of AI depends on robust IoT infrastructures capable of collecting and transmitting high-quality data. Modern sensor networks monitor thermal comfort, indoor environmental quality, occupancy, energy use, and equipment performance. Wireless IoT technologies such as LoRaWAN and NB-IoT provide scalable solutions with long battery life and support for large-scale sensor deployment, making AI-enabled building management increasingly practical.

Despite these opportunities, important challenges remain. Many AI models operate as "black boxes," providing highly accurate predictions without transparent explanations of their internal decision-making processes. This lack of explainability creates concerns regarding operator trust, troubleshooting, system validation, and legal liability, particularly in critical facilities such as hospitals and other mission-critical buildings. Future research should focus on explainable AI approaches that combine predictive power with transparent and auditable decision processes.

In conclusion, AI is transforming HVAC systems from reactive and rule-based infrastructures into intelligent, predictive, and adaptive ecosystems. Through predictive maintenance, dynamic optimization, advanced IAQ control, and Digital Twin integration, AI offers substantial opportunities for improving building energy efficiency, reliability, occupant comfort, and operational sustainability. Nevertheless, the successful deployment of these technologies will require continued advancements in explainability, data quality, interoperability, and human-AI collaboration.

References

1. European Parliament. What is Artificial Intelligence and How Is It Used? https://www.europarl.europa.eu-/topics/en/article/20200827STO85804/
2. IBM. Artificial Intelligence and Agentic AI. https://www.ibm.com/think/topics/artificial-intelligence
3. REHVA. Federation of European Heating, Ventilation and Air Conditioning Associations.
4. Relevant literature on AI-driven HVAC control, Digital Twins, Building Automation Systems, and Indoor Environmental Quality management.

Presenters Extended Summary

Meriç Sapçı
Metta Engineering

Speech Title: Hydraulic Design Verification and Performance Optimization of HVAC Systems Using Digital Twin Methodology:

A Case Study of a Water Loop Heat Pump System at BAU Campus, Istanbul

1. Introduction

Hydronic HVAC systems are widely used in buildings of all scales, from small commercial facilities to large campuses and high-rise developments. Regardless of system size or complexity, their performance fundamentally depends on how water is distributed, controlled, and balanced within the piping network.

Traditional HVAC design has focused primarily on thermodynamic calculations and equipment selection, including load determination, selection of chillers and heat pumps, and sizing of coils and pumps. While these aspects define system capacity, they do not guarantee that the system will operate as intended once installed.

In practice, many systems fail to achieve expected performance due to deficiencies in hydraulic behavior. A hydronic HVAC system is not only a thermal system but also a hydraulic network, where flow distribution, differential pressure availability, and control interactions determine how effectively thermal energy is delivered.

Improper hydraulic design can lead to:

I. Unbalanced flow distribution
II. Insufficient differential pressure at control valves
III. Excessive pumping energy consumption
IV. Degradation of system temperature difference (ΔT)

These issues are primarily the result of **unverified hydraulic assumptions** during the design phase, rather than incorrect equipment sizing.
Therefore, verification of hydraulic performance prior to installation is essential, particularly under part-load conditions where HVAC systems operate most of the time. Without such verification, discrepancies between design intent and actual operation often remain undetected until commissioning, when corrective actions become costly and limited.
This study investigates the HVAC system of the Bahçeşehir University (BAU) Beşiktaş South Campus in Istanbul, which utilizes a Water Loop Heat Pump (WLHP) system supported by seawater heat exchangers. The project provides a representative case for examining the interaction between hydraulic design, control strategy, and system performance.

A **Hydraulic Digital Twin (HDT)** is used to simulate and validate system behavior under both design and part-load conditions. By enabling quantitative verification of flow distribution, pressure stability, and control performance, the HDT transforms the design process from an assumption-based approach into a **performance-driven and verifiable methodology.**

This study demonstrates that hydraulic performance is not an inherent outcome of design, but a condition that must be explicitly defined, analyzed, and validated.

Presenters Extended Summary

2. Case Study: Coastal Campus System Description

2.1 Project Overview

The case study is based on a coastal university campus located along the Bosphorus in Istanbul, Türkiye, comprising academic and administrative buildings with a total enclosed area of approximately **27,500 m².**

A significant portion of the occupied spaces is located below grade, resulting in continuous internal heat gains and year-round cooling demand. Combined with diverse occupancy patterns, this creates **simultaneous heating and cooling requirements,** making the campus well suited for a **Water Loop Heat Pump (WLHP)** system.

The installed source-side capacities are:

- **Heat rejection capacity:** 3,100 kW (seawater heat exchangers)
- **Heat input capacity:** 1,040 kW (boiler system)

These values represent the total energy exchange at the source side of the system.
The system operates within a loop temperature range of approximately 19–32°C, allowing the water loop to function as a thermal energy buffer that supports load diversity and internal heat recovery.

2.2 System Architecture

The HVAC system is configured as a central water loop that functions both as a thermal energy buffer and a hydraulic distribution network.
The overall hydronic configuration is illustrated in Figure 1, showing the main loop, secondary substations, and source-side connections.
The system consists of a closed-loop piping network serving all buildings, incorporating a reverse return configuration to promote hydraulic balance and uniform pressure distribution. A total of 10 secondary substations (LP) is connected to the main loop, linking terminal systems to the central distribution network.

Hydraulic separation between the source and load sides is achieved through decoupling interfaces, allowing independent operation of primary and secondary circuits. This arrangement improves operational flexibility and prevents direct hydraulic interaction between source-side and distribution-side pumping systems.

Due to the diversity of building functions, the substations operate under simultaneous heating and cooling conditions, enabling internal heat recovery within the loop. As a result, the system behaves as an energy exchange network, redistributing thermal energy between zones with different load characteristics.

The hydraulic operating conditions of the substations under representative heating and cooling modes are summarized in Tables 1 and 2, respectively. These results indicate that flow regimes vary across substations in response to load conditions, while temperature differences are maintained within the expected operating range, enabling simultaneous energy exchange between zones.

At the substation level, the system exhibits flow-driven behavior, in which the design flow rate is maintained under normal operation, while the temperature difference (ΔT) adjusts according to the thermal load. Variations in substation flow occur only when connected terminal units (e.g., VRF or WLHP units) are out of operation, resulting in a reduction of active flow demand. This reflects the fundamental operating principle of hydronic terminal systems, where load variation is primarily accommodated through changes in ΔT rather than flow rate.

At the system level, operation is governed by temperature-driven behavior, which determines the activation of heating and cooling sources.

Presenters Extended Summary

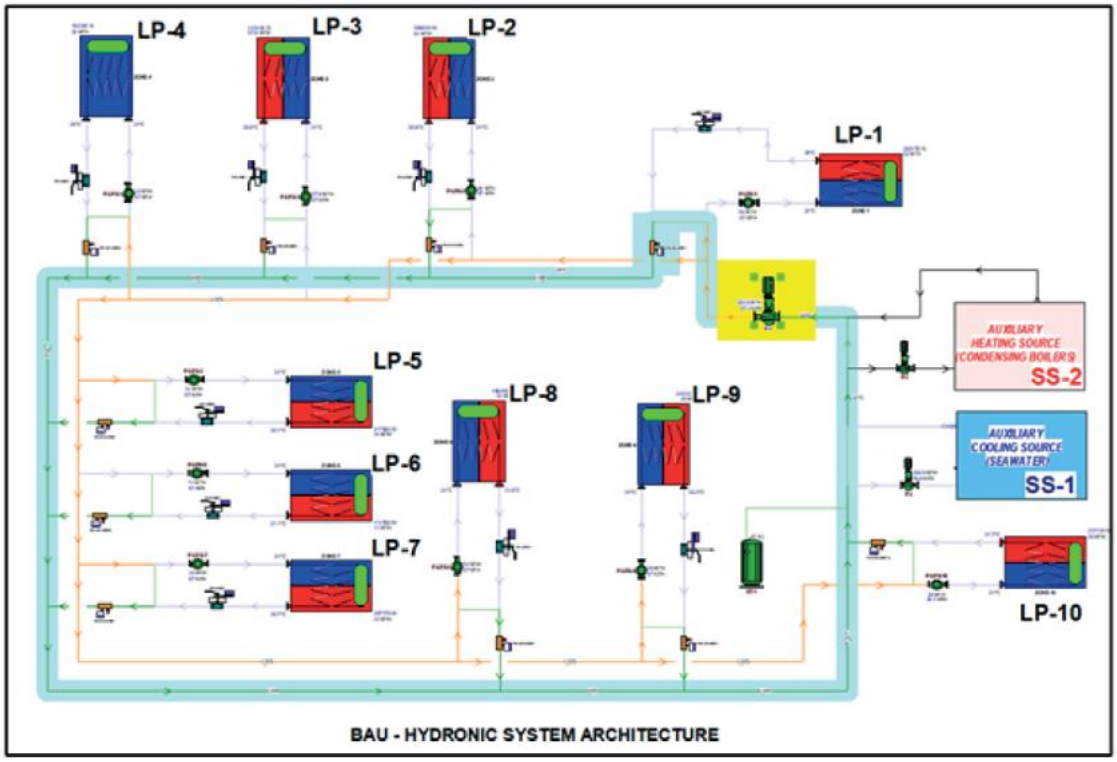


Figure 1– Hydronic System Architecture of the BAU Campus WLHP System

Sub-Stations	Pump Flow Rate (m^3/h)	Zone Heating Capacity [KW]	Input Power [KW]	Heat Absorption [kw]	Water Inlet Temp. (°C)	ΔT (°C)
LP1	52	59.66	3.05	56.61	26	-0.9
LP2	64	165.93	8.49	157.44	26	-2.1
LP3	57.8	87.79	4.49	83.3	26	-1.2
LP4	33	-125.00	26.04	-151.04	26	4.0
LP5	34	123.81	6.33	117.48	26	-3.0
LP6	14	51.78	2.65	49.13	26	-3.0
LP7	22	150.00	7.67	142.33	26	-5.6
LP8	54	196.09	10.03	186.06	26	-3.0
LP9	26	94.55	4.84	89.71	26	-3.0
LP10	26	100.75	5.15	95.6	26	-3.2
Total	**382.8**	**905.36**	**78.74**	**977.66**		**-1.9**

Table 1 – Hydraulic Performance of Substations under Heating Mode

Presenters Extended Summary

Sub-Stations	Pump Flow Rate (m^3/h)	Zone Cooling Capacity [KW]	Input Power [KW]	Heat Rejection [KW]	Water Inlet Temp. [°C]	ΔT (°C)
LP1	52	252.29	49.41	301.76	24	5.0
LP2	64	424.94	83.13	507.71	24	6.9
LP3	57.8	370.98	72.66	443.73	24	6.6
LP4	33	125	26.01	151.04	24	4.0
LP5	34	265	51.9	316.97	24	8.1
LP6	14	95.67	18.72	114.31	24	7.1
LP7	22	250	48.96	299.03	24	11.7
LP8	54	409.45	80.19	489.74	24	7.8
LP9	26	207.02	40.55	247.62	24	8.2
LP10	26	192.9	37.78	230.73	24	7.7
Total	**382.8**	**2593.25**	**509.31**	**3102.64**		**7.0**

Table 2 – Hydraulic Performance of Substations under Cooling Mode

2.3 Source Systems

The system employs a **hybrid energy concept,** combining internal heat recovery within the water loop with external energy sources to ensure reliable and efficient operation under varying load conditions.

Heating Source:

The heating system consists of eight condensing boilers (8 × 125 kW). Heat is transferred to the main loop via plate heat exchangers, providing hydraulic separation between the boiler circuit and the loop. The boiler plant operates as a supplementary heat source, activated only when the loop temperature falls below the defined lower limit. Under these conditions, heat is injected into the loop to maintain the target temperature range and ensure stable operation of the connected heat pump units.

Cooling Source:

The cooling system is based on a seawater heat rejection system consisting of three plate heat exchangers, each with a nominal capacity of approximately 1,550 kW. Under normal operation, two units provide a total heat rejection capacity of approximately 3,100 kW, while the third unit is reserved for standby and future expansion.

2.4 Loop Control Strategy

The loop control strategy is based on two coordinated control layers:

I. Temperature-based mode control and,
II. Pressure-based hydraulic control.

In this approach, the water loop functions both as a thermal energy buffer and as a hydraulic distribution network, ensuring stable and efficient operation under varying load conditions.

Presenters Extended Summary

Temperature-Based Mode Control:

The operating mode of the system is determined by the loop water temperature:

I. Economizing Mode (Dead-Band Operation):
When the loop temperature remains within the range of 23–26°C, neither the boiler nor the seawater system is activated. Under these conditions, the system operates as a thermal balancing network, where heat rejected by cooling-dominant zones is absorbed by heating-dominant zones.

II. Heating Mode:
When the loop temperature falls below 23°C, the boiler system is activated to supply heat to the loop.

III. Cooling Mode:
When the loop temperature exceeds 26°C, excess heat is rejected through the seawater system.

The loop volume (~40 m³), supported by buffer tanks, provides thermal inertia, reducing short-term load fluctuations and minimizing source cycling.

Pressure-Based Hydraulic Control:
Independently of the operating mode, the hydraulic behavior of the system is governed by a **variable differential pressure (ΔP) control strategy.**

The main loop pumps are equipped with **variable speed drives (VSDs)** and are controlled to maintain the required differential pressure at the **critical circuit**, ensuring sufficient pressure at all substations.

Flow at each substation is regulated by **pressure-independent control valves (PICVs).** Under varying load conditions, these valves modulate to adjust flow rates, while pump speed is reduced accordingly. This coordinated response prevents over-pressurization and minimizes pumping energy consumption.

At the substation level, the system exhibits **flow-driven behavior,** where device performance depends on maintaining the required flow rates. At the system level, operation is governed by temperature-driven behavior, which determines the activation of energy sources.

A key aspect of the design is the behavior of the hydraulic decouplers, which operate under near-zero differential pressure conditions when primary and secondary flow rates are balanced. Under these conditions, no flow passes through the decoupler, ensuring effective hydraulic separation between circuits.

A hydraulic decoupler does not inherently guarantee separation; it only provides the physical condition for separation. Effective separation is achieved only when primary and secondary flows are balanced.

3. Hydraulic Digital Twin (HDT) Modeling and Verification

3.1 Hydraulic Model Development

To verify the hydraulic performance of the system prior to implementation, a Hydraulic Digital Twin (HDT) model was developed. The model represents the complete hydronic network, including the main loop, secondary substations, control valves, pumps, and source-side components, enabling a consistent evaluation of system behavior under varying operating conditions.

The hydraulic model developed in the simulation environment is illustrated in Figure 2.

Presenters Extended Summary

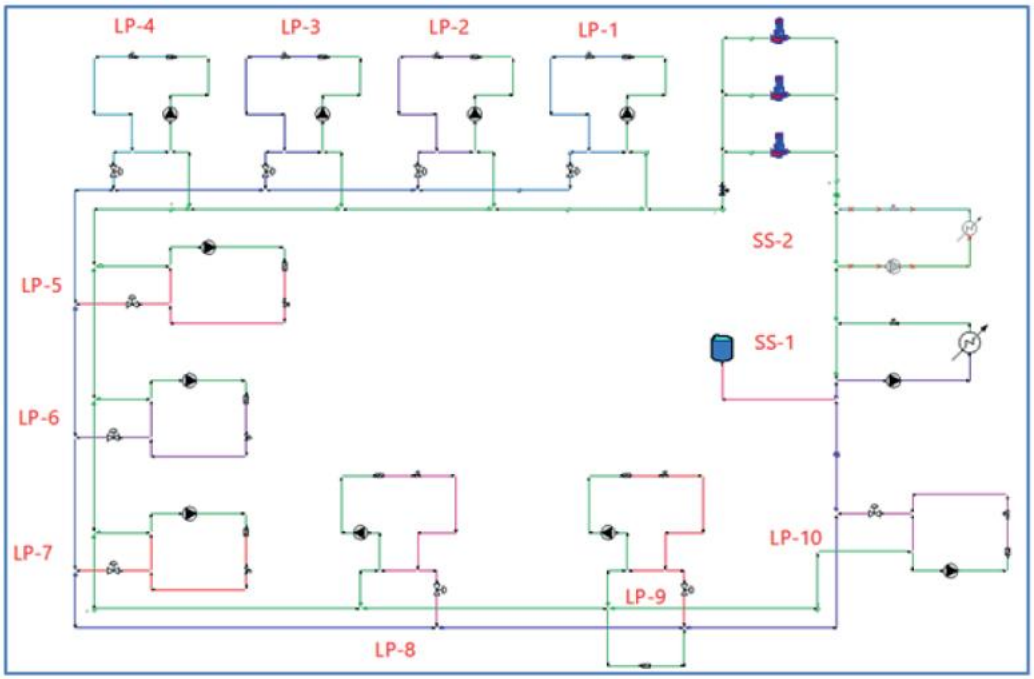


Figure 2- Hydraulic Model Representation Developed in Pipe-Flo

The model was constructed based on design data extracted from the BIM environment. Key parameters, including pipe lengths, diameters, fittings, and design flow rates, were transferred directly into the hydraulic simulation platform to ensure consistency between the digital model and the physical system.

All system components were defined with their corresponding hydraulic characteristics. Pipe networks were modeled with distributed pressure losses, while substations were represented with their respective design flow requirements. Pressure-independent control valves (PICVs) were implemented to reflect flow-regulating behavior, and pump performance curves were incorporated to represent realistic operating conditions.

The model also includes the representation of hydraulic decoupling interfaces between primary and secondary circuits, allowing the interaction between these circuits to be evaluated under different operating conditions.

This modeling approach ensures that the HDT provides an accurate and physically consistent representation of the system, forming the basis for the hydraulic performance verification presented in the following sections.

3.2 Simulation Scenarios

The Hydraulic Digital Twin (HDT) model was used to evaluate system behavior under both design and part-load conditions. Since hydronic HVAC systems operate predominantly under partial load, the analysis emphasizes performance under reduced load scenarios representative of actual operation.

The following load conditions were considered:

- 100% (design condition)
- 50% load
- 25% load
- 12.5% load

Presenters Extended Summary

For each scenario, system flow rates were adjusted proportionally to reflect the corresponding load level, while the control strategy—based on variable differential pressure (ΔP) pump control and pressure-independent control valve (PICV) modulation—was maintained.

The simulations were conducted under steady-state conditions to assess hydraulic performance. The evaluation focuses on key parameters governing system behavior, including:

- Differential pressure distribution across the network
- Flow distribution among substations
- Control valve operating conditions
- Pump operating points

This approach enables a consistent assessment of system response under varying load conditions, izolatın the impact of hydraulic control and system configuration on overall performance.

The simulation framework provides the basis for the hydraulic performance verification presented in Section

3.3 Hydraulic Performance Verification

The objective of the Hydraulic Digital Twin (HDT) analysis is to verify that the system operates in accordance with its design intent under all operating conditions. In variable flow hydronic systems, hydraulic performance is governed by the interaction between pressure, flow, and control elements, rather than by individual components alone.

The following verification steps are interdependent and collectively define the hydraulic behavior of the system:

I. Identification of the critical circuit to define the control reference point
II. Verification of sufficient differential pressure at control valves
III. Evaluation of pump operating points
IV. Assessment of flow distribution
V. Verification of decoupler behavior

This structured approach ensures that the system is evaluated from the most critical hydraulic condition toward overall system performance, establishing a complete and verifiable framework.

3.3.1 Identification of The Critical Circuit and Definition of The Control Reference Point

The identification of the critical hydraulic circuit is a fundamental step in establishing a reliable differential pressure (ΔP) control strategy for the system. The critical circuit represents the most hydraulically demanding flow path in the network and therefore defines the minimum pressure requirement that must be maintained by the main loop pumps.

Using the Hydraulic Digital Twin (HDT) model developed in Pipe-FLO, all substation circuits were analyzed under design operating conditions to determine the total pressure loss from the pump discharge to the most remote control point. Among the evaluated circuits, substation LP-9 was identified as the critical circuit, exhibiting the highest cumulative pressure drop.

Presenters Extended Summary

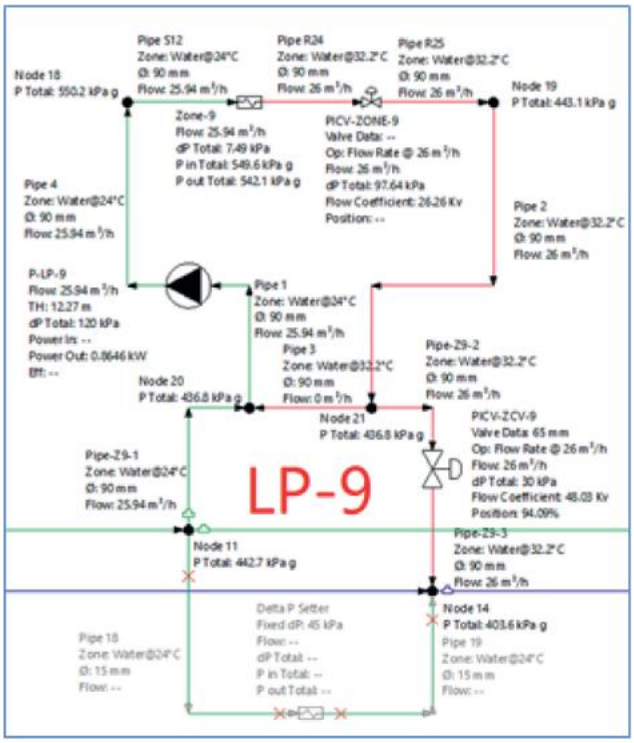


Figure 3-Identification of the Critical Circuit (LP-9)

The total pressures at the selected reference nodes along this circuit were determined as:

- **PNode11 (upstream): 442.7 kPa**
- **PNode14 (downstream): 403.6 kPa**

Accordingly, the differential pressure across the critical circuit is calculated as:

ΔP_critical=442.7-403.6=39.1" kPa

The minimum required differential pressure across the control valve PICV-ZCV-9 is 30 kPa, which represents the threshold necessary to ensure proper valve operation and flow regulation. The calculated ΔP of 39.1 kPa confirms that the critical circuit operates above this minimum requirement, thereby maintaining sufficient control authority.

Loop Station	Valve Name	Valve_Dia	Design Flow Rate		Min.Delta P		Valve position	
LP-9	PICV-ZCV-9	65 mm	26	m^3/h	30	kPa	94.09	%
LP-8	PICV-ZCV-8	100 mm	54	m^3/h	34.77	kPa	79.71	%
LP-2	PICV-ZCV-2	100 mm	64	m^3/h	38.46	kPa	82.84	%
LP-10	PICV-ZCV-10	65 mm	26	m^3/h	38.73	kPa	71.2	%
LP-1	PICV-ZCV-1	80 mm	52	m^3/h	39.02	kPa	83.29	%
LP-4	PICV-ZCV-4	80 mm	33	m^3/h	39.53	kPa	69.52	%
LP-3	PICV-ZCV-3	100 mm	57.8	m^3/h	39.82	kPa	79.84	%
LP-5	PICV-ZCV-5	80 mm	34	m^3/h	40.39	kPa	70.02	%
LP-7	PICV-ZCV-7	65 mm	22	m^3/h	42.08	kPa	81.71	%
LP-6	PICV-ZCV-6	50 mm	14	m^3/h	42.38	kPa	72.57	%

Table 3 – Hydraulic Performance of Zone Control Valves as per min set pressure of 30 kPa @ LP-9

Presenters Extended Summary

To ensure stable operation under varying load conditions and to provide a safety margin, the differential pressure setpoint for the main loop pumps is defined as:

$\Delta P_set=45"$ kPa

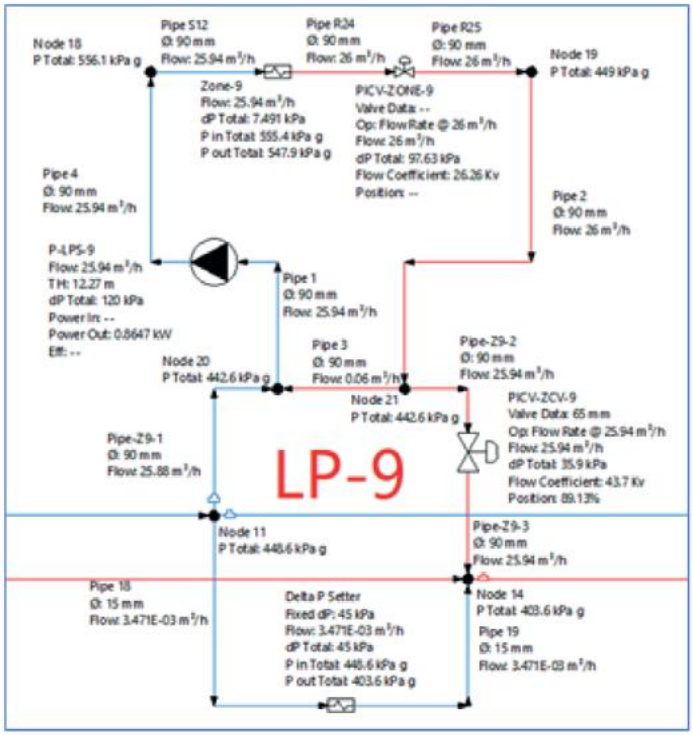


Figure 4– Identification of the Critical Circuit (LP-9) and ΔP Set Value between the Control Nodes

The main loop pumps are equipped with variable speed drives (VSDs) and are controlled based on the differential pressure measured between **PNode11 and PNode14**, corresponding to the critical circuit.

As shown in Figure 4, this control strategy ensures that the most hydraulically demanding circuit governs the system operation.

These results confirm that the identification of the critical circuit and the corresponding ΔP setpoint are not based on assumptions, but on validated hydraulic analysis, ensuring that the system is controlled according to the most demanding operating condition.

3.3.2 Verification Of Sufficient Differential Pressure at All Control Valves Under Varying Loads

The Hydraulic Digital Twin (HDT) was used to evaluate control valve performance under 100%, 75%, 50%, **25% and 12.5%** load conditions (Table 5,6, and 7). The results show that the differential pressure across all PICVs remains nearly constant at approximately 45 kPa, with minimal variation.

As flow demand decreases, valve positions modulate accordingly without reaching extreme limits, indicating that all valves operate within their effective control range. This confirms that the applied **variable ΔP control strategy** maintains a stable pressure regime while allowing independent flow regulation at each substation. In contrast, without proper ΔP control, part-load operation would lead to pressure imbalance and unstable valve behavior.

Presenters Extended Summary

Loop Station	Valve Name	Valve_Dia	100% Flow Rate		Delta P		Valve position		75% Flow Rate		Delta P		Valve position	
LP-9	PICV-ZCV-9	65 mm	26	m^3/h	35.86	kPa	89.23	%	19.5	m^3/h	39.68	kPa	79.22	%
LP-8	PICV-ZCV-8	100 mm	54	m^3/h	40.63	kPa	77.95	%	40.5	m^3/h	42.48	kPa	72.19	%
LP-2	PICV-ZCV-2	100 mm	64	m^3/h	44.34	kPa	81.01	%	48	m^3/h	44.53	kPa	74.74	%
LP-10	PICV-ZCV-10	65 mm	26	m^3/h	44.59	kPa	67.82	%	19.5	m^3/h	44.75	kPa	54.42	%
LP-1	PICV-ZCV-1	80 mm	52	m^3/h	44.91	kPa	79.8	%	39	m^3/h	44.87	kPa	71.91	%
LP-4	PICV-ZCV-4	80 mm	33	m^3/h	45.41	kPa	67.73	%	24.75	m^3/h	45.15	kPa	61.6	%
LP-3	PICV-ZCV-3	100 mm	57.8	m^3/h	45.69	kPa	78.25	%	43.35	m^3/h	45.32	kPa	72.81	%
LP-5	PICV-ZCV-5	80 mm	34	m^3/h	46.26	kPa	68.23	%	25.5	m^3/h	45.73	kPa	62.03	%
LP-7	PICV-ZCV-7	65 mm	22	m^3/h	47.96	kPa	79.97	%	16.5	m^3/h	46.72	kPa	73.98	%
LP-6	PICV-ZCV-6	50 mm	14	m^3/h	48.25	kPa	71.27	%	10.5	m^3/h	46.87	kPa	65.12	%

Table 4– Hydraulic Performance of Zone Control Valves under Variable Differential Pressure (ΔP) Control Using VSD Pumps at Part-Load Conditions (100% and 75%)

Loop Station	Valve Name	Valve_Dia	50% Flow Rate		Delta P		Valve position		25% Flow Rate		Delta P		Valve position	
LP-9	PICV-ZCV-9	65 mm	13	m^3/h	42.5	kPa	70.7	%	6.5	m^3/h	44.31	kPa	55.97	%
LP-8	PICV-ZCV-8	100 mm	27	m^3/h	43.83	kPa	62.94	%	13.5	m^3/h	44.69	kPa	43.27	%
LP-2	PICV-ZCV-2	100 mm	32	m^3/h	44.73	kPa	66.91	%	16	m^3/h	44.91	kPa	48.23	%
LP-10	PICV-ZCV-10	65 mm	13	m^3/h	44.87	kPa	37.53	%	6.5	m^3/h	44.95	kPa	19.64	%
LP-1	PICV-ZCV-1	80 mm	26	m^3/h	44.89	kPa	62.59	%	13	m^3/h	44.96	kPa	48.48	%
LP-4	PICV-ZCV-4	80 mm	16.5	m^3/h	45.02	kPa	53.16	%	8.25	m^3/h	44.99	kPa	36.94	%
LP-3	PICV-ZCV-3	100 mm	28.9	m^3/h	45.1	kPa	64.22	%	14.45	m^3/h	45.01	kPa	45.09	%
LP-5	PICV-ZCV-5	80 mm	17	m^3/h	45.34	kPa	53.64	%	8.5	m^3/h	45.1	kPa	37.72	%
LP-7	PICV-ZCV-7	65 mm	11	m^3/h	45.81	kPa	66.52	%	5.5	m^3/h	45.23	kPa	51.13	%
LP-6	PICV-ZCV-6	50 mm	7	m^3/h	45.86	kPa	56.53	%	3.5	m^3/h	45.24	kPa	37.9	%

Table 5– Hydraulic Performance of Zone Control Valves under Variable Differential Pressure (ΔP) Control Using VSD Pumps at Part-Load Conditions (50% and 25%)

Loop Station	Valve Name	Valve_Dia	12/5% Flow Rate		Delta P		Valve position	
LP-9	PICV-ZCV-9	65 mm	3.25	m^3/h	44.8	kPa	35.68	%
LP-8	PICV-ZCV-8	100 mm	6.75	m^3/h	44.91	kPa	24.46	%
LP-2	PICV-ZCV-2	100 mm	8	m^3/h	44.96	kPa	28.74	%
LP-1	PICV-ZCV-1	80 mm	6.5	m^3/h	44.98	kPa	31.14	%
LP-10	PICV-ZCV-10	65 mm	3.25	m^3/h	44.98	kPa	9.934	%
LP-3	PICV-ZCV-3	100 mm	7.225	m^3/h	44.99	kPa	26.07	%
LP-4	PICV-ZCV-4	80 mm	4.125	m^3/h	44.99	kPa	20.09	%
LP-5	PICV-ZCV-5	80 mm	4.25	m^3/h	45.03	kPa	20.68	%
LP-7	PICV-ZCV-7	65 mm	2.75	m^3/h	45.06	kPa	30.85	%
LP-6	PICV-ZCV-6	50 mm	1.75	m^3/h	45.06	kPa	17.09	%

Table 6 – Hydraulic Performance of Zone Control Valves under Variable Differential Pressure (ΔP) Control Using VSD Pumps at Part-Load Conditions (12.5%)

These findings validate the accuracy of the hydraulic design model, confirming that the system operates within the predicted control envelope and that valve performance remains stable under varying load conditions.

Presenters Extended Summary

3.3.3 Evaluation of pump operating points

The evaluation of pump operating points is essential to ensure that the pumping system operates within its efficient and stable performance envelope under varying load conditions. In variable flow hydronic systems, improper pump operation may result in over-pressurization, flow imbalance, excessive energy consumption, or unstable hydraulic behavior.

The main loop pumps are equipped with variable speed drives (VSDs) and operate under a variable differential pressure (ΔP) control strategy, whereby pump speed is continuously adjusted in response to system demand. The pump performance was analyzed using the Hydraulic Digital Twin (HDT), and the corresponding operating points were plotted on the manufacturer's pump performance curves, as shown in Figure 5 and Figure 6. Under design conditions, the pump operates close to its Best Efficiency Point (BEP), confirming that the pump selection is well matched with the system requirements. As the system load decreases, the operating points shift toward lower flow rates and reduced head values, following the system curve. This behavior indicates that the pump remains within its optimal performance region and avoids operation in inefficient or unstable zones.

At low-load conditions, the operating point approaches the minimum allowable flow limit, which defines the lower boundary of stable pump operation. Operation below this limit may result in internal recirculation, increased vibration, and loss of hydraulic stability. The analysis confirms that the system maintains operation above this minimum flow threshold under all evaluated scenarios.

This adaptive pump response ensures that the required differential pressure is maintained at the critical circuit while preventing over-pressurization in near branches. Consequently, stable control valve operation is preserved and unnecessary energy consumption is minimized.

In contrast, under constant ΔP control, the pump would maintain higher pressure levels regardless of load reduction, leading to excessive valve throttling and operation outside the optimal efficiency range.

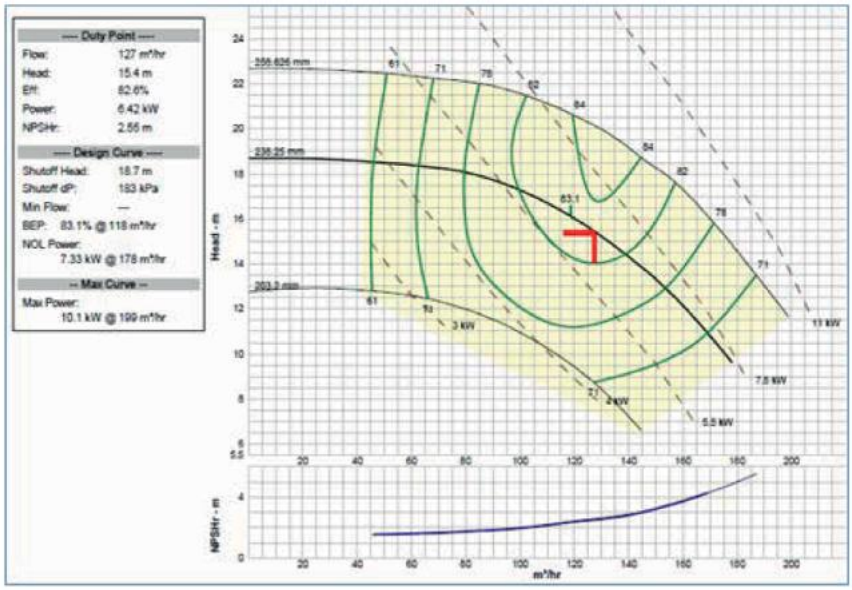


Figure 5– Main Loop Pump Operating Point @ 100% Flow

Presenters Extended Summary

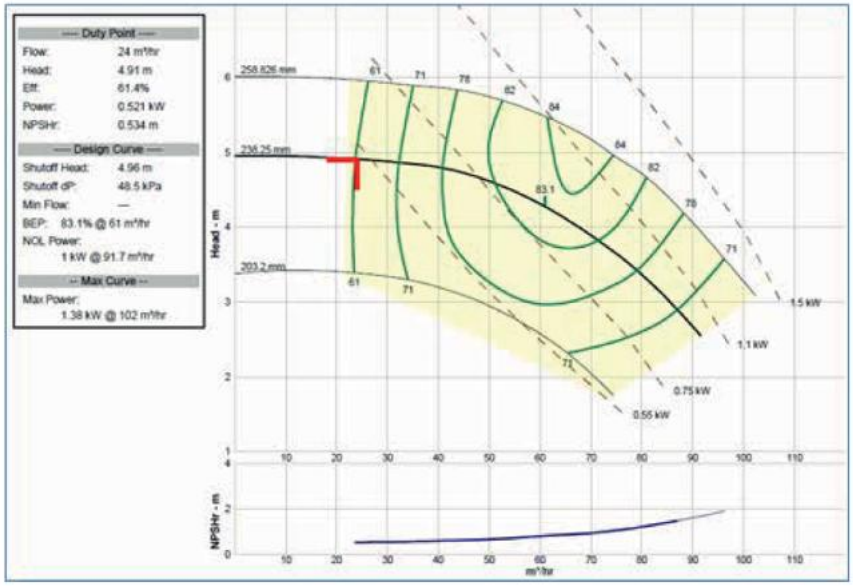


Figure 6 – Main Loop Pump Operating Point @ Min Flow Control Scenario

These findings confirm that the pump operates within its defined performance envelope and that the hydraulic model accurately predicts pump behavior, ensuring efficient, stable, and safe operation under varying load conditions.

3.3.4 Assessment of Flow Distribution to Prevent İmbalance, Overflow, Or Starvation

The flow distribution within the system is directly governed by the differential pressure conditions established in Section 3.3.2. Stable differential pressure across the control valves ensures that each valve can operate with sufficient authority, thereby enabling accurate and independent flow regulation at each substation.

Using the Hydraulic Digital Twin (HDT), the flow rates at each substation were evaluated under both design and part-load conditions. The results, summarized in Tables 4,5 and 6, indicate that flow distribution remains consistent with expected values across all operating scenarios.

The analysis confirms that no substation experiences excessive flow (overflow) or insufficient flow (starvation). As system load decreases, flow rates are reduced proportionally while maintaining balanced distribution across the network. This behavior demonstrates that the combination of stable ΔP control, PICV-based flow regulation, and reverse return piping configuration effectively ensures hydraulic balance.

The results further indicate that pressure losses are properly coordinated throughout the system, allowing uniform flow delivery even under reduced load conditions. This confirms that the hydraulic design avoids concentration of flow in low-resistance branches and ensures adequate supply to remote circuits.

In contrast, without stable differential pressure control, accurate flow distribution cannot be achieved. Under such conditions, part-load operation would typically result in over-pressurization of near branches and insufficient flow in remote zones, leading to hydraulic imbalance and degraded system performance.

Presenters Extended Summary

These findings confirm that the hydraulic model accurately predicts flow distribution as a direct outcome of stable valve operation and differential pressure control, ensuring that all substations operate within the intended flow range without imbalance, overflow, or starvation under varying load conditions.

3.3.5 Verification of Decoupler Behavior To Avoid Unintended Mixing Between Circuits

The hydraulic decoupler is implemented to achieve hydraulic separation between the primary (source) and secondary (distribution) circuits by minimizing pressure interaction between the two loops. In ideal operation, the decoupler should exhibit negligible differential pressure and near-zero flow, indicating that primary and secondary flow rates are balanced. The behavior of the decoupler was evaluated using the Hydraulic Digital Twin (HDT) by monitoring both the differential pressure (ΔP_dec) across the decoupler and the flow rate (Q_dec) through the decoupler under design and part-load conditions.
The results show that:

- The differential pressure across the decoupler remains approximately $\Delta P_dec \approx 0$ kPa
- The flow through the decoupler is $Q_dec \approx 0$ m³/h

These values confirm that the decoupler operates as a hydraulically neutral interface, with no measurable driving force for flow exchange between the primary and secondary circuits.

This condition is achieved when:

$$Q_primary \approx Q_secondary$$

indicating that the total flow supplied by the primary circuit matches the demand of the secondary circuits. Under this condition, no bypass or recirculation occurs through the decoupler.
The HDT analysis further confirms that this balance is maintained across varying load conditions. As demonstrated in Sections 3.3.2 through 3.3.4, stable differential pressure control, proper valve modulation, and balanced flow distribution ensure that primary and secondary flow rates always remain coordinated.

In contrast, any mismatch between primary and secondary flow rates would result in non-zero flow through the decoupler:

- If $Q_primary > Q_secondary$: excess flow bypasses from supply to return
- If $Q_primary < Q_secondary$: return water is drawn into the supply

Both conditions lead to mixing between supply and return streams, causing:

- Reduction of effective temperature difference (ΔT)
- Degradation of system energy efficiency
- Loss of thermal control accuracy

Therefore, the decoupler does not actively enforce separation; rather, it passively reflects the hydraulic balance of the system.
The HDT results confirm that the decoupler operates under near-zero flow and pressure conditions, validating that the system achieves true hydraulic separation and that the interaction between primary and secondary circuits is accurately predicted by the hydraulic model.

Presenters Extended Summary

3.4 Design Validation Outcomes

The simulation results demonstrate that the system operates within the defined hydraulic limits and maintains stable performance under all evaluated conditions.

The key validated outcomes are summarized as follows:

- All terminal units receive the required design flow rates under both design and part-load conditions
- Control valves operate within their required differential pressure range, ensuring stable and pres sure-independent flow control
- Pump operation remains within the efficient operating region of the performance curve, including part-load conditions
- System temperature difference (ΔT) is preserved through proper flow regulation
- Hydraulic uncertainties are eliminated through pre-construction verification using the Hydraulic Digital Twin (HDT) model

These results confirm that the hydraulic design is not only theoretically adequate but has been quantitatively validated to ensure stable, efficient, and reliable system operation prior to implementation.

3.5 Role of HDT in Design Process

The use of a Hydraulic Digital Twin (HDT) transforms the design process into a verifiable and performance-driven methodology.

By validating system behavior prior to installation, the HDT enables:

- Reduction of commissioning risks
- Verification of design assumptions
- Alignment of equipment selection with actual operating conditions
- Avoidance of costly post-installation modifications

The HDT approach shifts HVAC design from a predictive process based on assumptions to a validated process based on measurable system behavior.

4. Conclusions

From a design perspective, this study supports a shift toward a performance-based and verifiable approach, where hydraulic behavior is explicitly defined and validated rather than assumed. This approach reduces commissioning risks, minimizes the need for corrective actions, and ensures that the installed system performs in alignment with the original design intent.

Finally, while accurate design and verification are critical, the successful realization of system performance also depends on proper installation and workmanship. Adherence to the verified hydraulic design—particularly in piping implementation and equipment connections—is essential to fully achieve the intended operational efficiency.

Presenters Extended Summary

Volkan Doda
Atelier Ten
Head of Design Technologies
CIBSE Engineer of the year 2025

Speech Title: From Machine Learning to Learning from Machines

Abstract:
Artificial intelligence (AI) is swiftly permeating all aspects of life and the building services industry is no exception. This keynote argued that we engineers cannot afford to let AI happen to us while we watch it transform our world from the sidelines. As professionals with a commitment to designing and delivering for public good, we must engage with AI now, not next month, not tomorrow, but now. We also must do so both meaningfully by embracing emerging and yet-to-be-imagined opportunities AI offers, and responsibly by confronting its risks head-on rather than wishing them away. Drawing on recent data from acquisitions in our industry to signs of shifting hiring patterns for early-career professionals, the talk traced how AI is positioned to reshape our field, and how this may affect us all for the better, or possibly for the worse if we do not actively engage to shape it, now.

Building on that strand, the second part of the talk pivoted to discussing AI's possible impact on employment by challenging two opposing anxieties that AI is either incapable of doing an engineer's job or destined to replace it altogether. Both contain grains of truth. Today generative AI struggles with liability, context, and the kind of judgment that comes from years of internalized experience. But it is also improving fast, and some AI tools already outperform many humans in narrowly defined tasks. Yet the future remains ours to shape. Rather than a threat to be resisted, AI may well be part of the solution for the long-standing global productivity gap in the built environment sector. This in turn, the talk concluded, may offer us a runway to adopt AI deliberately and on our own terms, while empowering the next generation of AI-native engineers who will learn to work alongside these tools, and offer the rest of us many more new things to learn.

FULL PAPERS

TTMD
Turkish Society of HVAC & Sanitary Engineers
XVII TTMD INTERNATIONAL HVAC&R TECHNOLOGIES SYMPOSIUM
ARTIFICIAL INTELLIGENCE IN BUILDINGS
14-15 MAY 2026

Response Surface-Based Numerical Optimization of Opening Layouts for Natural Ventilation in Residential Buildings

Ahmetcan Yetiş[1], Ziya Haktan Karadeniz[1]
[1]İzmir Institute of Technology,Türkiye
Corresponding email: ahmetcanyetis@iyte.edu.tr

SUMMARY

Natural ventilation remains the dominant strategy in residential buildings despite the increasing adoption of mechanical and hybrid ventilation systems. Because its performance is strongly affected by façade opening configuration and external wind conditions, reliable evaluation during the design stage is essential. This study presents a computational framework for analyzing and optimizing floor-wise natural ventilation performance in a multi-storey residential building under realistic atmospheric boundary layer (ABL) conditions.

A full-scale benchmark building was analyzed using computational fluid dynamics (CFD). Inlet boundary conditions were reconstructed from validated wind tunnel data to represent ABL velocity and turbulence profiles realistically. The numerical model was first verified through empty-tunnel simulations, showing good agreement with the reference data and confirming preservation of the target ABL characteristics within the computational domain.

The influence of opening configuration was investigated using a Latin Hypercube Sampling (LHS)-based design of experiments with 45 cases. The resulting CFD dataset was used to construct Kriging-based response surfaces for each floor, enabling efficient exploration of the design space and identification of favorable configurations.

The results showed a clear non-linear relationship between opening configuration and floor-wise volume flow rate. The first floor was the most sensitive to opening configuration, while the upper floors showed comparatively smaller variations. Relative to the minimum observed values, the response-surface-based optimum configuration improved the volume flow rate by 42%, 25%, 18%, and 25% on the first to fourth floors, respectively.

INTRODUCTION

Despite the well-documented advantages of mechanical and hybrid ventilation systems, and the increasing encouragement of their adoption in building codes and standards, natural ventilation remains the predominant strategy in residential buildings. In many European countries, the majority of residential buildings rely on natural ventilation, and reducing the level of pollution is usually achieved simply by opening windows [1, 2]. Field studies indicate that the penetration of mechanical ventilation systems is still limited. A recent survey conducted in Germany involving 952 participants revealed that ventilation practices are largely influenced by situational, habitual, and goal-directed factors [3].

Although occupants generally recognize the benefits of mechanical ventilation systems, a significant majority of them -approximately 90%- still express a strong preference for maintaining control over window operation [3]. This persistent occupant behaviour highlights the continued reliance on, and importance of, natural ventilation in residential environments.

The relevance of natural ventilation and continuing practices/habits does not directly yield high energy consumption or inefficiencies. Tong et al. investigated the potential of natural ventilation on energy efficiency

and predicted that cooling energy requirements could be reduced by 8% to 78% through natural ventilation, depending on local climate and air quality [4]. Wang et al. analyzed the effects of different window usage strategies on building performance. The strategies were classified as: "open window model," where windows and mechanical ventilation systems are continuously open, "natural ventilation model," where only natural ventilation is applied, "change model," where natural and mechanical ventilation are activated according to indoor conditions, and "hybrid operating model," where these two methods are used simultaneously. According to the study results, keeping windows continuously open adds an additional load of 3.5% to 15.2% to ventilation energy consumption, while heating load can be reduced by 17% to 46.5% when natural and mechanical ventilation operate simultaneously [5]. Findings presented show that using natural ventilation strategies as a complementary element to mechanical systems can have positive effects on system efficiency.

Natural ventilation is unpredictable and unstable; thus, its design requires an understanding of the surrounding environment's characteristics [6]. Building façade elements, opening sizes, and their locations directly influence natural ventilation performance [7-10]. Apart from these building characteristics, environmental parameters such as wind velocity, direction, outdoor air quality, and temperature also influence indoor air quality and occupant comfort.

This study mainly investigates wind characteristics and building opening configurations to optimize natural ventilation performance through computational fluid dynamics (CFD) simulations. CFD provides a powerful tool for assessing airflow patterns and ventilation effectiveness for different cases. Reliable CFD-based natural ventilation optimization requires a realistic representation of atmospheric boundary layer (ABL) conditions, including velocity and turbulence quantities, which govern the wind-driven flow field around buildings [11]. Oversimplified or inaccurate boundary conditions may lead to misleading predictions of natural ventilation performance.

With emphasis placed on atmospheric boundary layer parameters, this study aims to optimize the opening layout of a multi-storey residential building model using response surface methodology. The proposed framework aims to provide a reusable methodology for improving natural ventilation in residential buildings. This study presents a workflow that integrates a validated ABL-consistent CFD framework with response surface modeling for the optimization of natural ventilation performance.

METHODOLOGY

The building model considered in this study is based on a benchmark configuration used by Karava et al. [8] and Ramponi et al. [10]. The building model has dimensions of 20 m x 20 m x 16 m (W x L x H). Karava et al. investigated a 1:200 scaled model in a wind tunnel using the Particle Image Velocimetry (PIV) method to assess different operable façade elements. Obtained experimental data, further used for the validation of CFD simulations by Ramponi et al.

In this study, a full-scale representation of the building model is adopted to directly evaluate ventilation performance without any geometric scaling. The inside domain of the building model is separated into 4 equal parts, representing each floor. Each floor is 3.5 m high, and the building walls have a thickness of 0.4 m. Each floor has equally sized 4.6 m x 1.8 m inlet and outlet openings, located at the horizontal center plane of opposite façade walls.

The building model is placed within a 148 m x 228 m x 100 m (W x L x H) computational domain. To match the velocity and turbulence quantities presented in reference studies, the building model was placed 48 m downstream of the inlet boundary. The domain size is selected to minimize blockage effects. Figure 1 shows the building model and computational domain dimensions.

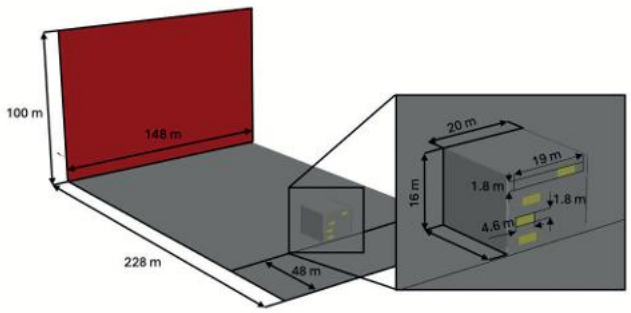


Figure 1. Computational Model and Dimensions

Atmospheric Boundary Layer Modelling and Model Validation

Inlet boundary conditions were defined based on measured mean wind velocity and turbulent intensity profiles, provided by Karava et al. [7]. The wind velocity profile follows the logarithmic law for neutral atmospheric conditions given in Eq. (1), where u_* is the friction velocity, κ is the von Kármán constant (0.42), and z_0 is the aerodynamic roughness length (0.05 m). The turbulent kinetic energy (k) is defined to be consistent with the reference study ABL's turbulent intensity profiles using Eq. (2), $I_u(z)$ is streamwise turbulent intensity and a is a constant with a value of 1.0 as recommended by Tominaga et al. (Tominaga et al., 2008). Turbulent dissipation rate (ε) is calculated by Eq. (3) and specific dissipation rate (ω) by Eq. (4). C_μ is a model constant which has a value of 0.09. These formulations ensure consistency between the velocity and turbulence quantities within the computational domain.

$$U(z) = \frac{u_*}{\kappa} \ln\left(\frac{z+z_0}{z_0}\right) \quad (1)$$

$$k(z) = a(I_u(z)U(z))^2 \quad (2)$$

$$\varepsilon(z) = \frac{u_*^3}{\kappa(z+z_0)} \quad (3)$$

$$\omega(z) = \frac{\varepsilon(z)}{C_\mu k(z)} \quad (4)$$

The inlet profiles are implemented using user-defined functions to ensure continuous variation with height. Turbulent kinetic energy (k) profile reconstructed from reference case, velocity, and specific dissipation rate (ω) profiles are defined by equations 1 and 4. Surface roughness effects are incorporated through equivalent sand-grain roughness (roughness constant, C_s=0.874 and sand-grain roughness height, k_s=0.056 m) parameters at the ground boundary according to the guidelines derived by Blocken et al. [11]. Building surfaces are treated as smooth walls with zero sand-grain roughness height.

An empty tunnel was simulated with defined ABL profiles to validate the computational domain. Figure 2 shows velocity, k and ε profiles of reconstructed reference cases for representing the full-scale model (Figure 2a), and the computational domain investigated in this study (Figure 2b). At the inlet, the investigated profiles showed good agreement with the reference data with a coefficient of determination (R^2) ≥ 0.99, while at the building position, the minimum coefficient of determination was calculated (R^2) ≥ 0.96.

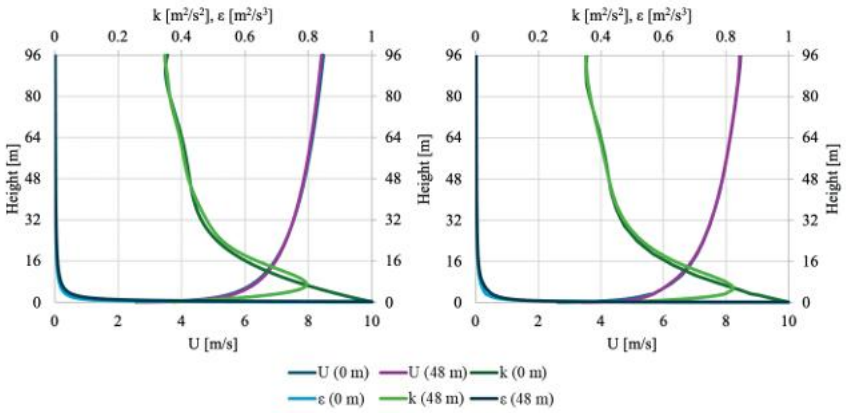


Figure 2. Velocity (U), turbulent kinetic energy (k), and turbulent dissipation rate (ε) profiles at the inlet (0 m) and building position (48 m). a) Reference case reconstructed for full scale, b) Empty tunnel simulation of the computational domain investigated in this study.

The SST k-ω turbulence model was employed to simulate the flow field, as it provides reliable predictions for flows involving separation and external aerodynamics. The computational mesh consisted of approximately 2.16 million cells, with refinement applied near the building, on the ground surface, and in opening regions. The computational domain mesh incorporating the building model is shown in Figure 3.

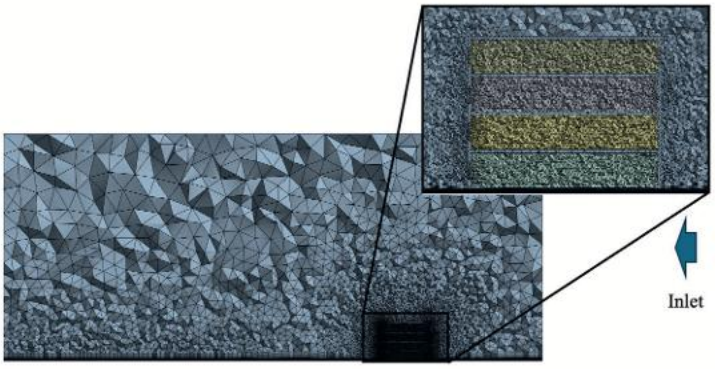


Figure 3. Computational Domain Mesh

Design of Experiments and Response Surface Methodology

The influence of opening configurations is investigated using a Latin Hypercube Sampling–based design with 45 samples. The horizontal positions of openings on each floor are treated as design variables; each variable ranges from 1 m to 14.4 m, to vary the opening positions along the façade surfaces, while their dimensions are kept constant.

Each sample was evaluated using CFD simulations, and the resulting data were used to construct a Kriging surrogate model. The response surface enables efficient exploration of the design space and identification of configurations that improve ventilation performance, while acknowledging limitations in capturing highly non-linear interactions.

RESULTS AND DISCUSSION

The response surfaces for each floor are presented in Figure 4. Each surface was generated by varying the opening position of the corresponding floor horizontally while keeping the opening positions on the other floors fixed at their mid-range values. Accordingly, the presented surfaces should be interpreted as conditional floor-wise responses. The results indicate that the ventilation performance on each floor is still affected by the overall opening configuration of the building. In all cases, the response exhibited a distinctly non-linear dependence on the windward and leeward opening positions, indicating that ventilation performance cannot be described by a simple monotonic relationship.

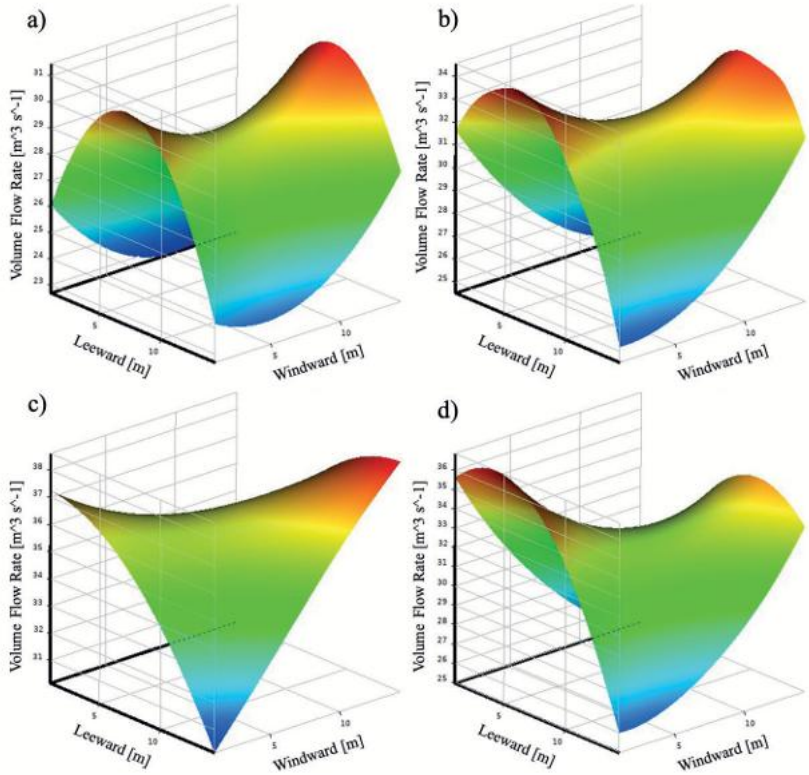


Figure 4. Response surfaces for each floor, a) first, b) second, c) third, d) fourth floors

The first floor showed the widest response range, whereas the upper floors exhibited comparatively smaller variations. Across the investigated cases, the volume flow rate ranged from 19.38 to 29.39 m^3/s on the first floor, 26.20 to 34.03 m^3/s on the second floor, 29.87 to 38.36 m^3/s on the third floor, and 28.16 to 35.27 m^3/s on the fourth floor. These ranges correspond to floor-wise variations of 52%, 30%, 28%, and 25%, respectively, indicating that the first floor was the most sensitive to opening configuration.

The response-surface-based optimum configuration also provided a marked improvement over the low-performance regions of the design space. Relative to the minimum observed volume flow rate on each floor, the selected configuration increased the volume flow rate by 42%, 25%, 18%, and 25% for the first to fourth floors, respectively. Since these minimum values were obtained independently for each floor, they do not correspond to a single common design point. Nevertheless, the results demonstrate that the selected configuration shifted the solution toward a high-performance region of the design space.

Additional simulations were also conducted using a uniform inlet velocity profile, which produced higher predicted volume flow rates, particularly in the lower half of the building. Although only a limited number of such

cases were evaluated, the results consistently indicated an overprediction tendency. This suggests that adopting a uniform inlet profile may lead to an unrealistically favorable prediction of ventilation performance in the present study.

Although the study examined the effect of opening configuration on volume flow rate in detail, the internal airflow structure within each floor was not investigated explicitly. Therefore, the findings mainly reflect the quantitative aspect of ventilation performance. For a more comprehensive assessment, ventilation effectiveness indicators such as airflow pattern, age of air, and air change efficiency should also be considered, as these parameters provide additional information on ventilation effectiveness within the occupied space.

CONCLUSION

This study investigated the effect of façade opening configuration on floor-wise volume flow rates in a multi-storey naturally ventilated building using response surface analysis. The results showed that ventilation performance was strongly dependent on the opening arrangement and exhibited a clearly non-linear response on all floors. Among the investigated cases, the first floor showed the highest sensitivity to opening configuration, with a variation of 52% between the minimum and maximum observed values, whereas the upper floors exhibited narrower but still significant ranges. The response-surface-based optimum configuration yielded improvements of 42%, 25%, 18%, and 25% relative to the minimum observed values on the first to fourth floors, respectively, demonstrating the usefulness of the approach for identifying favorable design regions.

The findings also showed that the response of each floor depended not only on its local opening position but also on the overall opening configuration of the building. In addition, simulations performed with a uniform inlet velocity profile produced higher volume flow rates, particularly in the lower part of the building, indicating that this assumption may lead to unrealistically favorable ventilation predictions.

Although the present study examined volume flow rates in detail, it did not explicitly assess the internal airflow distribution within each floor. Therefore, the results should be interpreted primarily in terms of ventilation quantity. For a more comprehensive evaluation of natural ventilation performance, future work should also consider ventilation effectiveness indicators such as airflow pattern, age of air, and air change efficiency.

REFERENCES

[1] A. Litiu, “Introduction Ventilation system types in some EU countries,” 2012.

[2] J. Ferdyn-Grygierek and K. Grygierek, “Ventilation Methods for Improving the Indoor Air Quality and Energy Efficiency of Multi-Family Buildings in Central Europe,” Energies (Basel)., vol. 17, no. 9, May 2024, doi: 10.3390/en17092232.

[3] J. Berneiser, S. Auerswald, D. Maier, S. Gölz, N. Carbonare, and T. Pflug, “Feeling the breeze? Ventilation practices and occupant requirements for mechanical ventilation in residential buildings,” Energy Build., vol. 302, Jan. 2024, doi: 10.1016/j.enbuild.2023.113702.

[4] Z. Tong, Y. Chen, A. Malkawi, Z. Liu, and R. B. Freeman, “Energy saving potential of natural ventilation in China: The impact of ambient air pollution,” Appl. Energy, vol. 179, pp. 660–668, Oct. 2016, doi: 10.1016/j.apenergy.2016.07.019.

[5] L. Wang and S. Greenberg, “Window operation and impacts on building energy consumption,” Energy Build., vol. 92, pp. 313–321, Apr. 2015, doi: 10.1016/j.enbuild.2015.01.060.

[6] Sait Cemil SOFUOĞLU et al., Konutlarda İç Hava Kalitesi ve Havalandırma I, 1st ed. İzmir: TMMOB Makina Mühendisleri Odası İzmir Şubesi, 2024.

[7] Panagiota. Karava, Airflow prediction in buildings for natural ventilation design: Wind tunnel measurements and simulation. [Concordia University (Canada)], 2008.

[8] P. Karava, T. Stathopoulos, and A. K. Athienitis, "Airflow assessment in cross-ventilated buildings with operable façade elements," Build. Environ., vol. 46, no. 1, pp. 266–279, Jan. 2011, doi: 10.1016/j.buildenv.2010.07.022.

[9] Y. Tominaga and B. Blocken, "Wind tunnel analysis of flow and dispersion in cross-ventilated isolated buildings: Impact of opening positions," Journal of Wind Engineering and Industrial Aerodynamics, vol. 155, pp. 74–88, Aug. 2016, doi: 10.1016/j.jweia.2016.05.007.

[10] R. Ramponi and B. Blocken, "CFD simulation of cross-ventilation for a generic isolated building: Impact of computational parameters," Build. Environ., vol. 53, pp. 34–48, Jul. 2012, doi: 10.1016/j.buildenv.2012.01.004.

[11] B. Blocken, T. Stathopoulos, and J. Carmeliet, "CFD simulation of the atmospheric boundary layer: wall function problems," Atmos. Environ., vol. 41, no. 2, pp. 238–252, Jan. 2007, doi: 10.1016/j.atmosenv.2006.08.019.

[12] Y. Tominaga et al., "AIJ Guidelines for Practical Applications of CFD to Pedestrian Wind Environment around Buildings," Yokohama, Nov. 2007.

NUMERICAL INVESTIGATION OF SINGLE CYCLE TRANSIENT THERMAL RESPONSE OF GYROID HEAT EXCHANGER

Alper Mete Genç[1]
[1]Bosch Thermotechnology, Manisa, Türkiye
Corresponding email: alpermete.genc@tr.bosch.com

SUMMARY

In this study, the initial regenerative heat transfer performance of a Gyroid structure—one of the triply periodic minimal surfaces (TPMS)—is numerically investigated for a single charging and discharging cycle. The Gyroid geometry is selected because of its continuous surface topology, high surface-area-to-volume ratio, and structural uniformity, which make it a promising candidate for compact and efficient heat exchanger applications. A constant porosity value of 0.6 is considered throughout the simulations to isolate the influence of geometric characteristics based on previous studies. Aluminium is selected as the heat exchanger material due to its high thermal conductivity, allowing direct comparison with previously reported studies. The analysis is performed under transient conditions to evaluate the immediate dynamic thermal response of the structure during the first regenerative operation. For the hot cycle, the inlet fluid temperature and the initial temperature of the heat exchanger are assumed as 298.15 K and 278.15 K, respectively. For the cold cycle, the inlet fluid temperature is specified as 263.15 K. These boundary conditions represent a typical regenerative heat exchange process in which the solid alternately stores and releases thermal energy. The numerical investigation aims to characterize the time-dependent temperature distribution, instantaneous heat storage capacity, and the start-up thermal performance under the defined operating conditions.

INTRODUCTION

In recent years, the integration of triply periodic minimal surface (TPMS) geometries into the architecture of heat exchangers has attracted substantial interest, primarily due to their exceptional surface area-to-volume ratios, uninterrupted flow conduits, and elegant curvatures. These structural attributes facilitate superior thermo-hydraulic capabilities when contrasted with traditional compact heat exchanger configurations. Particularly in decentralized environments characterized by severe spatial constraints, the high degree of compactness inherent in TPMS frameworks presents a revolutionary opportunity for downscaled thermal management. As a result, TPMS-based thermal devices have been extensively explored across a diverse range of fields, from compact energy recovery systems to high-performance electronic cooling solutions.

The bulk of existing literature is centred on the numerical characterization of TPMS topologies, where observed performance gains are typically credited to intensified convective heat transfer mechanisms. These include local flow acceleration, the continuous stripping of thermal boundary layers, and the development of intricate vortex structures within the complex geometric matrix. To mitigate the computational overhead while upholding the fidelity of the architecture, researchers frequently employ a porous media modeling strategy. This approach facilitates macro-scale simulations while effectively capturing the fundamental fluid flow and heat exchange characteristics. Within this context, Genç and Karadeniz (2024) investigated a gyroid-type TPMS structure under low Reynolds number regimes, concluding that thermal efficacy is profoundly influenced by both the thermophysical properties of the material and the prevailing flow dynamics.

Further investigations have delved into the impact of topological diversity and geometric modification. Beer and Rybár (2024) conducted a comparative analysis of various gyroid-based layouts, demonstrating that specialized TPMS variants can augment heat transfer rates while maintaining hydraulic resistance at manageable levels. In a similar vein, Yanagihara et al. (2025) utilized a Darcy–Forchheimer-informed porous media model to report efficiency improvements of approximately 28% through rigorous structural optimization. Furthermore, Ohtani et al. (2025) highlighted the potential of functionally graded designs, showing that non-uniform wall thickness distributions in gyroid structures can significantly enhance the overall performance evaluation criterion (PEC).

Despite these clear benefits, the implementation of TPMS geometries is often hampered by substantial pressure drop penalties. Comparative assessments, such as those by Raza (2025), indicate that while TPMS-based exchangers can outperform conventional fin-and-tube systems in terms of heat transfer, this enhancement is almost invariably coupled with increased hydraulic losses. In fan-assisted ventilation systems, such resistance is a pivotal design constraint that directly affects power consumption and acoustic quality; thus, the equilibrium between thermal gain and pressure loss remains a subject of critical inquiry.

While the literature regarding TPMS heat exchangers is vast, studies dedicated specifically to air-side performance are notably scarce. Air, characterized by its low density and minimal thermal capacity, demonstrates thermo-hydraulic patterns that differ significantly from those of liquids, necessitating specialized investigation. Research by Saghir et al. (2025) and Kilic et al. (2025) has confirmed that TPMS architectures can catalyze heat transfer in air-flow conditions; however, the pressure gradient remains a primary bottleneck, particularly in the low Reynolds number regimes typical of HVAC operations.

Concurrently, decentralized heat recovery ventilation (HRV) systems have been the subject of intensive study within the building science sector. These systems generally utilize honeycomb or ceramic thermal storage matrices and operate under cyclic flow reversal (push–pull) protocols. The naturally symmetrical and streamlined flow channels of specific TPMS topologies make them excellent candidates for such bi-directional flow environments. Experimental work by Pekdoğan et al. (2020, 2021) has documented heat recovery efficiencies between 60% and 80%, while Galiszewska et al. (2023) showed that integrating phase-change materials could further amplify these gains.

Notwithstanding the wealth of independent research on TPMS geometries and decentralized ventilation, the intersection of these two domains remains largely unexplored. Most available studies prioritize multi-cycle operations to determine quasi-steady state efficiencies. However, the initial transient response occurring during the very first flow-reversal cycle—which dictates the thermal inertia and start-up dynamics of the unit—has not been thoroughly investigated. Understanding this first-cycle behavior is essential, as it illuminates the immediate thermal penetration and energy exchange between the fluid and the solid matrix before the system reaches periodic equilibrium.

Consequently, the present work offers a first-of-its-kind numerical investigation into the single-cycle transient thermal response of a TPMS-based heat exchanger. The analysis is specifically designed to isolate the initial charging and discharging phases under low Reynolds number air-side conditions. by examining the instantaneous heat storage capacity and thermal lag during the debut cycle, this research seeks to provide fresh perspectives on the viability of TPMS cores for decentralized HVAC applications. In contrast to earlier studies that rely on periodic boundary conditions, this investigation employs a configuration that mirrors actual ventilation start-up sequences, allowing for a more precise evaluation of the dynamic thermal performance of TPMS-based recuperators.

MATERIAL AND METHOD

The heat exchanger geometries used in the simulations are generated by modifying a code developed in the Mathematica program. Since honeycomb heat exchangers employed in mono unit systems typically have a cylindrical form, this characteristic is also incorporated into the TPMS geometry design. Therefore, in Figure 1, gyroid geometry at 0.6 porosity is shown.

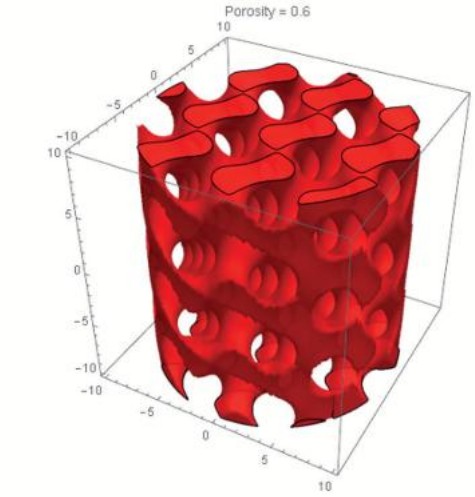


Figure 1. Cylindrical gyroid geometry at 0.6 porosity which is created by Mathematica

The transient 3D numerical model is developed by ANSYS CFX for heat transfer and fluid flow. However, instead of analysing the entire system, a representative volume element (RVE) or a repeating unit cell can be analysed. An RVE is a material volume whose effective behaviour represents the behaviour of the material as a whole. The RVE is shown in Figure 2. This approach is used for all geometries used in the analysis. In this case, system dimensions have been shown in Table 1.

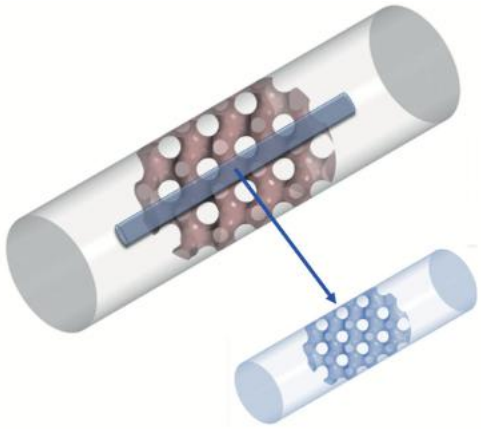


Figure 2. Representative volume element (RVE) (Genc 2024)

The geometrical configuration of the computational domain and boundary conditions are shown in Figure 3.7. Analyses are carried out for 0.1 m/s, which correspond to 19.12 Reynolds number for pore diameter at laminar flow. This value is corresponded to 96 for channel diameter. As the boundary condition in the analysis, the outer surfaces of the fluid and solid domains are defined as adiabatic walls. The inlet temperatures of the fluid to the system are assumed to be 298.15 K and 268.15 K for hot flow and cold flow, respectively. Where the initial temperature of the heat exchanger is assumed to be 278.15 K (Table 2).

Table 1. RVE System dimensions.

System Properties	
Diameter	15 (mm)
Inlet Length	20 (mm)
HEX Length	20 (mm)
Outlet Length	20 (mm)

When choosing these temperatures, the change in the heat capacity of a certain mass over time is considered. Here, indoor, and outdoor temperatures used in ventilation systems are taken as the basis. It is envisaged to be used effectively in heat processes such as heat recovery. Aluminium, ceramic, and PLA are chosen as heat exchanger materials to compare the differences in thermal properties. The thermophysical properties of the materials are given in Table 3. The thermophysical properties of air at 298.15 K are used for the fluid. Natural convection effects have been neglected.

Table 2. CFD and heat transfer model boundary conditions.

Boundary Conditions	
Thot flow,initial	298.15 (K)
THEX,initial	278.15 (K)
Tcold flow,initial	263.15 (K)
Vinlet	0.1 (m/s)
Outlet	$\Delta P = 0$
Outer surface of fluid domain	Adiabatic
Outer surface of solid domain	Adiabatic
Wall influence	Free-slip wall

Geometrical configuration of the computational domain and boundary conditions is shown in Figure 4.

Table 3. Thermophysical properties of heat exchanger materials

Material	**k (W/mK)**	**c_p (J/kgK)**	**ρ (kg/m^3)**	**α (m^2/s)**	**ρ^*c_p (J/m3K)**
Aluminium	237.00	903.00	2700.00	9.71E-05	2.44E+06

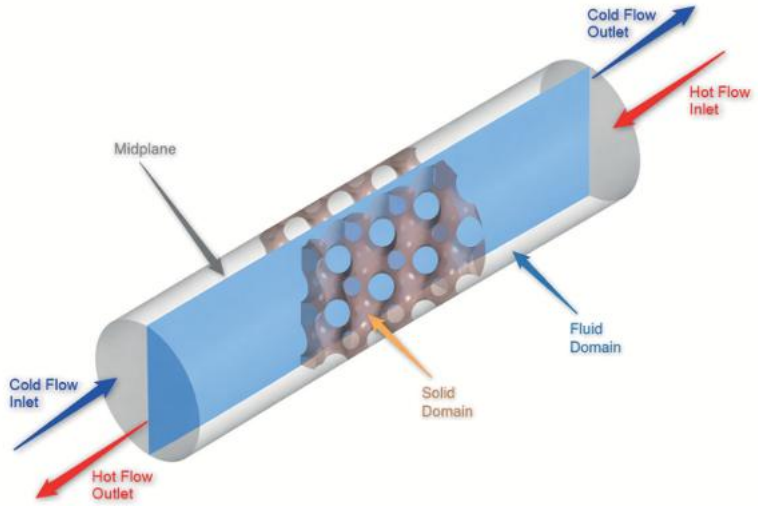


Figure 4. Geometrical configuration of the computational domain and boundary conditions for hot and cold sides.

The Navier-Stokes equations are shown in Equations (1) and (2), respectively. Convergence criteria are set to 10–6 for all the governing equations. The Shear Stress Transport (SST) turbulence model is used to understand the developed vortexes along the heat exchanger. SST model is prepared by Menter for some missing points of k- ω model. Menter improved the spurious free-stream sensitivity of k- ω model. Two region formularization which utilize k- ω model close wall, k- ε is used for the other part of flow are also improved. A high-resolution scheme is used to solve advection terms. For the transient scheme Second Order Backward Euler is used.

$$\frac{\partial \rho}{\partial t} + \vec{\nabla}.(\rho \vec{V}) = 0 \quad (1)$$

$$\rho \frac{\partial V}{\partial t} = -\vec{\nabla} P + \rho \vec{g} + \mu \nabla^2 \vec{V} \quad (2)$$

$$\rho c_p \left[\frac{\partial T}{\partial t} + (\vec{\nabla}.\vec{V})T\right] = k\vec{\nabla}^2 T + \phi \quad (3)$$

Mesh independency analysis is conducted for four different mesh element numbers (M1 = 2371748, M2 = 3557621, M3 = 5352423 and M4 = 8884799) that are shown in Figure 3.9. Heat rate values, which are critical parameters for the comparison of numerical data, are calculated using M1, M2, M3, and M4 to evaluate mesh independence (Figure 5). According to Figure 5, all meshes are matched up with each other. To evaluate temperature and velocity distributions at higher resolution with reduced computational costs, M2 is chosen. In here, fluid -solid interface element size 0.15 mm, fluid body element size 0.3 mm, solid-fluid interface 0.4 mm, solid body element size. It is determined as 0.8 mm. In places where the element size is small, more frequent mesh is generated. This allows the areas with frequent mesh to be analysed better. The grid quality is ensured with Skewness to be less than 0.8 for all meshes.

In addition, time-step independency is also carried out for 0.05, 0.1, 0.2, 0.4 and 0.5 s. Figure 6 shows that 0.2 s is suitable for obtaining an accurate solution due to the occurring deviation for the first 5 s at 0.4 and 0.5 s time steps. It is clear that the variation of the total number mesh and/or time step size did not cause any remarkable changes in the time-dependent variation of the heat rate. The maximum deviation between the M1 and the M4 mesh is found to be less than 0.1%. Besides, regarding the time-step size, the maximum difference is obtained as 0.1%. Consequently, the preliminary survey ensures that the results are independent of the mesh number and the time-step size.

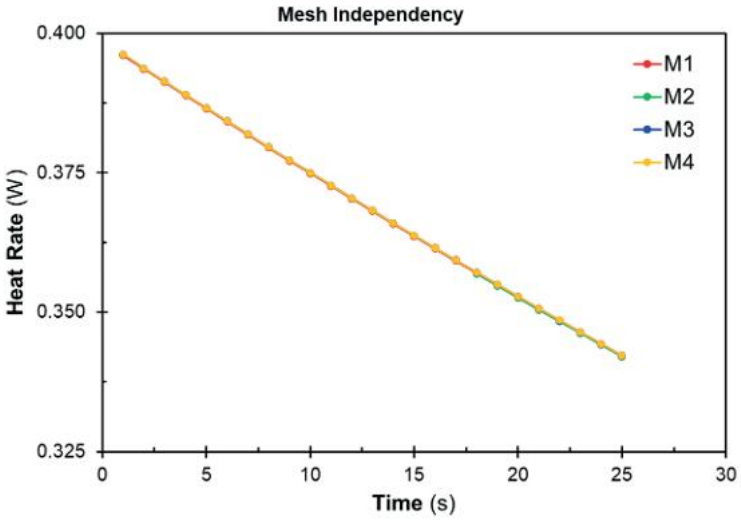


Figure 5. Mesh independency analysis.

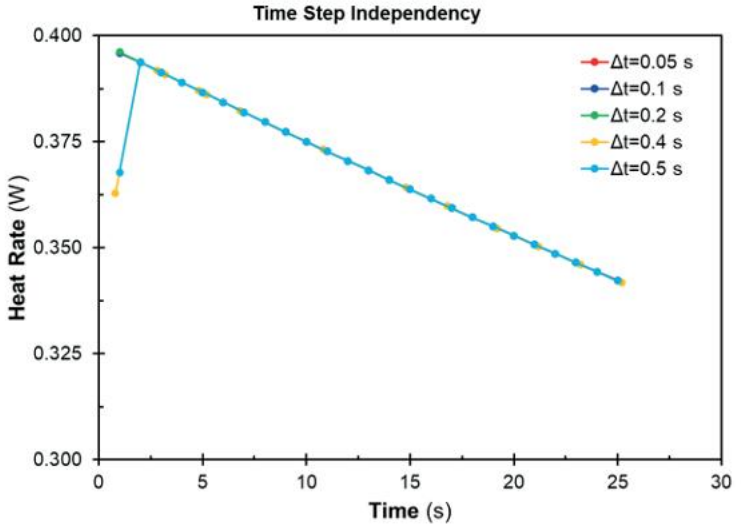


Figure 6. Time step independency

RESULT AND DISCUSSIONS

The single-cycle transient thermal response of a TPMS-based heat exchanger is numerically investigated for the first time. The analysis focuses on isolating the initial charging and discharging phases under low Reynolds number air flow conditions.

In the hot flow (Figure 7), the fluid enters the domain at 298.15 K, creating a 20 K temperature gradient relative to the initial state of the solid matrix. The contours reveal a thermal distribution within the Gyroid architecture, where the continuous curvature effectively disrupts the air-side thermal boundary layer even at a low inlet velocity of 0.1 m/s. Despite the high thermal conductivity of the Aluminium struts, the solid-phase temperature only reaches approximately 282 K by the end of the first 25-second cycle. This indicates that a significant portion of the inlet thermal energy is consumed by the thermal inertia of the matrix to overcome its initial cold state (278.15 K), which explains the relatively lower efficiency of the first cycle compared to stabilized periodic operations.

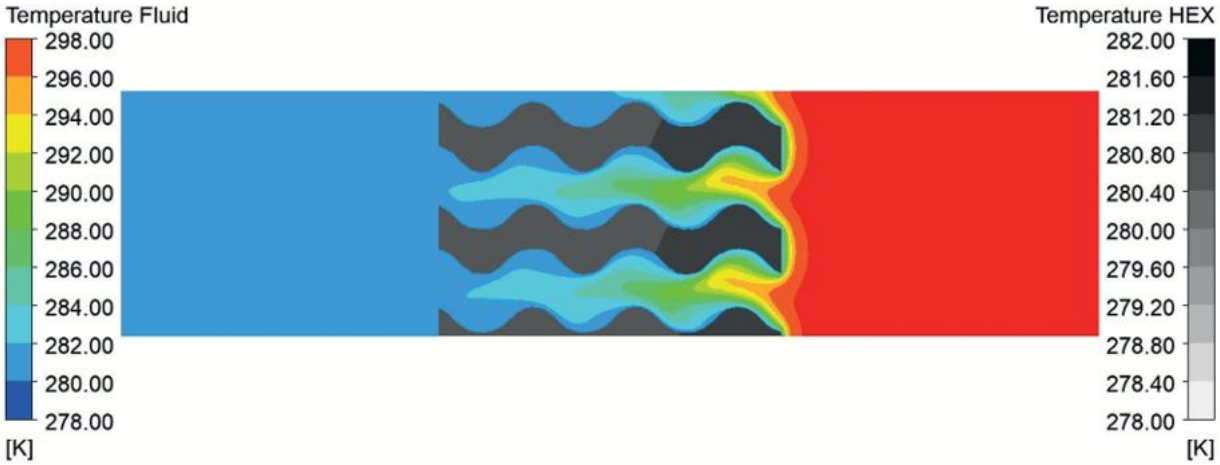


Figure 7. Temperature profiles of the fluid and the regenerative heat exchanger core during the hot flow phase.

During the cold flow (Figure 8), the flow reversal introduces cold outdoor air at 263.15 K into the pre-heated core. The temperature contours illustrate an efficient energy release mechanism, where the cold air is rapidly warmed as it passes through the Gyroid channels, reaching significantly higher temperatures at the outlet. The HEX temperature scale shows a decrease toward 276 K, demonstrating that the stored sensible heat is effectively transferred to the supply air. The inherent symmetry and non-tortuous pathways of the Gyroid topology facilitate this bi-directional heat exchange with minimal stagnant zones, ensuring that the 25-second switching duration provides sufficient time for the matrix to act as a functional thermal reservoir without reaching premature thermal saturation.

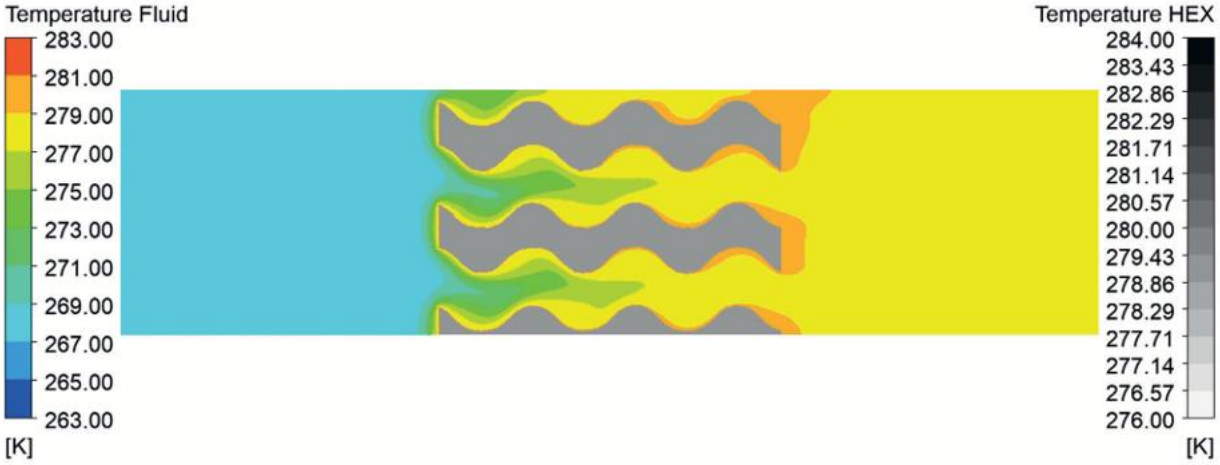


Figure 8. Temperature profiles of the fluid and the regenerative heat exchanger core during the hot flow phase.

CONCLUSION

In this study, the single-cycle transient thermal response of a Gyroid-based TPMS heat exchanger was numerically investigated to characterize its initial charging and discharging behavior. Unlike multi-cycle steady-state analyses, this research isolates the immediate fluid-structure interaction during the first 50 seconds of operation. The following conclusions are drawn:

The Gyroid matrix exhibits a rapid temperature response during the first 25-second charging phase. Due to the high thermal conductivity of the Aluminium struts, the internal temperature of the solid phase closely follows the surface temperature, indicating a low-Biot-number regime that facilitates uniform volumetric heating.

The continuous curvature of the Gyroid topology effectively prevents the development of a stable thermal boundary layer. Even at a low inlet velocity of 0.1 m/s, the geometry promotes passive mixing (chaotic advection), which significantly enhances the heat transfer rate between the 298.15 K hot air and the 278.15 K solid matrix.

During the first charging cycle, a significant portion of the inlet thermal energy is absorbed to overcome the thermal inertia of the matrix. The temperature contours confirm that the Gyroid architecture allows for deep thermal penetration, ensuring that the core acts as an effective heat sink before the flow reversal occurs.

Upon flow reversal, the pre-heated Gyroid core successfully transfers its stored sensible heat to the 263.15 K cold inlet air. The rapid warming of the supply air during this phase demonstrates the structure's high instantaneous heat exchange effectiveness, even in the absence of cyclic stabilization.

This fundamental single-cycle characterization provides the necessary baseline for evaluating the initial thermal response of TPMS-based cores. However, to fully understand the long-term operational performance, future research will focus on:

Future studies will investigate a significantly higher number of flow-reversal cycles to determine the point of cyclic stability. Reaching a quasi-steady state is essential to accurately calculate the stabilized heat recovery efficiency and to observe how the mean matrix temperature shifts over time.

By analysing multiple successive cycles, the optimal duration for the charging and discharging phases can be identified to prevent thermal saturation of the core.

The multi-cycle performance will also be evaluated using technical ceramics to increase volumetric heat storage, alongside the development of low-order numerical models (e.g., in MATLAB) for rapid parametric optimization across thousands of operational scenarios.

REFERENCES

- Genç, M. S., & Karadeniz, Z. H. (2024). Investigation of flow and heat transfer performance of gyroid structure as porous media. Isı Bilimi ve Tekniği Dergisi. https://doi.org/10.47480/isibted.1471713
- Beer, M., & Rybár, R. (2024). Optimization of heat exchanger performance using modified gyroid-based TPMS structures. Applied Thermal Engineering. Advance online publication.
- Yanagihara, T., et al. (2025). Porous media modeling and optimization of triply periodic minimal surface heat exchangers. arXiv. https://arxiv.org/abs/2512.10207
- Ohtani, K., et al. (2025). Optimization of wall thickness distribution in gyroid TPMS heat exchangers using homogenization-based modeling. arXiv. https://arxiv.org/abs/2510.10622
- Raza, F. (2025). Performance evaluation of gyroid lattice heat exchangers compared to conventional fin-tube systems (Master's thesis). LUT University.
- Saghir, M. Z., et al. (2025). Experimental and numerical investigation of gyroid TPMS-based heat sink and heat exchanger systems. Processes, 13(6), 1786. https://doi.org/10.3390/pr13061786
- Kilic, M., et al. (2025). Thermal performance analysis of TPMS-based heat exchangers under turbulent flow conditions. Applied Sciences, 15(8), 4140. https://doi.org/10.3390/app15084140
- Pekdoğan, T., et al. (2020). Experimental investigation of a decentralized heat recovery ventilation system. Energy and Buildings.
- Pekdoğan, T., et al. (2021). Performance analysis of a push–pull type decentralized ventilation system. Building and Environment.

- Galıśzewska, M., Jóźwik, K., & Nowak, A. (2023). Thermal performance enhancement of decentralized ventilation systems using phase change materials. Energies, 16(8), 3310. https://doi.org/10.3390/en16083310
- Genç, M. S. (2024). Investigation of triply periodic minimal surface-based heat exchangers for decentralized ventilation systems (Master's thesis). İzmir Kâtip Çelebi University.
- Menter, F. R. (1994). Two-equation eddy-viscosity turbulence models for engineering applications. AIAA journal, 32(8), 1598-1605.

TTMD
Turkish Society of HVAC & Sanitary Engineers
XVII TTMD INTERNATIONAL HVAC&R TECHNOLOGIES SYMPOSIUM
ARTIFICIAL INTELLIGENCE IN BUILDINGS
14-15 MAY 2026

NUMERICAL INVESTIGATION OF THERMAL COMFORT AND AIR QUALITY IN A BUS CABIN EQUIPPED WITH HEAT RECOVERY VENTILATION (HRV) SYSTEM

Alper Mete Genç[1], Begüm Karataş[2] and İbrahim Atmaca[3]
[1]Bosch Thermotechnology, Manisa, Türkiye
[2]Graduate School of Natural and Applied Sciences, Akdeniz University, Antalya, Türkiye
[3]Faculty of Engineering, Mechanical Engineering Department, Akdeniz University, Antalya, Türkiye
Corresponding email: alpermete.genc@tr.bosch.com

SUMMARY

This preliminary study numerically investigates the effects of a Heat Recovery Ventilation (HRV) system on indoor air quality and thermal comfort within a commercial bus cabin. Utilizing Computational Fluid Dynamics (CFD) with a high-resolution k-ε turbulence model, the airflow dynamics, temperature distributions, and Mean Age of Air (MAoA) were analysed for a realistic 3D bus geometry housing 53 occupants. Six different scenarios were simulated, considering indoor temperatures of 22 °C and 25 °C at an outdoor temperature of 5 °C, with HRV efficiencies of 50% and 70%. The results indicate that while the HRV system maintains air velocities within the comfort limits defined by ASHRAE 55 (below 0.24 m/s), heat recovery alone is insufficient to provide optimal thermal comfort in cold climates. High velocity and lower temperatures were specifically observed around the heads of hall-side passengers. The findings suggest that while HRV significantly reduces energy losses, supplemental heating systems are required to ensure a homogeneous and comfortable thermal environment in sustainable public transportation.

INTRODUCTION

Passenger comfort, indoor air quality, and the minimization of transmission risks—especially following the global pandemic that emerged in 2020—have gained significant importance in public transportation. In buses, which are among the most essential and widely used modes of transport, it is necessary to maintain control over cabin temperature and airflow under varying climatic conditions (Genç et al. 2023).

In addition to these considerations, energy efficiency remains a crucial aspect. In an era where countries worldwide are shifting toward sustainable energy sources, the efficient use of existing energy resources has become a necessity rather than a preference. A significant portion of the energy consumed by buses originates from auxiliary systems, among which Heating, Ventilation, and Air Conditioning (HVAC) systems account for the largest share.

To achieve energy savings, it is not feasible to restrict or eliminate ventilation components. Maintaining a specific level of air quality inside the bus is essential for the health and comfort of passengers traveling in an enclosed space. This requirement can only be met by continuously supplying fresh air into the cabin. However, conditioning this fresh outdoor air to match the cabin temperature requires a substantial amount of energy. At this point, Heat Recovery Ventilation (HRV) systems provide an effective solution. These systems transfer heat from the exhaust air leaving the cabin to the incoming fresh air through a heat exchanger. In this way, the fresh air is pre-heated or pre-cooled without additional energy input, thereby minimizing ventilation-related energy losses (Şentürk, 2016).

If air is blown directly onto passengers at high velocity, it creates a "draft" effect, causing localized cooling sensations and discomfort. Conversely, if the air velocity is too low, "dead zones" may form within the cabin where air is not properly renewed, leading to temperature stratification—for example, the head level may be warm while the foot level remains cold. Therefore, when designing a heat recovery system, it is necessary not only to conserve energy but also to distribute air within the cabin in accordance with comfort criteria defined in standards such as ISO 7730 and ASHRAE 55 (Branco, 2024).

At this stage, Computational Fluid Dynamics (CFD) becomes a critical tool. Advances in computational power and decreasing costs have established CFD as a strong alternative or complement to experimental methods in the analysis of indoor air distribution, contaminant transport, and thermal comfort (Nielsen, 2004). Numerical methods solve the Navier–Stokes equations, based on the conservation laws of mass, momentum, and energy, enabling the simulation of airflow within a virtually modelled bus cabin. Through CFD analyses, different vent designs, blowing angles, and flow rates can be tested in a virtual environment. By visualizing airflow paths, temperature contours, and velocity vectors, potential design flaws can be identified before the production stage.

Atmaca et al. (2009) and Zhu et al. (2010) stated that the air speed that will not disturb occupants is approximately 0.2 m/s. Furthermore, Zhu et al. (2010) investigated CO_2 levels relative to passenger density in a numerical and experimental study, concluding that CO_2 levels and the risk of disease transmission increase in the absence of natural or mechanical ventilation. Zhu et al. (2012) examined how different vent sizes and locations affect air velocities and particle distributions, concluding that displacement ventilation (bottom discharge, top suction) at an air velocity of 0.23 m/s is the most suitable method.

Vignesh et al. (2013) examined various bus ventilation methods using CFD and concluded that the interior environment can be improved with properly placed mechanical ventilation systems on the bus ceiling, which was found to increase in-cabin air velocity by 131%. Chaudhry and Elumalai (2020) investigated the effect of school bus ventilation scenarios on in-cabin PM concentration and air exchange rates. Querol et al. (2022) studied the effects of CO_2 levels for different bus sizes and seating arrangements. Accordingly, various studies have been presented to improve ventilation rates, such as the placement of CO_2 sensors that allow the driver to increase ventilation flow according to passenger density.

In a study by Atmaca (2015), it was mentioned that numerous parameters (air speed, ventilation type, CO_2 concentration, temperature, etc.) affect comfort and indoor air quality. An ASHRAE Position Document provided an analysis that can serve as a basis for a 1000 ppm limit; however, there is no explicit statement in ASHRAE Standard 62.1-2022 regarding the acceptance of 1000 ppm as a strict limit. Toksoy and Sofuoğlu (2022) stated that the 1000 ppm value is accepted as a standard in almost every country and recommended it as the current limit. Similarly, Atmaca (2015) accepted 1000 ppm as the limit and stated that supplying fresh air up to 25% of the air conditioner's flow rate would be sufficient.

This preliminary study aims to numerically investigate the effects of a bus HVAC system equipped with heat recovery technology on in-cabin comfort parameters. Within the scope of the study, a realistic three-dimensional bus geometry is modelled and analysed using validated turbulence models. The primary objective is to determine whether the fresh air supplied by the heat recovery unit can create a homogeneous temperature distribution and whether the resulting air velocities pose any risk to passenger comfort. Based on the findings, it is intended to develop optimal air distribution scenarios that preserve energy efficiency while maximizing passenger satisfaction. This study is expected to contribute to the literature by emphasizing the importance of simulation-based engineering in the design of sustainable public transportation.

MATERIAL AND METHOD

In this study, the bus geometry was developed using a commercial CAD software. The dimensions of the vehicle and the occupant capacity were modelled to represent standard commercial buses. The bus has an approximate length of 12.3 m, a width of 2.6 m, and a height of 2.9 m. The model includes a total of 52 passengers and one driver.

The total area for both suction and discharge vents was determined to be 2.35 m^2. The ventilation configuration consists of İwo separate discharge vents located on the right and left sides of the cabin, near the ceiling. The suction vent is designed as a single-piece unit positioned along the centre of the ceiling. The detailed locations of these vents within the bus cabin are illustrated in Figure 1 (Genç et al. 2023).

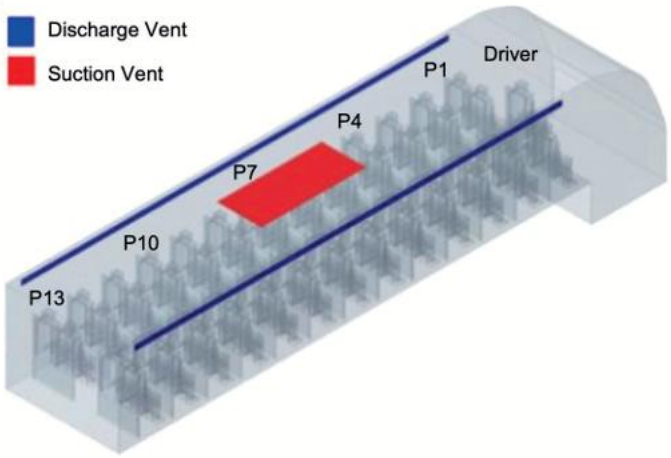


Figure 1. The location of the vents in the bus.

The developed geometry was subsequently imported into commercial CFD software (ANSYS CFX) to establish a 3D steady-state numerical model. The standard k-ε turbulence model, with a turbulence intensity of 5%, was employed for the turbulence closure. A high-resolution scheme was utilized for the discretization of the advection terms to ensure numerical accuracy. The convergence criteria for all governing equations were set to a residual target of 10-6.

To evaluate the temperature, velocity, and mean age of air (MAoA) distributions in detail, spherical air regions were defined around the heads of the driver and all passengers. The regions serve as virtual surfaces within the fluid domain; they do not influence the flow field but facilitate the visualization and calculation of localized air quality and thermal comfort indicators. Consequently, this study presents an alternative and more focused representation of indoor air quality and comfort results within a bus cabin.

The computational domain was discretized using a multi-scale meshing approach. A fine mesh with an element size of 20 mm was applied to the passengers' heads and the volume within the spherical regions, as illustrated in Figure 2. A coarser mesh with an element size of 50 mm was utilized for the passengers' bodies and the remaining parts of the cabin geometry. Additionally, the mesh element size at the discharge and suction sections was refined to 25 mm. The final mesh consists of a total of 6,717,548 elements.

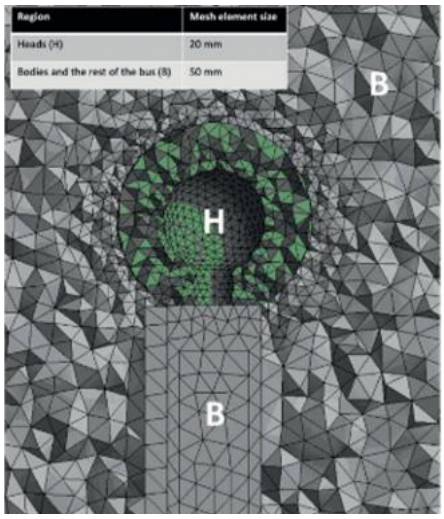


Figure 2. Mesh distribution in the numerical model.

Atmaca (2015) reported that for commercial HVAC systems used in buses, the maximum airflow rate is 6,900 m^3/h at low outdoor temperatures, while the minimum airflow rate is 8,400 m^3/h for high outdoor temperatures. The upper limit for CO_2 concentration in non-industrial environments is specified as 1,000 ppm, and it was concluded that supplying fresh air at 25% of the air conditioner's total airflow rate is sufficient. In the present study, the average of these two airflow rates was utilized, and 25% of this mean value was calculated, resulting in an airflow rate of approximately 1,950 m3/h. Under these conditions, the air velocity at the discharge vents is approximately 0.23 m/s. This value aligns with the findings of Atmaca et al. (2009) and Zhu et al. (2010, 2012), who emphasized that an average air speed of around 0.2 m/s is ideal for providing comfortable indoor conditions without causing occupant discomfort. Temperature is another critical parameter for indoor thermal comfort. According to the literature, the most suitable temperature range for thermal comfort is approximately 21-28°C (Velt and Daanen, 2017; Zhang et al., 2020). Consequently, a heat transfer analysis (thermal energy model) was conducted to evaluate the thermal environment within the bus. The simulations considered indoor temperatures (Tindoor) of 22°C and 25°C, an inlet temperature (Tinlet) of 5°C, and two heat recovery (HRV) efficiencies of 50% and 70%. The remaining boundaries of the geometry, such as the bus walls, were defined as adiabatic. For all simulated cases, the boundary condition at the suction vent was defined as a pressure outlet with a relative static pressure of 0 Pa. The comprehensive set of defined boundary conditions is compiled in Table 1.

Table 1. Boundary Conditions

Scenarios	T_{indoor} (°C)	Inlet			Outlet
		HRV (%)	$T_{in,IGK}$ (°C)	V_{inlet} (m/s)	
1	22°C	-	-	0.23 m/s	ΔP = 0
2	25°C	-	-		
3	22°C	0,5	13,5°C		
4	25°C	0,5	15,0°C		
5	22°C	0,7	16,9°C		
6	25°C	0,7	19,0°C		

The Mean Age of Air (MAoA) is defined by the duration for the air entering the indoor environment from the discharge vent to reach a certain value, and it is also an indicator of the freshness of the air. MAoA is defined as a scalar quantity (φ) in this numerical model, and the transport of the scalar (φ) was calculated with additional convection diffusion equation as given by Eq. 1 (Chanteloup and Mirade, 2009).

$$\frac{\partial(\rho\phi)}{\partial t} = \nabla \cdot (\rho\vec{V}\phi) + S_\phi \quad (1)$$

Here t is the time, ρ is the density, $\vec{V}$ is the average velocity of the moving quantity and $S\phi$ is the source of the scalar term. For steady flow, Eq. 1 can be simplified to Eq. 2.

$$\nabla \cdot (\rho\vec{V}\phi - \rho D\nabla\phi) = S_\phi \quad (2)$$

The source term $S\phi$ is 1 (Chanteloup and Mirade, 2009; Bartak et al., 2002; Gan, 2000). D is the kinematic diffusivity of the scalar magnitude and has two components, laminar and turbulent as given in Eq. 3.

$$D = \frac{\mu}{\sigma_L} + \frac{\mu_T}{\sigma_T} \quad (3)$$

where μ is the viscosity and μ_T is the turbulent viscosity. σ_L and σ_T are laminar and turbulent Schmidt numbers, respectively. Since the fluid is turbulent in this study, the turbulent viscosity will be higher than the laminar viscosity and therefore the laminar component will have a weaker effect than the turbulent component (Chanteloup and Mirade, 2009). For turbulent flows in ANSYS CFX, turbulent diffusion is included by default as a result of averaging the advection term. Therefore, kinematic diffusion is not defined but included in the solution.

RESULTS AND DISCUSSIONS

In this section, the airflow dynamics within a bus cabin equipped with a Heat Recovery Ventilation (HRV) system were analysed using coloured velocity contour maps. Before evaluating the findings, it is important to specify the fundamental boundary conditions applied in the analyses. For all temperature cases examined, the air inlet velocity was kept constant at 0.23 m/s, following the approach adopted by Genç et al. (2023). Additionally, to optimize computational cost in the high-resolution mesh cabin model, the thermophysical properties of air were assumed to be constant at a reference temperature of 25°C (Versteeg, 2007). Under these assumptions, the resulting velocity distribution contours are presented sequentially.

One of the most critical factors in evaluating the performance of cabin HVAC systems is the local velocity effect of the conditioned air on passengers. Studies in the literature indicate that the head and neck regions of the human body are the most thermally sensitive areas to airflow (draft) (Fanger, 1988). For this reason, Figure 3 presents a three-dimensional contour map showing the air velocity (m/s) distribution over spherical surfaces representing the head and shoulder regions of the passengers.

In this study, the inlet velocity was kept constant for all temperature conditions according to the previous study of authors. In the analyses, the thermophysical properties of air were assumed to be constant as 25°C due to the computational costs. Thus, the change of temperature did not affect the velocity distribution on the spherical air regions (Figure 3) and velocity streamlines inside the bus (Figure 4). Locating the suction vent at the upper centre of the bus results in higher velocity values on the spherical air regions of the passengers sitting at the hall-side as approximately 0.2 m/s. However, the velocity reached 0.05 m/s for the passengers sitting at the window-side. The airflow was directed to the suction vent with a narrow area, and this resulted in higher velocity values.

For seated occupants, the maximum allowable air velocity limits that do not cause local draft discomfort in indoor environments are defined by various international standards. According to the ASHRAE 55 standard, in

moderate thermal environments, the air velocity should not exceed 0.25 m/s in order to prevent draft discomfort.

Based on the CFD results obtained, it was determined that the maximum local surface velocity inside the bus remained around 0.24 m/s and did not exceed the reference limit value. This indicates that the designed HRV system provides ventilation within safe limits without causing thermal discomfort such as cold drafts for the passengers (Khatoon, 2020).

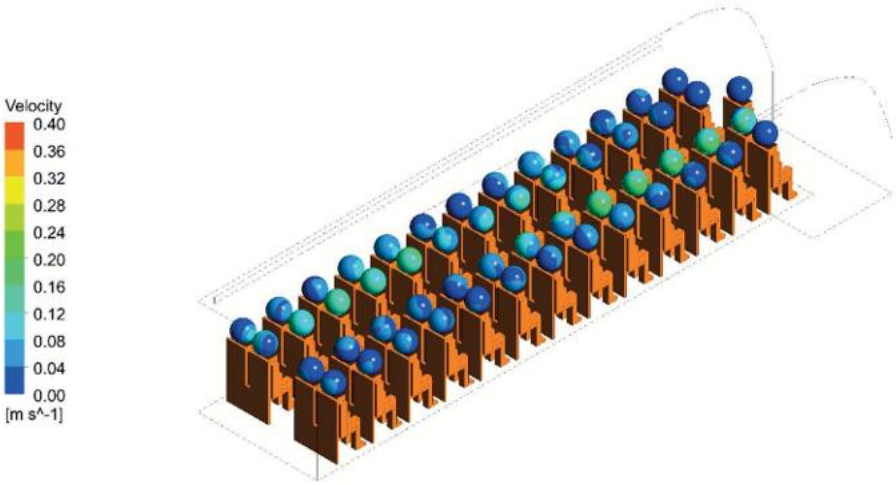


Figure 3. Velocity distributions on spherical air regions

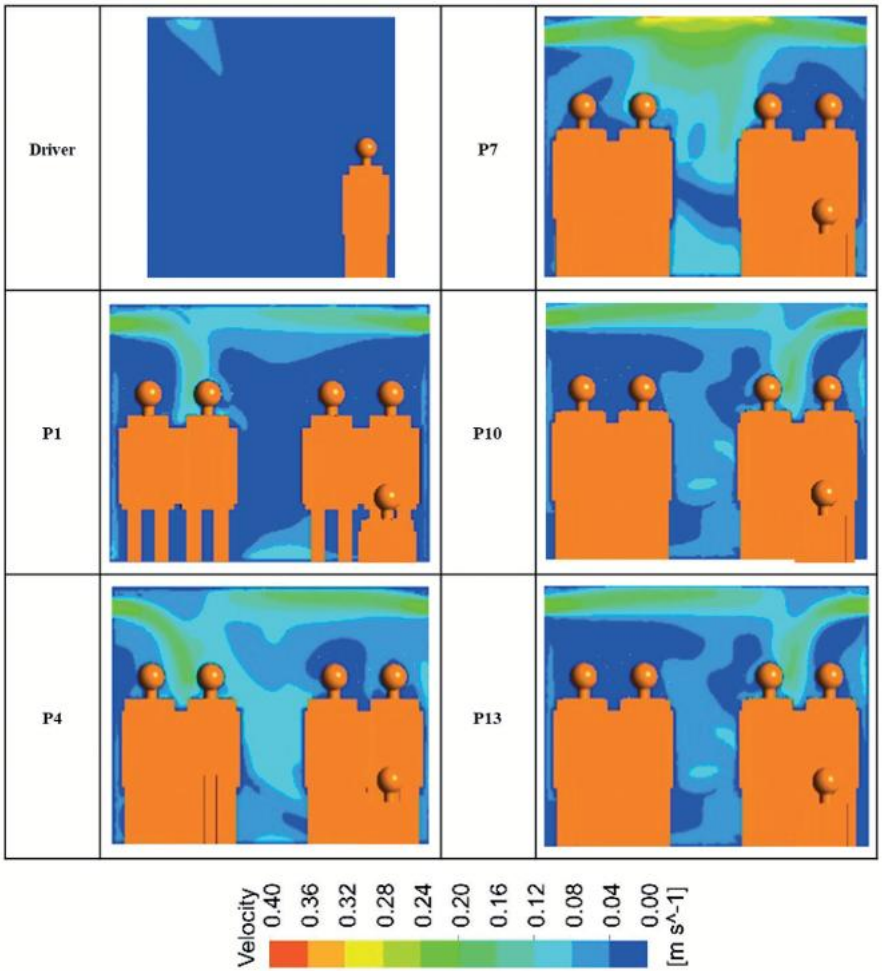


Figure 4. Velocity distributions on selected rows in the bus

The numerical results of the velocity distribution across various cross-sections (Driver, P1–P13) provide a detailed understanding of the airflow dynamics within the bus cabin (Figure 4). The velocity contours illustrate that the conditioned air exiting the discharge vents follows the ceiling profile before descending into the occupant zone, distribute air without direct impingement. In all passenger rows, a clear disparity is observed between seating positions; while hall-side occupants are exposed to moderate air velocities ranging from 0.16 to 0.24 m/s, window-side occupants remain in lower-velocity zones below 0.12 m/s. Crucially, the maximum local air velocity at the head level of all occupants does not exceed 0.24 m/s, which strictly adheres to the ASHRAE 55 and ISO 7730 draft risk limit of 0.25 m/s. This confirms that the HRV system's discharge velocity of 0.23 m/s is successfully optimized to ensure adequate air renewal while maintaining high thermal comfort by preventing localized cooling sensations or 'draft' effects.

The mean age of air is directly related to air velocity, and thus it was not affected by temperature differences like velocity distribution. In Figure 5, higher age of air values was observed at points away from the suction vent where air velocities were lower, which were the driver and the rows behind the driver as 500 s. This shows that the airflow remained unchanged in these regions because the suction vent was only located in the middle of the ceiling of the bus. As mentioned in Figures 3 and 4, since the change of the thermophysical properties with temperature was neglected, there were no changes observed for all cases in Figure 5.

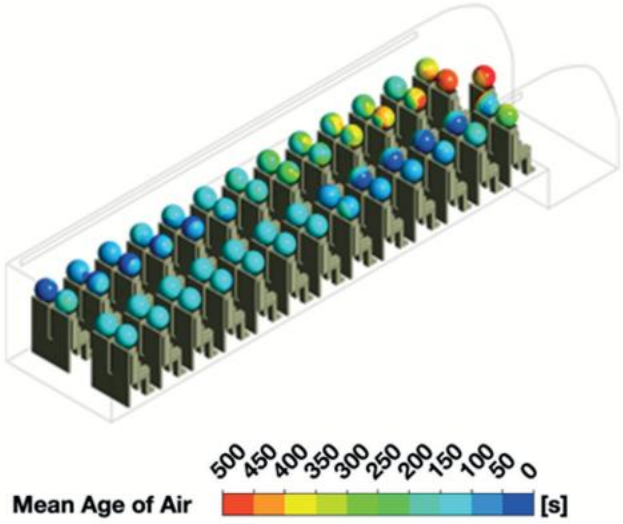


Figure 5. Mean age of air distributions on spherical air regions

Figure 6 shows the temperature distributions on the spherical air regions. For the Scenarios 1 and 2 (without HRV), the indoor temperature drops to 6°C, especially for the passengers sitting on the hall-side. Considering that the air entering the indoor environment at low temperatures affects thermal comfort, it is seen that providing the airflow by heat recovery or pre-heating plays an important role. For the

When the indoor temperature is 22 °C, using a system with 50% heat recovery efficiency increases the inlet temperature from 5 °C to 13.5 °C. This raises the air temperature around the heads of passengers, especially those sitting on the hall side, to 16 degrees Celsius. In Scenario 4, the indoor temperature is assumed to be 25 °C compared to Scenario 3, and the air temperature around the heads of passengers rises to 18 °C. However, this does not provide adequate thermal comfort. In Scenarios 5 and 6, the heat recovery efficiency is increased to 70%, resulting in inlet temperatures of 16.9 and 19 °C, respectively. While the air temperature around their

heads reaches approximately 20 °C in Scenario 5, this value is around 22 °C in Scenario 6, especially for passengers near the exit vent and those sitting on the hall side. Based on the results, it is observed that a 70% heat recovery efficiency is low at an outdoor temperature of 5 °C, and that the indoor inlet temperature should be increased with a higher heat recovery efficiency or using a pre-heater.

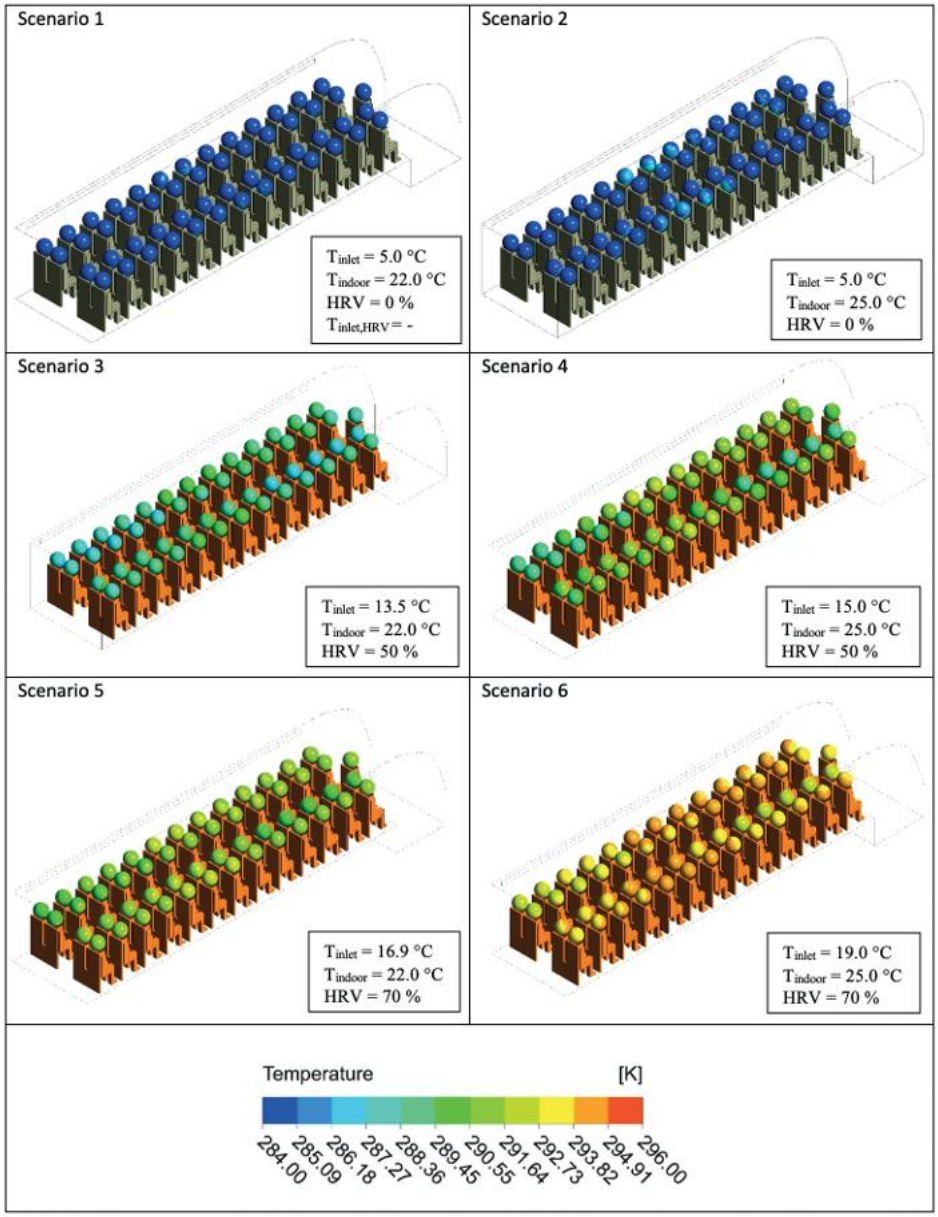


Figure 6. Temperature distributions on spherical air regions

CONCLUSION

In this study, the impact of a heat recovery-integrated HVAC system on the thermal comfort and air freshness of a bus cabin was evaluated through steady-state CFD simulations. The following key conclusions were drawn:

- The maximum local air velocity remained around 0.24 m/s, complying with the ASHRAE 55 "no-draft" limit of 0.25 m/s. This confirms that the designed HRV system does not cause localized cooling discomfort due to high-velocity air.

- The Mean Age of Air (MAoA) analysis revealed that the central suction vent configuration provides effective air renewal in the middle of the cabin, though higher MAoA values (up to 500 s) were observed near the driver and rear sections, suggesting a need for more distributed suction points.
- Increasing HRV efficiency from 50% to 70% significantly improved the supply air temperature. However, at an outdoor temperature of 5 °C, the air temperature around passengers—particularly those on the hall-side—remained below the desired 21-28 °C comfort range.
- To achieve ideal thermal comfort in winter conditions, it is concluded that HRV systems should be supported by **auxiliary heating units (e.g., PTC heaters)**. Furthermore, the implementation of high-performance heat exchanger geometries, such as **Triply Periodic Minimal Surfaces (TPMS)** (Genc and Karadeniz 2024), is recommended to maximize efficiency and achieve a more homogeneous temperature distribution without increasing the system's footprint.

Overall, this study demonstrates that simulation-based engineering is a vital tool for optimizing energy-efficient ventilation strategies in public transport, balancing the trade-off between energy savings and passenger satisfaction.

REFERENCES

- ANSYS, Inc. (2017), "ANSYS Fluent User's Guide, Release 18.2", Equation (6.58).
- ANSYS, Inc. (2017), "ANSYS Fluent User's Guide, Release 18.2", Equation (6.59).
- ASHRAE. (2020). ANSI/ASHRAE Standard 55-2020: Thermal Environmental Conditions for Human Occupancy. American Society of Heating, Refrigerating and Air-Conditioning Engineers.
- ASHRAE Position Document on Indoor Carbon Dioxide". February 2, 2022, February 2, 2022, Expires February 2, 2025.
- Atmaca, İ. (2015). Şehirlerarası Otobüslerde Havalandırma ve İç Hava Kalitesi. 12. Ulusal Tesisat Mühendisliği Kongresi Bildiriler Kitabı
- Atmaca, İ., Demirezen, A., & Çağlar, A. (2025). Energy-efficient heat exchanger design for indoor air quality in intercity buses. Energy Sources, Part A: Recovery, Utilization and Environmental Effects, 47(1), 5207–5224. https://doi.org/10.1080/15567036.2021.1891158
- Bartak, M., Beausoleil-Morrison, I., Clarke, J. A., Denev, J., Drkal, F., Lain, M., ... & Stankov, P., 2002, Integrating CFD and building simulation, Building and Environment, 37(8-9), 865-871.
- Branco, P. T. B. S., Pinto, A. J. S., & Sousa, S. I. V. (2024). Characterising indoor air quality in private vehicle cabins under unprecedented traffic conditions during COVID-19 lockdown. Building and Environment, 262. https://doi.org/10.1016/j.buildenv.2024.111797
- Chaudhry, S. K., & Elumalai, S. P. (2020). The influence of school bus ventilation scenarios over in-cabin PM number concentration and air exchange rates. Atmospheric Pollution Research, 11(8), 1396-1407.
- Chanteloup, V., & Mırade, P. S., 2009, Computational fluid dynamics (CFD) modelling of local mean age of air distribution in forced-ventilation food plants, Journal of Food Engineering, 90(1), 90-103.
- Gan, G., 2000, Effective depth of fresh air distribution in rooms with single-sided natural ventilation, Energy and buildings, 31(1), 65-73.
- Genç A. M., Atmaca İ. & Karadeniz Z.H., 2023, Şehirlerarasi Otobüslerde Menfez Konumlarının Kabin İçi Hava Dağılımı Üzerine Etkisinin İncelenmesi, 15. Ulusal Tesisat Mühendisliği Kongresi, İzmir, 1-8.

- Genç, A. M., Çobanoğlu, N., Atmaca, İ., & Haktan Karadeniz, Z. (2023). The Effect Of Temperature And Aır Velocıty Insıde The Bus Cabın On Passengers.
- Genc, A. M., & Karadeniz, Z. H. (2024). Investigation of Flow and Heat Transfer Performance of Gyroid Structure as Porous Media. Isı Bilimi ve Tekniği Dergisi, 44(2), 351-358.
- Khatoon, S., & Kim, M. H. (2020). Thermal comfort in the passenger compartment of vehicles: A review. Renewable and Sustainable Energy Reviews, 121, 109703.
- Patankar, S. V. (1980). Calculation of the flow field. Numerical heat transfer and fluid flow içinde. Hemisphere Publishing Corporation.
- Şentürk, U., Aktakka, S., Toksoy, M. (2016). Havalandırmada Enerji Geri Kazanımı: Araştırma Ve Geliştirme.
- TOKSOY, M., & SOFUOĞLU (2022), S. C. KARBONDİOKSİT ve SINIFLAR.
- Querol, X., Alastuey, A., Moreno, N., Minguillón, M. C., Moreno, T., Karanasiou, A., ... & Felisi, J. M. (2022). How can ventilation be improved on public transportation buses? Insights from CO2 measurements. Environmental research, 205, 112451.
- Versteeg, H. K., & Malalasekera, W. (2007). An introduction to computational fluid dynamics: the finite volume method. Pearson education.
- Vignesh, S., & Sachin, P. (2013). Evaluation of Bus Ventilation Methods Using CFD (No. 2013-26-0043). SAE Technical Paper.
- Zhu, S., Srebric, J., Spengler, J. D., & Demokritou, P. (2012). An advanced numerical model for the assessment of airborne transmission of influenza in bus microenvironments. Building and Environment, 47(1), 67–75. https://doi.org/10.1016/j.buildenv.2011.05.003
- Zhu, S., Srebric, J., Spengler, J. D., & Demokritou, P. (2012). An advanced numerical model for the assessment of airborne transmission of influenza in bus microenvironments. Building and Environment, 47(1), 67–75. https://doi.org/10.1016/j.buildenv.2011.05.003

TTMD
Turkish Society of HVAC & Sanitary Engineers
XVII TTMD INTERNATIONAL HVAC&R TECHNOLOGIES SYMPOSIUM
ARTIFICIAL INTELLIGENCE IN BUILDINGS
14-15 MAY 2026

A Case Study on AI-Driven, Sensor-Free HVAC Control for Energy Efficiency in Large-Scale Commercial Buildings

Bahadır Karaca[1] and Onur Behzat Tokdemir[2]
[1]General Manager, Nesil Teknik Engineering, Istanbul, Türkiye
bahadir.karaca@yahoo.com
[2]Istanbul Technical University, Department of Civil Engineering, Istanbul, Türkiye
otokdemir@itu.edu.tr

ABSTRACT

Buildings account for approximately 40% of global energy consumption, and heating, ventilation, and air conditioning (HVAC) systems represent a substantial share of building energy use. This paper provides a focused conference adaptation of the AI-based occupant-centric HVAC control framework previously developed by Yayla et al. (2022), to which both present authors contributed. The framework replaces real-time occupancy detection with day-ahead hourly occupancy predictions generated by an Artificial Neural Network (ANN) from historical, environmental, and calendar-related inputs. A two-year dataset from a shopping mall in Istanbul was used to develop the model and evaluate four HVAC control scenarios in IDA Indoor Climate and Energy (IDA-ICE). The preferred ANN configuration achieved a Mean Absolute Percentage Error (MAPE) of 13.23% and an R^2 of 0.776; prediction accuracy for a held-out national holiday was approximately 87%. The reported simulations showed that the AI-based scenarios reduced energy consumption by at least 10% relative to traditional sensor-based control and by at least 35% relative to continuous full-power operation, with savings approaching 20% and 40%, respectively, under hotter conditions. Thermal comfort was also maintained more consistently because the control strategy anticipated changes in occupancy rather than reacting after they occurred.

Keywords: AI-based HVAC control; sensor-free occupancy prediction; artificial neural network; energy efficiency; commercial buildings; occupant-centric control

1. INTRODUCTION

Buildings are among the most energy-intensive sectors of the global economy. The built environment accounts for approximately 40% of global energy consumption, while HVAC systems are responsible for roughly 40% of building energy use (IEA, 2019; Yang et al., 2014). In large commercial buildings such as shopping malls, energy management is further complicated by rapidly changing and difficult-to-predict occupancy patterns.

Traditional HVAC controllers generally rely on fixed schedules or feedback from temperature, humidity, CO_2, and occupancy sensors. Such systems are inherently reactive: environmental effects caused by a sudden increase in occupants must first develop and then be detected before corrective action begins. Motion-based sensors can also undercount stationary occupants, while CO_2-based estimates respond gradually and may lag behind rapid population changes in large spaces (Erickson & Cerpa, 2010; Yayla et al., 2022).

Occupant-centric and predictive control strategies seek to overcome these limitations by anticipating demand. User-interactive control, machine-learning prediction, and deep reinforcement learning have demonstrated potential to reduce HVAC energy use while preserving comfort (Lee et al., 2020; Liu et al., 2021; Du et al., 2021). Nevertheless, many proposed approaches still depend on real-time occupancy sensing, which introduces installation, calibration, maintenance, privacy, and reliability constraints.

This paper presents a focused adaptation of the previously published framework by Yayla et al. (2022). It concentrates on the ANN-based occupancy prediction component and its integration with a sensor-free cooling schedule. The method is evaluated using a two-year shopping-mall dataset and IDA-ICE simulations that compare continuous full-power operation, conventional sensor-based control, AI-based control, and AI-based control with pre-cooling.

2. LITERATURE REVIEW

A focused overview of the literature identifies three closely related research areas: occupant-centric HVAC operation, machine-learning-based occupancy prediction, and predictive control that combines occupancy and weather information.

2.1 Occupant-Centric Control Systems

Occupant-centric HVAC control aims to align building operation with actual demand rather than relying solely on fixed schedules. Lee et al. (2020) developed a less intrusive feedback-request strategy for human-centered HVAC operation, while Liu et al. (2021) demonstrated an interactive thermal-control system that balanced occupant satisfaction and energy performance. Du et al. (2021) further showed the potential of deep reinforcement learning for multi-zone HVAC control.

Occupancy-responsive scheduling has also produced substantial savings in earlier studies. Erickson et al. (2009) reported approximately 14% HVAC energy savings using occupancy information. Capozzoli et al. (2017) achieved a similar reduction by learning occupancy patterns and adapting HVAC schedules, while Peng et al. (2018) reported savings of up to 52% for occupancy-prediction-based cooling control in office buildings.

2.2 AI and Machine Learning for Occupancy Prediction

Machine-learning methods can estimate or predict occupancy from visual, environmental, temporal, and behavioral inputs. Tien et al. (2022) demonstrated improved performance for vision-based occupancy detection, whereas the present framework uses camera counts only as historical ground-truth data during model development and does not require real-time camera input during control.

Weather information is also important for proactive HVAC scheduling. Ignjatović et al. (2022) showed that short-term weather forecasts can support building energy-performance evaluation and control decisions. Combining occupancy forecasts with day-ahead weather information therefore provides a basis for adjusting HVAC operation before internal loads and outdoor conditions produce a measurable comfort deviation.

2.3 Sensor-Free Occupancy-Based Control

Most occupancy-based control studies assume real-time input from cameras, motion detectors, RFID systems, or CO_2 sensors. Yayla et al. (2022) demonstrated an alternative in which historical occupancy patterns, weather conditions, time variables, and social-calendar indicators are used to predict hourly demand in advance. The present conference paper condenses that framework and clarifies the relationship between occupancy prediction, control scheduling, and energy-simulation results.

3. METHODOLOGY

3.1 Case Study Building and Dataset

The study used two years of occupancy and environmental data spanning portions of 2017–2019 from a multi-story shopping mall in Istanbul, Türkiye. The building was modeled in Autodesk Revit and imported into IDA-ICE 4.8 in Industry Foundation Classes (IFC) format. The simulation model represented the actual building elements, including insulated light-steel external walls, double low-emissivity glazing, and an insulated standing-seam roof.

Entrance cameras installed for security and visitor counting provided the historical ground-truth occupancy series. The mall operated from 10:00 a.m. to 10:00 p.m.; the ANN dataset therefore used twelve hourly operating intervals per day, represented by time indices 10–21. These camera data were used for model training and validation rather than as a real-time input to the proposed HVAC controller.

3.2 ANN-Based Occupancy Prediction

The ANN used nine inputs: outdoor temperature (°F), relative humidity (%), weather-condition category, day of week, month, day of month, year, time of day, and day type. Day type distinguished normal days, public holidays, the first day of religious holidays, and the remaining days of religious holidays. The model output was the predicted number of visitors for each hourly interval.

The network was implemented with TensorFlow/Keras using the Adam optimizer and rectified linear unit (ReLU) activation. Model development included a 90/10 training-test division and five-fold cross-validation, as reported in the source study. Eight-hidden-layer configurations with 8–64 neurons per layer and 250–1000 training epochs were compared. ANN-1, with 8 neurons per hidden layer and 500 epochs, was selected as the preferred configuration because it provided a favorable balance between prediction performance and processing time. It achieved a MAPE of 13.23% and an R^2 of 0.776.

3.3 HVAC Control Scenarios

Four IDA-ICE scenarios were used to compare control strategies:

S1, Full-Power Baseline: The HVAC system operates continuously at full power with a maximum cooling setpoint of 24°C. This scenario represents the highest-energy reference case.

S2, Traditional Sensor-Based Control: HVAC operation responds to temperature measurements and occupancy information represented by CO_2 sensing. Thermostat deadband and sensor-response delay can produce wider indoor-temperature fluctuations during rapid occupancy changes.

S3, AI-Based Occupancy-Predictive Control: The control schedule is generated from ANN-predicted occupancy and day-ahead weather information. No real-time occupancy detector is required for the simulated control logic. In a practical installation, existing comfort and indoor-air-quality sensors may remain available as safety or override inputs, although those overrides were not used in the sensor-free simulations.

S4, AI-Based Control with Pre-Cooling: S4 extends S3 by initiating cooling 30 minutes before a predicted sharp increase in occupancy. The pre-cooling condition is activated when the following-hour increase exceeds 250 visitors.

S3 and S4 were simulated using both actual and ANN-predicted occupancy series. This comparison was used to determine whether prediction errors materially altered energy consumption or thermal-comfort performance.

4. RESULTS AND DISCUSSION

4.1 ANN Prediction Accuracy

ANN-1 achieved a MAPE of 13.23% and an R^2 of 0.776. Four days were excluded from model training for a more interpretable test: Sunday, 18 August; Monday, 19 August; Thursday, 29 August; and the national holiday on Friday, 30 August 2019. For the holiday case, which represented an atypical occupancy profile, the hourly predictions were approximately 87% accurate.

Training and validation losses for ANN-1 and ANN-3 remained within an acceptable complexity range without clear evidence of overfitting. By contrast, larger models using 64 neurons per layer and 1,000 epochs showed increasing separation between training and validation losses after approximately 600 epochs. These results supported the selection of the more compact ANN-1 model.

4.2 Energy Simulation Results

Detailed simulations were examined for Thursday, 29 August 2019, a hot summer day, and Friday, 7 June 2019, a milder early-summer day. The corrected weekday labels are used here; the dates themselves are unchanged from the source study.

Across the two selected days, the published comparison showed that S3 and S4 reduced energy consumption by approximately 10% relative to S2 on 7 June and by approximately 22% on 29 August. Relative to the full-power S1 baseline, the overall results reported savings of at least 35%, approaching 40% during hotter outdoor conditions (Yayla et al., 2022).

Thermal-comfort performance was also more consistent in the AI-based scenarios. S2 showed wider indoor-temperature fluctuations and periods outside the desired comfort range during rapid changes in occupancy and outdoor conditions. S3 responded in advance using the predicted occupancy trend. On 7 June, S4 activated cooling at 12:30 p.m., 30 minutes before an increase of more than 250 visitors between 1:00 and 2:00 p.m., bringing indoor temperature toward the setpoint before the surge. Simulations using actual and predicted occupancy produced only slight differences in energy use and indoor temperature.

4.3 Discussion

The principal advantage of the proposed approach is temporal anticipation. A conventional sensor-based controller acts after occupancy has affected temperature or CO_2 concentration, whereas the ANN provides a day-ahead schedule that can position HVAC capacity before the load materializes. This proactive behavior explains the combined improvement in energy efficiency and thermal comfort.

The reported 10–22% savings relative to traditional sensor-based control are consistent with the broader occupancy-control literature, in which reported savings vary according to building type, baseline, control logic, and climate (Erickson et al., 2009; Capozzoli et al., 2017; Peng et al., 2018). The present framework is distinct because real-time occupancy detection is not required by the predictive schedule.

The small differences between simulations using actual and ANN-predicted occupancy suggest that moderate prediction errors do not eliminate the operational benefit of the control strategy. Nevertheless, this conclusion is limited to the studied shopping mall, cooling season, selected simulation days, and model assumptions. Field implementation should retain appropriate safety limits, commissioning procedures, and optional sensor-based overrides.

5. CONCLUSIONS

This paper summarized an AI-driven, occupancy-predictive HVAC control framework for a large commercial building. A two-year shopping-mall dataset was used to train an ANN that estimated hourly occupancy from environmental, temporal, and social-calendar variables. The preferred model achieved a MAPE of 13.23%, an R^2 of 0.776, and approximately 87% accuracy for a held-out national-holiday profile.

IDA-ICE simulations compared continuous full-power operation, conventional sensor-based control, AI-based predictive control, and AI-based control with pre-cooling. The published analysis reported minimum energy savings of approximately 10% relative to sensor-based control and 35% relative to continuous full-power operation, with savings approaching 20% and 40%, respectively, in hotter conditions. The AI-based scenarios also maintained indoor temperature closer to the intended comfort level during rapid occupancy changes.

Three conclusions follow. First, historical occupancy combined with weather, time, and day-type variables contains sufficient information to generate useful day-ahead forecasts. Second, predictive scheduling enables proactive thermal management that reactive occupancy sensing cannot provide by itself. Third, the simulation outcomes remained broadly stable when ANN-predicted occupancy replaced actual occupancy, although field validation is still required before generalizing the results.

Future research should extend the method to the heating season, evaluate other commercial-building types, conduct full-scale field trials, and investigate adaptive thresholds and variable pre-cooling periods. Integration with real-time temperature, indoor-air-quality, and equipment-status signals as fail-safe overrides may further improve robustness in operational buildings.

SOURCE NOTE

This conference paper is a condensed and clarified adaptation of Yayla et al. (2022), published under the Creative Commons Attribution 4.0 license. Both authors of the present paper were co-authors of the original study. The dataset, ANN framework, control algorithms, and simulation findings summarized here originate from that publication; no new experimental dataset is claimed.

REFERENCES

- Capozzoli, A., Piscitelli, M. S., Gorrino, A., Ballarini, I., & Corrado, V. (2017). Data analytics for occupancy pattern learning to reduce the energy consumption of HVAC systems in office buildings. Sustainable Cities and Society, 35, 191–208. https://doi.org/10.1016/j.scs.2017.07.016
- Du, Y., Zandi, H., Kotevska, O., Kurte, K., Munk, J., Amasyali, K., McKee, E., & Li, F. (2021). Intelligent multi-zone residential HVAC control strategy based on deep reinforcement learning. Applied Energy, 281, 116117. https://doi.org/10.1016/j.apenergy.2020.116117
- Erickson, V. L., Lin, Y., Kamthe, A., Brahme, R., Surana, A., Cerpa, A. E., Sohn, M. D., & Narayanan, S. (2009). Energy efficient building environment control strategies using real-time occupancy measurements. In Proceedings of the 1st ACM Workshop on Embedded Sensing Systems for Energy-Efficiency in Buildings (BuildSys '09), 19–24. https://doi.org/10.1145/1810279.1810284
- Erickson, V. L., & Cerpa, A. E. (2010). Occupancy based demand response HVAC control strategy. In Proceedings of the 2nd ACM Workshop on Embedded Sensing Systems for Energy-Efficiency in Buildings (BuildSys '10), 7–12. https://doi.org/10.1145/1878431.1878434
- IEA (International Energy Agency). (2019). Energy efficiency: Buildings. https://www.iea.org/topics/energy-efficiency/buildings

- Ignjatović, M. G., Blagojević, B. D., Stojiljković, M. M., Anđelković, A. S., Blagojević, M. B., & Mitrović, D. M. (2022). Energy performance of air-conditioned buildings based on short-term weather forecast. Science and Technology for the Built Environment, 28(4), 491–507. https://doi.org/10.1080/23744731.2021.1989907
- Lee, S., Karava, P., Tzempelikos, A., & Bilionis, I. (2020). A smart and less intrusive feedback request algorithm towards human-centered HVAC operation. Building and Environment, 182, 107190. https://doi.org/10.1016/j.buildenv.2020.107190
- Liu, X., Lee, S., Bilionis, I., Karava, P., Joe, J., & Sadeghi, S. A. (2021). A user-interactive system for smart thermal environment control in office buildings. Applied Energy, 293, 117005. https://doi.org/10.1016/j.apenergy.2021.117005
- Peng, Y., Rysanek, A., Nagy, Z., & Schlüter, A. (2018). Using machine learning techniques for occupancy-prediction-based cooling control in office buildings. Applied Energy, 211, 1343–1358. https://doi.org/10.1016/j.apenergy.2017.12.002
- Tien, P. W., Darkwa, J., Wei, S., Wood, C., Chow, T. W., & Calautit, J. K. (2022). Enhancing the detection performance of a vision-based occupancy detector for buildings. Proceedings of the Institution of Civil Engineers – Engineering Sustainability, 175(4), 198–210. https://doi.org/10.1680/jensu.22.00013
- Yang, L., Yan, H., & Lam, J. C. (2014). Thermal comfort and building energy consumption implications: A review. Applied Energy, 115, 164–173. https://doi.org/10.1016/j.apenergy.2013.10.062
- Yayla, A., Świerczewska, K. S., Kaya, M., Karaca, B., Arayici, Y., Ayözen, Y. E., & Tokdemir, O. B. (2022). Artificial intelligence (AI)-based occupant-centric heating ventilation and air conditioning (HVAC) control system for multi-zone commercial buildings. Sustainability, 14(23), 16107. https://doi.org/10.3390/su142316107

Resilience Approaches for Adapting HVAC Systems, Built Environments, and Communities to Climate Change and Urban Heat Island Effects

Birol Yavuz Author
Birol Yavuz Consultancy Turkey
birolyavuz65@gmail.com

SUMMARY

The intensification of climate change and Urban Heat Island effects poses significant challenges for HVAC systems, built environments, and urban communities. Rising ambient temperatures, increasing frequency and duration of extreme heat events, and changing climatic conditions directly affect the performance, energy efficiency, reliability, and long-term sustainability of HVAC systems. These developments necessitate a re-evaluation of not only technical infrastructures but also urban living conditions, social vulnerabilities, and public health frameworks.

This study examines resilience-based approaches for adapting HVAC systems and built environments to climate change and Urban Heat Island effects. Conceptualizing HVAC systems not merely as technical infrastructures but as integral socio-technical components of urban resilience, the study adopts a multi-scalar perspective. Accordingly, adaptation strategies are analyzed at the building, neighborhood, urban, and community levels in an integrated manner.

The paper ultimately proposes an interdisciplinary, systems-based, and socially inclusive resilience framework to enhance the flexibility, adaptability, and sustainability of HVAC systems under changing climatic conditions.

Keywords: Climate change, heat island, resilience, HVAC systems, built environment, communities.

1. INTRODUCTION

Global temperature increases and the intensification of extreme heat events have become defining characteristics of contemporary climate dynamics. Urban areas are particularly vulnerable due to the Urban Heat Island effect, which amplifies ambient temperatures through dense construction, reduced vegetation, and anthropogenic heat emissions.

In this context, HVAC systems play a critical role in maintaining indoor environmental quality and thermal comfort. However, rising cooling demand, higher peak loads, and increased operational stress challenge the long-term sustainability and reliability of these systems. Traditional HVAC design methodologies rely heavily on historical climatic datasets, which no longer accurately represent future climate realities.

Therefore, HVAC resilience must be redefined as a strategic component of urban climate adaptation, extending beyond technical efficiency toward systemic adaptability and socio-technical integration.

2. CONCEPTUAL FRAMEWORK: RESILIENCE AND SOCIO-TECHNICAL SYSTEMS

Resilience refers to the capacity of systems to absorb disturbances, adapt to changing conditions, and maintain essential functions. While engineering resilience focuses on system recovery speed, ecological and socio-technical perspectives emphasize adaptability, transformation, and learning capacity.

HVAC systems should be conceptualized as socio-technical systems consisting of:

Mechanical and thermal equipment

Energy supply infrastructure

Digital control and automation systems

User behavior and occupancy patterns

Institutional regulations and energy policies

This integrated perspective enables a broader understanding of vulnerability and adaptation pathways.

3. IMPACTS OF CLIMATE CHANGE AND URBAN HEAT ISLAND ON HVAC SYSTEMS

Climate change and Urban Heat Island effects impose multidimensional pressures on HVAC systems:

3.1 Increased Cooling Demand

Higher ambient temperatures significantly increase cooling energy consumption. Studies indicate that cooling demand may rise disproportionately in already warm climates, increasing electricity peak loads and grid stress.

3.2 Reduced System Efficiency

As outdoor temperatures rise, heat rejection efficiency declines, reducing coefficient of performance (COP) values in cooling systems.

3.3 Equipment Degradation and Failure Risk

Extreme heat conditions accelerate mechanical wear, refrigerant stress, and electrical component degradation, increasing failure probabilities.

3.4 Grid Vulnerability

Simultaneous peak demand during heatwaves can overload electricity networks, creating cascading system risks.

These impacts demonstrate that resilience must address both system robustness and adaptive capacity.

4. RESILIENCE-ORIENTED ADAPTATION STRATEGIES

A multi-scale approach is essential for enhancing HVAC resilience.

4.1 Building-Scale Technical Strategies

Climate-responsive HVAC design

Modular and flexible system architecture

Passive cooling integration (shading, thermal mass, natural ventilation)

Evaporative and hybrid cooling systems

Smart building automation systems

Real-time data-driven adaptive controls

Reducing cooling loads through passive design significantly lowers mechanical system stress and enhances long-term resilience.

4.2 Urban-Scale Planning Strategies

Expansion of green infrastructure

High-albedo roofing and pavement materials

Climate-sensitive urban morphology

District cooling networks

Renewable energy integration

Urban ventilation corridor planning

Urban-scale interventions create multiplier effects that reduce overall cooling demand and mitigate Urban Heat Island intensity.

4.3 Community and Governance-Level Approaches

Participatory resilience planning

Heatwave early warning systems

Cooling support programs for vulnerable populations

Energy poverty mitigation mechanisms

Public–private partnerships

Resilience depends not only on technological capacity but also on institutional and social adaptability.

5. DISCUSSION

Enhancing HVAC resilience requires integration across engineering, urban planning, policy, and social systems. Merely increasing system capacity does not guarantee sustainability under uncertain climate futures. Instead, adaptive and flexible design paradigms must replace static performance assumptions.

Key transitions include:

From efficiency-only metrics to resilience metrics

From reactive maintenance to predictive analytics

From isolated building systems to integrated urban energy networks

From centralized control to distributed adaptive intelligence

This systemic transition aligns HVAC development with broader climate adaptation and decarbonization goals.

6. CONCLUSION

Climate change and Urban Heat Island effects necessitate a redefinition of HVAC system design and governance. This paper presented a socio-technical, multi-scale resilience framework integrating building, urban, and community-level strategies.

Future research should focus on:

Climate-projection-informed design standards

AI-driven adaptive HVAC control systems

Integrated district energy resilience modeling

Policy instruments linking climate mitigation and adaptation

Equity-centered cooling access strategies

HVAC systems must evolve from static thermal infrastructure into adaptive, intelligent, and socially embedded resilience mechanisms for climate-responsive cities.

References

- Akbari, H., Pomerantz, M., & Taha, H. (2001). Cool surfaces and shade trees to reduce energy use and improve air quality in urban areas. Solar Energy, 70(3), 295–310. https://doi.org/10.1016/S0038-092X(00)00089-X□
- Artmann, N., Manz, H., & Heiselberg, P. (2007). Climatic potential for passive cooling of buildings by night-time ventilation in Europe. Applied Energy, 84(2), 187–201. https://doi.org/10.1016/j.apenergy.2006.05.004□
- Georgescu, M., Morefield, P. E., Bierwagen, B. G., & Weaver, C. P. (2014). Urban adaptation can roll back warming of emerging megapolitan regions. PNAS, 111(8), 2909–2914. https://doi.org/10.1073/pnas.1322280111□
- Holling, C. S. (1973). Resilience and stability of ecological systems. Annual Review of Ecology and Systematics, 4, 1–23.
- IPCC. (2021). Climate change 2021: The physical science basis. Cambridge University Press.
- Oke, T. R. (1982). The energetic basis of the urban heat island. Quarterly Journal of the Royal Meteorological Society, 108(455), 1–24.
- Santamouris, M. (2015). Regulating the damaged thermostat of the cities. Energy and Buildings, 91, 43–56.
- Santamouris, M. (2020). Recent progress on urban overheating research. Energy and Buildings, 207, 109482.
- Ürge-Vorsatz, D., et al. (2015). Heating and cooling energy trends in buildings. Renewable and Sustainable Energy Reviews, 41, 85–98.
- World Bank. (2022). Türkiye country climate and development report. World Bank Group.

TTMD
Turkish Society of HVAC & Sanitary Engineers
XVII TTMD INTERNATIONAL HVAC&R TECHNOLOGIES SYMPOSIUM
ARTIFICIAL INTELLIGENCE IN BUILDINGS
14-15 MAY 2026

Artificial Intelligence in Thermal Energy Storage Building Applications

Burcu Koçak[1], Sedat Emir[1], Abou Baker A. Ibrahim[1,2], Fatma Alma[1], Filiz Hoplamaz[1], Gülfeza Kardaş[1], Halime Paksoy[1]

[1]Department of Chemistry, Çukurova University, Adana, Türkiye

[2]Department of Mechanical Engineering, University of Blue Nile, Blue Nile, Sudan

Corresponding email: hopaksoy@cu.edu.tr

SUMMARY

Increasing use of solar energy introduces challenges such as intermittency and mismatch between energy supply and demand. TES systems play a critical role in addressing these challenges; however, conventional control approaches are often limited in adapting to dynamic operating conditions. In this context, AI techniques such as machine learning, predictive analytics, and intelligent control algorithms are reviewed with respect to key functions including demand forecasting, optimal charging and discharging, thermal comfort management, and energy cost reduction. The applicability of these methods is evaluated through the HECTAPUS Project, which develops a PCM-based TES system for heating and cooling of refugee shelters. The observations indicate that AI-supported TES systems can significantly improve system performance, flexibility, and user comfort.

Keywords: Artificial intelligent, buildings, thermal energy storage, heating- cooling systems

INTRODUCTION

Thermal Energy Storage (TES) systems play a critical role in improving energy efficiency and flexibility in building applications by enabling load shifting, peak shaving, and enhanced integration of renewable energy sources. However, the variability of energy consumption in buildings and renewable energy generation throughout the day significantly complicates the optimal operation of TES systems. Recent studies indicate that AI has become an effective tool for improving the performance and control TES systems in building applications [1]. AI-based methods are widely used for system modeling, performance prediction, optimal control, and energy management in buildings.

Artificial Neural Networks (ANNs) have been extensively applied to predict temperature distribution, stored thermal energy, and charging–discharging efficiency of sensible and latent heat storage systems with significantly low computational cost [2].

ANN and machine learning models can be employed to analyze the thermal behavior of phase change material (PCM)-enhanced walls and roofs, as well as their impact on indoor thermal comfort and energy savings [3].

AI techniques are also widely adopted for optimal control and energy management of TES-integrated HVAC systems. Reinforcement learning, genetic algorithms, and machine-learning-assisted model predictive control have been proposed to optimize TES charging and discharging schedules in buildings [4]. The primary objectives include minimizing energy consumption and costs, reducing peak demand, and maintaining thermal comfort.

Furthermore, AI-based demand forecasting plays a key role in enhancing TES operation in smart buildings. Machine learning models are used to predict heating and cooling loads, enabling demand response and load

shifting strategies through storage systems [5]. These approaches support higher penetration of renewable energy sources and improve building energy flexibility.

Overall, this study explores the application of AI-based methods in TES systems for building applications. It reviews AI techniques in relation to key functions such as demand forecasting, optimal charging and discharging strategies, and thermal comfort management. Particular emphasis is placed on the integration of TES with solar energy technologies for both heating and cooling. In addition, the potential of using these methods is assessed through a real-life case study, namely the HECTAPUS Project. Within this framework, the study not only provides a comprehensive reviews relevant AI methods applicable to active TES systems in buildings but also identifies potential AI approaches and system requirements for optimizing TES operation in the HECTAPUS system, thereby bridging the gap between theory and practical implementation.

2. THERMAL ENERGY STORAGE IN BUILDING APPLICATIONS

TES allows thermal energy to be stored and used at the appropriate time. Sensible, latent and thermo chemical heat storage techniques are known as TES techniques. Latent heat storage is the storage of energy during phase changes. Latent heat storage provides several advantages over sensible heat storage, such as up to 5 times higher energy storage density and isothermal properties during the TES process [6]. Phase-change materials (PCMs) are used for this purpose [7]. PCMs are classified into three groups: organic, inorganic, and mixtures. Thermal energy can be stored by selecting PCMs that undergo phase changes under desired conditions and within specific temperature ranges [8]. One of the many applications of PCMs is their use in buildings [9]. Thanks to their ability to store and release large amounts of energy within a narrow temperature range, PCMs are attracting increasing interest for use in buildings (Fig. 1).

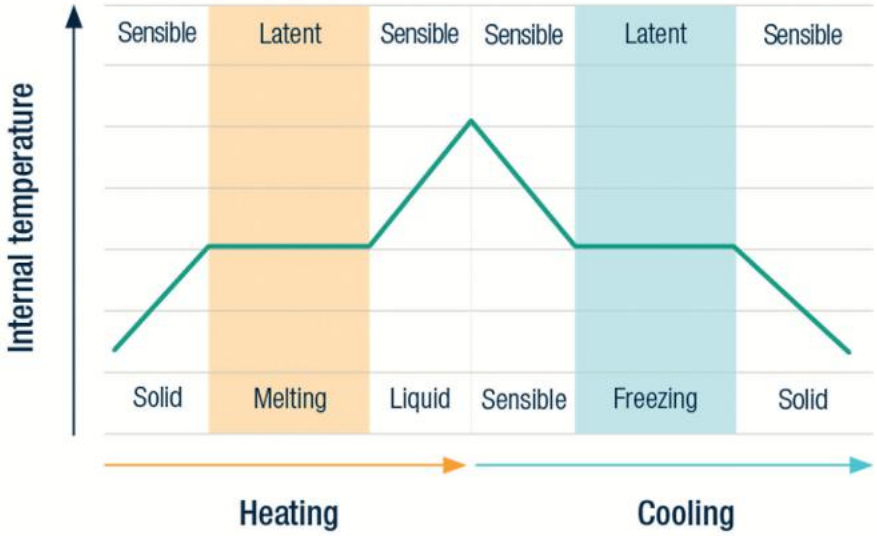


Figure 1. PCM heating and cooling currve

Previous studies indicate that PCM integration can significantly improve indoor temperature stability, reduce HVAC loads, and enhance demand shifting capabilities. The selection of PCM melting temperature is critical, with values between 21 °C and 25 °C being optimal depending on seasonal and climatic conditions. While PCM applications show notable benefits in light weight (LW) buildings, some studies report that heavy weight (HW) buildings without PCM may still outperform PCM-enhanced LW structures in maintaining thermal comfort [10].

Heating and cooling in buildings can be provided by active and passive systems. Passive systems are approaches that enhance thermal performance without relying on mechanical equipment. These include the use of high thermal mass materials, effective insulation, controlled solar gains, and natural ventilation strategies. In passive approach, PCM is incorporated into building envelopes, such as walls and ceilings, to reduce indoor temperature fluctuations and improve thermal stability. By storing and releasing latent heat within a narrow temperature range, PCMs contribute to lowering overall energy demand while maintaining occupant comfort.

Active heating and cooling systems in buildings rely on mechanical equipment such as HVAC systems, heat pumps, and chillers to maintain indoor thermal comfort and air quality. Their performance is enhanced through advanced control strategies, including programmable thermostats and demand response, which optimize operation based on occupancy and energy demand. Integration with TES can further improve efficiency by storing energy during off-peak periods and using it during peak times. This reduces energy costs and peak loads. Overall, combining efficient technologies, smart controls, and TES enables flexible, energy-efficient and sustainable building operation.

3.HEATING AND COOLING IN HECTAPUS PROJECT

3.1 Hectapus System Overview

Turkey hosts over 3.5 million registered refugees, the highest number worldwide, with temporary camps spread across multiple provinces. These regions experience extreme climate conditions, with summer temperatures exceeding 40°C and winter temperatures dropping below 0 °C. Heating in refugee camps is mainly provided by fossil fuel systems, while air conditioning is rarely used due to high costs. Overall, these conventional heating and cooling solutions are both expensive and inefficient in terms of primary energy use.

The HECTAPUS project supported under the Geothermica Smart Energy Systems ERA-Net framework focuses on the development of a prototype heating and cooling system for refugee shelters using PCM-based TES. In HECTAPUS project a dual-mode, solar-assisted latent heat TES unit is developed to provide heating and cooling for temporary shelters (Fig. 2). The infrastructure is housed within a prefabricated cabinet measuring 3.0 × 7.0 × 2.8 m. The core components include flat-plate solar collectors, two PCM-based TES tanks (for heating and cooling), and four fan-coil units for indoor climate control. Double-spiral copper coil heat exchangers are integrated into the TES tanks for charging and discharging of heat and cold.

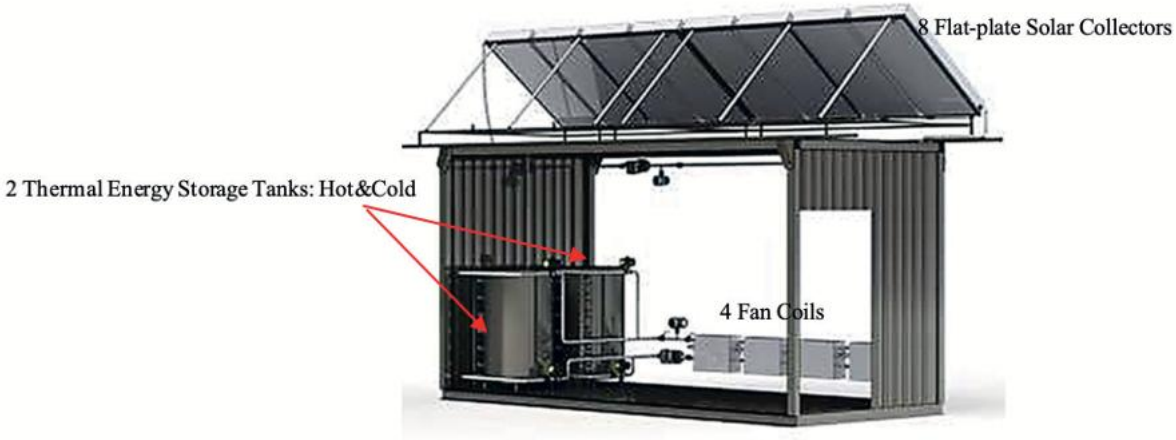


Figure 2. Refugee shelter with dual mode solar assisted latent heat units [11]

The system architecture utilizes two primary hydraulic circuits: a charging circuit connecting the solar collectors to the TES units, and a discharging circuit linking the TES units to the fan-coil system.

The operation is governed by predefined temperature threshold values to automate the transition between modes as heating and cooling. The system operates according to defined control strategies to ensure efficient and reliable performance. In storage mode, the system is activated when the collector temperature reaches 45°C, and storage mode is deactivated when the outlet temperature of the heat transfer fluid from the TES tank is higher than the inlet temperature. In recovery mode, it operates when the indoor air temperature is below 23°C and the inside the PCM tank is above 25°C, and stops when the indoor air temperature exceeds 26°C.

During heating operation, thermal energy collected from solar collectors during the daytime is used to melt the PCM in the hot TES, thereby storing heat. At night, the energy stored in the hot TES is released and used to heat the cabin through fan coil units, ensuring indoor thermal comfort.

For cooling operation, the system utilizes the energy stored in the cold TES during the previous night to cool the cabin during daytime via fan coil units. During nighttime, the heat transfer fluid is cooled in solar collectors positioned horizontally to take advantage of night sky radiation, allowing the PCM in the cold TES to solidify and store cooling for the next day.

To evaluate system performance, temperature, flow rate, and solar irradiance are monitored and recorded with data logger. Temperature is measured at 8 points in the TES tanks and at indoor/outdoor, collector, and fan-coil inlets/outlets. Flow rates in charging and discharging circuits are measured using a flowmeter, and solar radiation is measured with a pyranometer.

3.2. Operational Challenges in the HECTAPUS System

The HECTAPUS system is designed to effectively utilize solar energy by integrating TES with building heating applications. By storing solar energy and using it when needed, the system addresses the inherent intermittency of renewable energy sources and contributes to improved energy efficiency and indoor thermal comfort [12]. Nevertheless, certain operational challenges may arise under specific conditions.

1. Temporal change of solar energy availability: While the system is capable of storing and supplying solar energy under normal conditions, reduced solar radiation on overcast days can temporarily affect the charging performance of the TES unit. In addition, sudden changes in weather conditions may lead to short-term mismatches between energy generation and system response, as the system operates based on predefined control conditions that may not always adapt instantly to rapid climatic variations.
2. Limited utilization of full storage capacity of paraffin TES tank: Incomplete melting of PCM seen in the central regions of the TES tank can limit the utilization of its full storage capacity. This is primarily associated with the relatively low thermal conductivity of paraffin-based materials [13]. Heat transfer within the storage unit may not always be uniform, which can influence the timing and efficiency of energy recovery under certain operating conditions. To improve thermal performance and maintain indoor comfort, different flow rate configurations of the heat transfer fluid have been tested. Adjusting the flow rate allows better control of heat transfer between the heat transfer fluid and the PCM, supporting more effective charging and discharging processes. However, the selection of optimal flow conditions may vary depending on external conditions and system demand, requiring adaptive rather than fixed operational settings.
3. Delay in system response: The control strategy based on fixed temperatures are used to ensure stable operation and help maintain indoor thermal comfort within the desired range. However, in some cases, the activation or deactivation of these control conditions may occur with a delay under rapidly changing conditions, which can affect system responsiveness. This also can translate into reduced storage/recovery and overall system efficiencies.

4. POTENTIAL AI-BASED STRATEGIES FOR THE HECTAPUS SYSTEM

The employment of AI approaches in the HECTAPUS system provides significant opportunities to address operational limitations arising from solar variability and mismatches between energy generation and demand.

4.1. Model Predictive Control (MPC)

Integrating model predictive control (MPC) with machine learning can be used to predict short-term solar radiation, ambient temperature, and heating demand from historical operational data [14, 15]. The predicted values can then be incorporated into an MPC framework to proactively adjust system operation, such as modifying flow rates or preheating the PCM tank before anticipated cloudy periods. Previous studies have demonstrated that these strategies remarkably improve the utilization of TES and enhance system flexibility under intermittent renewable energy conditions [16, 17]. For example, MPC coupled with machine learning models has been successfully applied to residential heating systems with TES, which enables improved management of energy generation and consumption based on short-term solar forecasts [16, 18]. Furthermore, MPC strategies applied to solar thermal systems with storage have shown enhanced energy utilization and reduced auxiliary energy consumption compared with conventional rule-based control approaches [19, 20, 21]. The adoption of such an MPC in the HECTAPUS system would improve responsiveness to weather fluctuations, reduce temperature deviations, and increase overall system efficiency.

4.2. Reinforcement Learning (RL)

AI techniques can also address the thermal performance limitations of the PCM-based storage tank, particularly incomplete melting due to paraffin's low thermal conductivity. Reinforcement learning (RL) algorithms can dynamically optimize operational parameters, such as flow rate and charging duration, by interacting with a digital twin of the TES unit [22]. Through iterative learning, the RL agent identifies optimal control policies that enhance heat transfer uniformity and maximize energy recovery [23].

4.3. Artificial Neural Networks (ANN)

In addition, surrogate machine learning models or artificial neural networks can approximate the internal thermal state of the PCM tank in real time, enabling faster decision-making compared to computationally intensive numerical simulations [24]. MPC strategies integrating neural networks have been experimentally validated for TES systems, showing improved charging and discharging optimization and operational cost reductions compared with rule-based control [21, 25]. These intelligent optimization approaches would improve the degree of PCM utilization and enhance charging/discharging efficiency in the HECTAPUS system, ultimately supporting more stable indoor thermal comfort under variable operating conditions.

4.4. Adaptive Intelligent Controls (AIC)

Further improvements can be achieved by replacing fixed rule-based control strategies with adaptive intelligent control methods [26]. Fuzzy logic controllers, combined with reinforcement learning or neuro-fuzzy systems, can handle uncertainty and gradual transitions between operating modes more effectively than threshold-based control [27]. Such controllers simultaneously consider multiple variables, including collector temperature, PCM tank temperature, indoor temperature, and predicted weather conditions, enabling smoother switching between storage and recovery modes [28]. Reinforcement learning can further refine fuzzy rules through continuous learning from operational data, allowing the system to adapt to changing environmental conditions. Recent studies have demonstrated that hybrid reinforcement learning and fuzzy logic approaches can optimize HVAC

operation, improving thermal comfort while reducing energy consumption [29]. Additionally, advanced MPC strategies for solar thermal heating systems with TES have shown substantial improvements in energy savings and operational flexibility under variable occupancy and environmental conditions [30]. Implementing such adaptive AI-based control methods in the HECTAPUS system would enhance reliability, minimize control delays, reduce unnecessary cycling, and maintain indoor thermal comfort more consistently.

4.5. Solutions to Challenges of HECTAPUS with AI Based Methods

The AI based methods reviewed here can provide opportunities to overcome the challenges seen in HECTAPUS operation. These are summarized in Table 1. Application of these methods can improve system performance and flexibility under variable solar resources.

Table 1. Potential application of AI based methods in overcoming challenges in HECTAPUS Project

Challenges	Suggested AI- based method	Expected result	Reference
Temporal change of solar energy availability	MPC	Improve responsiveness to weather fluctuations and increase overall system efficiency	[16-21]
Limited utilization of full storage capacity	RL	Provide optimal control policies that enhance heat transfer uniformity	[22, 23]
Delay in system response	ANN AIC	Enhance charging/discharging efficiency, enhance reliability, minimize control delays, reduce unnecessary cycling, support more stable indoor thermal comfort	[24,28-30]

6. CONCLUSION

This study highlights the significant potential of AI-based methods to enhance the performance of TES systems in building applications. By addressing key challenges such as solar intermittency, control limitations, and storage inefficiencies, AI-driven approaches offer promising solutions for improving system efficiency, flexibility, and thermal comfort. For the HECTAPUS case study, different intelligent and adaptive control strategy opportunities are identified. By integrating such strategies into TES systems can support more reliable and sustainable heating and cooling solutions with intermittent solar energy resources. Particularly in challenging environments such as refugee shelters, more effective results can be achieved. The findings underline the potential of AI-enabled TES as a key component in the transition toward smart and low-carbon building energy systems. Furthermore, the integration of latent heat TES with solar energy across different building typologies can support the transition to clean energy systems and achieve greater impact when optimized using AI-driven strategies.

ACKNOWLEDGEMENT

The authors would like to acknowledge funding provided by TÜBİTAK (Project No: 218M182), British Council (Project ID: 414707599), HECTAPUS project funded by TÜBİTAK (Project No:122N750/222N357) under the umbrella of GEOTHERMICA Joint Call Smart Energy Systems ERA-Net.

REFERENCES

[1] Ahmad, T., Chen, H., Guo, Y., Wang, J. (2018). A comprehensive overview on the data driven and large scale based approaches for forecasting of building energy demand: A review. Energy and Buildings, 165, 301–320.

[2] Neto, A. H., Krarti, M. (2017). Artificial neural network based predictive control for energy efficiency improvement in buildings. Energy and Buildings, 150, 82–97.

[3] Ascione, F., Bianco, N., De Masi, R. F., de' Rossi, F., Vanoli, G. P. (2014). Energy refurbishment of existing buildings through the use of phase change materials: Energy savings and indoor comfort in the cooling season. Applied Energy, 113, 990–1007.

[4] Drgoňa, J., Arroyo, J., Cupeiro Figueroa, I., Blum, D., Arendt, K., Kim, D., … Wetter, M. (2020). All you need to know about model predictive control for buildings. Annual Reviews in Control, 50, 190–232.

[5] Mocanu, E., Nguyen, P. H., Gibescu, M., Kling, W. L. (2016). Deep learning for estimating building energy consumption. Sustainable Energy, Grids and Networks, 6, 91–99.

[6] Alva, G., Lin, Y., Fang, G. (2018). An overview of thermal energy storage systems. Energy, 144, 341-378.

[7] Nie, B., Palacios, A., Zou, B., Liu, J., Zhang, T., Li, Y. (2020). Review on phase change materials for cold thermal energy storage applications. Renewable and sustainable energy reviews, 134, 110340.

[8] Sharma, A., Tyagi, V. V., Chen, C. R., Buddhi, D. (2009). Review on thermal energy storage with phase change materials and applications.Renewable and Sustainable energy reviews, 13(2), 318-345.

[9] Pomianowski, M., Heiselberg, P., Zhang, Y. (2013). Review of thermal energy storage technologies based on PCM application in buildings. Energy and Buildings, 67, 56-69.

[10] Saffari, M., Roe, C., Finn, D. P. (2022). Improving the building energy flexibility using PCM-enhanced envelopes. Applied Thermal Engineering, 217, 119092.

[11] Paksoy H., Mahkamov K., Kardaş G., Südaş İ., Emir S., Göktepe Biçer G., Güngör Ö., Alma F., Hoplamaz F. Solar heating and cooling with latent heat storage for temporary shelters, ENERSTOCK the 16th IEA ES TCP International Conference on Energy Storage, 5-7 Haziran 2024, Lyon, Fransa, 467-469.

[12] Mao, Q., Wang, Y. (2025). Recent development of thermal heat storage technology coupling with phase change material. Journal of Energy Storage, 139, 118739.

[13] Mjbel, H. M., Hamzah, H. K., Alkhazaleh, R., Alahmer, A. (2025). A roadmap for high-performance phase change materials in thermal energy applications. International Communications in Heat and Mass Transfer, 169, 109921.

[14] Çeçen, M., Rivera, M., Wheeler, P., Zerdali, E. (2025, 1-4 Sept. 2025). Predictive Control for Solar Radiation Forecasting: A Case Study. Paper presented at the 2025 Energy Conversion Congress and Expo Europe (ECCE Europe).

[15] Gao, Y., Miyata, S., Akashi, Y. (2022). Multi-step solar irradiation prediction based on weather forecast and generative deep learning model. Renewable Energy, 188, 637-650.

[16] Maltais, L.-G., Gosselin, L. (2022). Energy management of domestic hot water systems with model predictive control and demand forecast based on machine learning. Energy Conversion and Management: X, 15, 100254.

[17] Yang, S., Wan, M. P., Chen, W., Ng, B. F., Dubey, S. (2020). Model predictive control with adaptive machine-learning-based model for building energy efficiency and comfort optimization. Applied energy, 271, 115147.

[18] Eseye, A. T., Lehtonen, M. (2020). Short-Term Forecasting of Heat Demand of Buildings for Efficient and Optimal Energy Management Based on Integrated Machine Learning Models. IEEE Transactions on Industrial Informatics, 16(12), 7743-7755.

[19] Bianchini, G., Casini, M., Vicino, A., Zarrilli, D. (2016). Demand-response in building heating systems: A Model Predictive Control approach. Applied energy, 168, 159-170.

[20] Pintaldi, S., Li, J., Sethuvenkatraman, S., White, S., Rosengarten, G. (2019). Model predictive control of a high efficiency solar thermal cooling system with thermal storage. Energy and Buildings, 196, 214-226.

[21] Thieblemont, H., Haghighat, F., Ooka, R., Moreau, A. (2017). Predictive control strategies based on weather forecast in buildings with energy storage system: A review of the state-of-the art. Energy and Buildings, 153, 485-500.

[22] Zhang, H., Seal, S., Wu, D., Bouffard, F., Boulet, B. (2022). Building Energy Management With Reinforcement Learning and Model Predictive Control: A Survey. IEEE Access, 10, 27853-27862.

[23] de Gracia, A., Fernández, C., Castell, A., Mateu, C., Cabeza, L. F. (2015). Control of a PCM ventilated facade using reinforcement learning techniques. Energy and Buildings, 106, 234-242.

[24] Li, Y., Huang, X., Huang, X., Gao, X., Hu, R., Yang, X., He, Y.-L. (2023). Machine learning and multilayer perceptron enhanced CFD approach for improving design on latent heat storage tank. Applied energy, 347, 121458.

[25] Lee, D., Ooka, R., Matsuda, Y., Ikeda, S., Choi, W. (2022). Experimental analysis of artificial intelligence-based model predictive control for thermal energy storage under different cooling load conditions. Sustainable Cities and Society, 79, 103700.

[26] Zhou, X., Xue, S., Du, H., Ma, Z. (2023). Optimization of building demand flexibility using reinforcement learning and rule-based expert systems. Applied energy, 350, 121792.

[27] Kang, C.-S., Hyun, C.-H., Park, M. (2015). Fuzzy logic-based advanced on–off control for thermal comfort in residential buildings. Applied energy, 155, 270-283.

[28] Marvuglia, A., Messineo, A., Nicolosi, G. (2014). Coupling a neural network temperature predictor and a fuzzy logic controller to perform thermal comfort regulation in an office building. Building and Environment, 72, 287-299.

[29] Yao, L., Huang, L.-Y., Teo, J. C. (2025). HVAC control based on reinforcement learning and fuzzy reasoning: Optimizing HVAC supply air temperature, flow rate, and velocity. Journal of Building Engineering, 103, 112143.

[30] Wei, Z., Calautit, J. (2023). Evaluation of model predictive control (MPC) of solar thermal heating system with thermal energy storage for buildings with highly variable occupancy levels. Building Simulation, 16(10), 1915-1931.

THE IMPACT OF CONDENSER DESIGN ON THE PERFORMANCE OF HEAT PUMP INTEGRATED WATER HEATERS

İmge KARAKOÇ[1], Levent ÇOLAK[2]
[1]Başkent University, Graduate School of Natural and Applied Sciences, Mechanical Engineering, Ankara, Türkiye
[2]Başkent University, Faculty of Engineering, Mechanical Engineering Department, Ankara, Türkiye
Corresponding email: imgekarakoc@gmail.com

SUMMARY

This study investigates the impact of condenser geometry and tank thermal stratification on the performance of a heat pump integrated domestic hot water system. Unlike conventional approaches that assume uniform or average temperature conditions, this work considers the condenser–tank interaction as a spatially and temporally varying process. An experimental setup consisting of an air-source heat pump integrated with a storage tank was analyzed. The condenser was configured as a wrapped-around serpentine coil on the external surface of the tank. Surface temperature measurements were obtained at multiple points along the condenser using an infrared thermometer, while internal tank temperatures were monitored at three vertical positions. A data processing methodology was developed to define region-specific reference tank temperatures based on a vertically continuous temperature profile, enabling a more physically representative evaluation of local driving temperature differences. The results indicate that the condenser does not operate under uniform temperature conditions. Significant temperature differences were observed along the vertical direction of the condenser, directly influenced by the stratified temperature distribution inside the tank. The experimental coefficient of performance (COP) was calculated as 2.45, showing deviation from typical nominal values due to non-uniform boundary conditions. The findings further reveal that thermal interaction is not uniformly distributed along the condenser, with certain regions exhibiting higher relative thermal driving potential than others, particularly in the middle-lower section. The study demonstrates that condenser performance in such systems should not be evaluated based on average temperature assumptions. Instead, a regional and time-dependent analysis is required. The presented methodology provides a foundation for future parametric and thermodynamic analysis of condenser design, including variations in geometry, coil spacing, and surface area.

Keywords: Heat pump water heating, Thermal stratification, Condenser design, Spatial temperature distribution, Regional analysis

1 INTRODUCTION

Heat pump integrated water heaters are increasingly used due to their high energy efficiency and role in low-carbon heating applications [1], [2]. The performance of such systems is strongly influenced by condenser configuration and thermal stratification within the storage tank [1]–[4].

In conventional analyses, the condenser is typically assumed to operate under uniform temperature conditions. However, in storage-type systems, thermal stratification leads to inherently non-uniform temperature distributions, resulting in spatially varying boundary conditions along the condenser surface.

In wrapped-around condenser configurations, the interaction between condenser geometry and tank stratification plays a critical role in determining system performance. Despite this, most studies still rely on simplified approaches that neglect local temperature variations.

This study experimentally investigates the influence of condenser geometry and tank stratification on system performance by treating the condenser as a spatially distributed heat transfer component. To the best of the authors' knowledge, a regional analysis based on profile-derived local driving temperature differences combined with area-weighted heat transfer indicators has not been systematically applied in this context.

2 MATERIAL AND METHOD

2.1 System description

The system analyzed in this study consists of an air-source heat pump integrated with a domestic hot water storage tank. The condenser is configured as a serpentine coil wrapped around the external surface of the tank, allowing heat transfer through the tank surface without an intermediate heat exchanger.

The condenser tube has a D-shaped cross-sectional geometry, as shown in Figure 1, which increases the effective contact interface between the condenser and the tank wall and influences local heat transfer behavior.

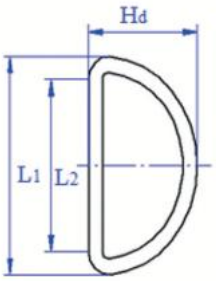


Figure 1. Cross-sectional geometry of the condenser tube used in the study, showing the D-shaped profile that increases the contact surface with the tank wall.

Due to this configuration, the thermal boundary conditions along the condenser vary in the vertical direction. Therefore, the condenser is treated as a spatially distributed heat transfer component rather than an isothermal surface.

The vertical distribution of the coil results in distinct thermal regions along the tank height. These regions interact with the stratified temperature field inside the tank, making condenser geometry a key parameter affecting local heat transfer potential.

2.2 Experimental setup and measurements

Temperature measurements along the condenser surface were performed using an infrared thermometer (IR) at selected spiral locations. The measurement points and the defined vertical regions (B1–B5) are illustrated in Figure 2.



Figure 2. Experimental observation of the wrapped-around condenser and definition of vertical regions (B1–B5) used for analysis

The condenser was divided into five vertical regions to capture spatial variations in heat transfer behavior along the tank height. The corresponding tank temperature levels (T1–T3) represent the upper, middle, and lower regions of the tank.

The tank temperature distribution was monitored using three vertically positioned sensors (T1–T3). The experiment was conducted from an initial representative tank temperature of 16.9 °C to a final tank temperature of 47.8 °C, with a set temperature of 55.0 °C. Measurements were recorded at 5-minute intervals during the initial phase and at approximately 30-minute intervals thereafter.

Electrical energy consumption was measured using an energy analyzer, and the electric heater was disabled during the test. The main experimental conditions and measurement parameters are summarized in Table 1.

Table 1. Experimental test conditions and measurement parameters

Parameter	**Value**
Initial representative tank temperature based on measured sensor values (T1-T2-T3)	16.9 °C
Final tank temperature	47.8 °C
Temperature increase (ΔT)	30.9 °C
Set temperature	55.0 °C
Average ambient temperature	17.4 °C
Measurement interval	5 min (initial), 30 min (later stage)
Surface measurement method	Infrared thermometer
Tank temperature measurement	3 vertical sensors (T1–T3)
Electrical energy measurement	Energy analyzer (power meter)
Electric heater status	Disabled

2.3 Determination of condenser temperature distribution

A vertically continuous temperature profile T(z) was reconstructed based on the discrete tank temperature measurements (T1–T3). This profile was used to determine spatially representative reference tank temperatures for each condenser region by averaging T(z) over the corresponding vertical boundaries.

2.4 Coupling between condenser and tank temperature

The spatial relationship between condenser regions and corresponding tank temperature levels is illustrated in Figure 3.

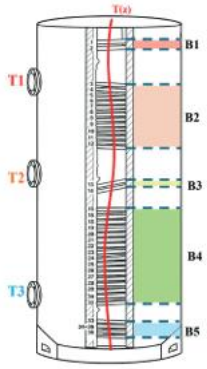


Figure 3. Schematic representation of condenser regions (B1–B5) and their corresponding tank temperature levels (T1–T3), illustrating the spatial coupling between condenser surface and stratified tank temperature distribution.

As shown in Figure 3, each condenser region is associated with a reference tank temperature obtained from the vertically continuous temperature profile T(z), calculated as the average temperature over the spatial boundaries of the corresponding region.

2.5 Thermodynamic analysis

The thermal energy stored in the tank was calculated using:

$$Q_{tank} = m \cdot c_p \cdot (T_{final} - T_{initial}) \quad (1)$$

where m is the effective water mass (180 kg), c_p is the specific heat capacity of water (4.186 kJ/kg·K), and ΔT represents the temperature difference between the initial and final states.

Based on the experimental measurements, the stored thermal energy was 6.44 kWh, while the electrical energy consumption was 2.63 kWh.

The experimental coefficient of performance (COP) was calculated as:

$$COP = \frac{Q_{tank}}{W_{el}} \quad (2)$$

resulting in a value of 2.45.

The experimentally obtained COP value of 2.45 is lower than the manufacturer-declared value of 3.66, indicating the impact of real operating conditions. This deviation can be attributed to several real operating condition effects, including non-uniform thermal boundary conditions and stratification phenomena, which are not fully represented in nominal performance ratings. Similar deviations have been reported in the literature due to condensation temperature variations, pressure drops, and system-level inefficiencies [6], [7].

Assumptions

2.6 The following assumptions were made:

- Temperature variations between unmeasured spiral locations were approximated using linear interpolation.
- Regional reference temperatures are defined based on the vertically continuous tank temperature profile T(z), representing the average thermal state of the fluid within the spatial extent of each condenser region.
- Tank temperature distribution was assumed to be primarily vertical, consistent with stratified storage tank behavior.
- Surface temperature measurements were performed using an infrared thermometer with a manufacturer-specified accuracy of ±1 °C under laboratory conditions, which was considered sufficient for capturing the relative temperature variations along the condenser.

3 RESULTS AND DISCUSSION

3.1 Condenser temperature distribution

Surface temperature measurements along the condenser, presented in Figure 4, indicate a clear non-uniform temperature distribution in the vertical direction. Upper regions heat up faster and reach higher temperatures, while lower regions remain at lower temperature levels for a longer duration.

This behavior demonstrates that the condenser cannot be accurately represented using uniform temperature assumptions.

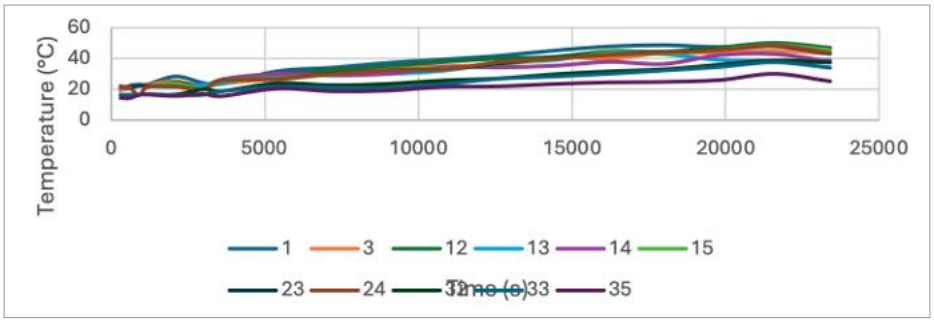


Figure 4. Surface temperature variation along the condenser serpentine

3.2 Tank stratification

The temperature measurements inside the tank confirm the presence of strong thermal stratification. Figure 5 shows the temperature evolution at three vertical levels inside the tank.

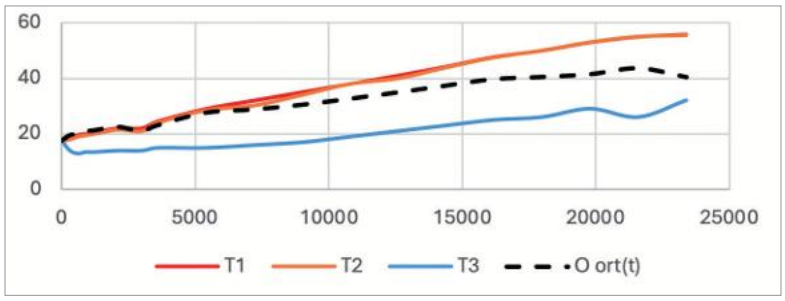


Figure 5. Tank temperature distribution at three vertical levels

The upper region (T1) reaches the target temperature faster, whereas the lower region (T3) remains at a significantly lower temperature throughout most of the heating process. This stratification behavior directly influences the temperature distribution along the condenser, as discussed in the following section.

3.3 Interaction between condenser and tank

The experimental results show that the condenser temperature distribution is directly influenced by the stratified temperature field inside the tank. The regional condenser surface temperatures, presented in Figure 6, highlight clear non-uniform thermal behavior along the vertical direction.

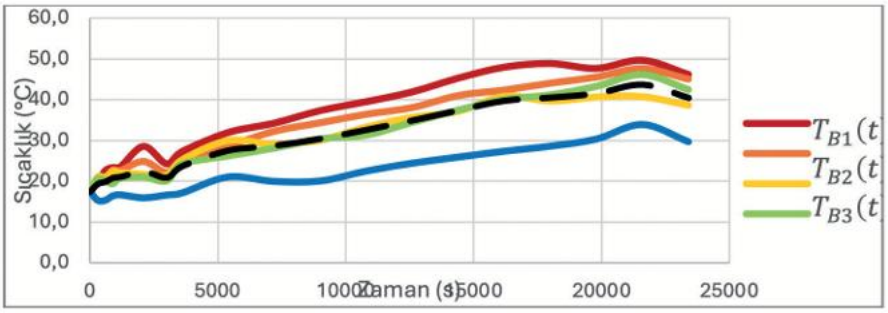


Figure 6. Regional average condenser surface temperatures

Different regions of the condenser operate under distinct temperature levels, indicating that the condenser behaves as a spatially distributed heat transfer component rather than an isothermal surface. Consequently, it cannot be accurately represented using a single average temperature and must be evaluated based on region-specific boundary conditions.

This non-uniform behavior directly affects the local driving temperature difference, which is analyzed in the following section.

3.4 Performance evaluation

The time-dependent variation of the representative driving temperature differences (ΔT_1–ΔT_5) is presented in Figure 7.

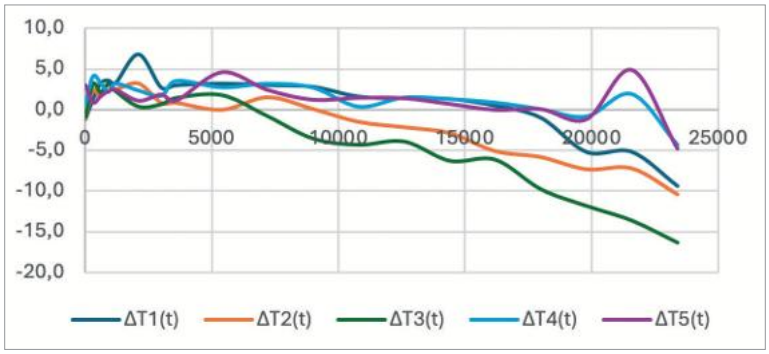


Figure 7. Time-dependent variation of regional driving temperature difference (ΔT)

These results indicate that the thermal interaction between the condenser and the tank varies both spatially and temporally throughout the heating process. In the early stage of the test, higher ΔT values were observed in the upper condenser regions, while the middle and lower regions exhibited relatively higher thermal driving potential during the later stages due to the evolving vertical temperature distribution inside the tank.

The results reveal a region-dependent thermal behavior associated with tank stratification. Among the evaluated regions, ΔT_4 maintained relatively high positive values during a significant portion of the heating period, indicating a comparatively stronger thermal driving potential in the middle-lower section of the condenser. In contrast, ΔT_5 exhibited lower but more sustained positive values over time.

Negative ΔT values observed in certain regions do not directly indicate a reversal of local heat transfer direction. These values arise from the relative relationship between the regional condenser surface temperature and the corresponding reference tank temperature defined by the vertical temperature profile approach.

Overall, the findings indicate that condenser performance is strongly influenced by stratified tank conditions and region-dependent thermal interaction. Consistent with these findings, previous studies have also reported that local temperature variations and spatially varying thermal interaction characteristics can significantly influence overall system performance and efficiency under stratified operating conditions [2], [4]. This behavior is considered one of the factors contributing to the deviation between experimental and nominal COP values.

3.5 Implications for condenser design

The findings demonstrate that condenser design should not be based solely on total heat transfer area. Instead, the results show that thermal interaction varies along the condenser, with some regions exhibiting higher relative thermal driving potential than others.

In particular, the middle-lower region exhibited relatively higher thermal driving potential compared to the other regions, indicating that geometric parameters such as coil distribution, vertical placement, and spacing should be evaluated together with tank stratification characteristics.

These results highlight that effective condenser design requires consideration of region-dependent heat transfer behavior rather than relying on uniform or average assumptions.

The proposed methodology provides a physically grounded basis for future parametric and thermo-economic evaluations of condenser design.

CONCLUSION

This study experimentally investigated the influence of condenser geometry and tank stratification on the performance of a heat pump integrated water heater system. The results demonstrate that:

- The condenser operates under spatially non-uniform temperature conditions.
- Thermal stratification significantly influences condenser performance.
- Thermal interaction varies along the condenser under stratified conditions.
- Average temperature assumptions are insufficient for accurate performance evaluation.

The proposed methodology enables the evaluation of condenser behavior based on regional temperature distributions and time-dependent thermal interaction characteristics.

The experimentally measured electrical energy consumption was 2.63 kWh, whereas an equivalent electric resistance heating system would require approximately 6.44 kWh to provide the same thermal energy increase, corresponding to an estimated electrical energy demand reduction of approximately 59%.

Future work will focus on evaluating the effects of condenser surface area, contact geometry, vertical coil distribution, and spiral spacing on the thermal interaction behavior of the system. These investigations will be supported by exergy-based and thermo-economic approaches to identify condenser configurations that improve performance while maintaining cost effectiveness.

REFERENCES

[1] B. Shen, K. Nawaz, V. D. Baxter and A. F. Elatar, "Development and validation of quasi-steady-state heat pump water heater model having stratified water tank and wrapped-tank condenser," International Journal of Refrigeration, vol. 87, pp. 78–90, 2018, doi: 10.1016/j.ijrefrig.2017.10.023.

[2] J. D. Rendall, K. Nawaz, A. F. Elatar, W. Asher and W. Worek, "Performance evaluation of a wrapped around condenser for heat pump water heater applications," Applied Thermal Engineering, vol. 207, p. 118097, 2022, doi: 10.1016/j.applthermaleng.2022.118097.

[3] S. Valencia-Cañola, C. A. Bustamante, C. Mira-Hernández and C. A. Isaza-Roldán, "Effect of geometric parameters on the heat transfer performance of a submerged coil condenser for heat-pump water heating," International Journal of Thermo-Fluids, vol. 24, p. 100808, 2024, doi: 10.1016/j.ijft.2024.100808.

[4] F. Ju, Z. Mu, H. Liu, X. Fan, Q. Hou, L. Hou, Q. Liu, W. Liu and H. Zheng, "Experimental investigation on system performance of an instant heat pump water heater with combined condenser," Case Studies in Thermal Engineering, vol. 53, p. 103819, 2024, doi: 10.1016/j.csite.2023.103819.

[5] K. Kusakana and S. Tangwe, "Evaluating thermal dynamics of air to water heat pump due to stratification: Experiment and modelling," Energy Reports, vol. 8, pp. 1118–1125, 2022, doi: 10.1016/j.egyr.2021.11.154.

[6] N. Koruga, M. Dobrnjac, D. Golubović and N. Dobrnjac, "Analysis of the influence of condensation temperature and compressor efficiency on heat pump system efficiency," IOP Conference Series: Materials Science and Engineering, vol. 1208, no. 1, p. 012015, 2021, doi: 10.1088/1757-899X/1208/1/012015.

[7] T. Koopman, T. Zhu and W. Rohlfs, "Performance evaluation of air-source heat pump based on a pressure drop embedded model," Heliyon, vol. 10, p. e24634, 2024, doi: 10.1016/j.heliyon.2024.e24634.

XVII TTMD INTERNATIONAL HVAC&R TECHNOLOGIES SYMPOSIUM
ARTIFICIAL INTELLIGENCE IN BUILDINGS
14-15 MAY 2026

Physics-Constrained Deep Learning for Sparse Data Reconstruction in Data Center Thermal Management

Koray Omercan Saçlı[a], Ömer Yiğit Türkarslan[a], Seyhan Onbaşıoğlu[a]
[a]Mechanical Engineering Department, Istanbul Technical University
sacli24@itu.edu.tr, turkarslano23@itu.edu.tr, onbasiogl1@itu.edu.tr

Abstract

This study addresses the inverse problem of reconstructing high-resolution thermal fields in air-cooled data centers from sparse sensor measurements. Unlike conventional surrogate modeling approaches that focus on forward prediction, the proposed framework employs a Physics-Constrained Neural Network (PCNN) to infer complete temperature distributions from limited observations. The model integrates thermodynamic principles and heat transfer constraints into the learning process, ensuring physically consistent reconstruction in regions without direct measurements. Trained on CFD-generated data, the framework achieves a mean absolute error of 0.75 °C across unseen conditions. Importantly, the model maintains accuracy not only at observed locations but also in unobserved regions, demonstrating strong generalization under sparse data conditions. In contrast, unconstrained neural networks exhibit non-physical artifacts and systematically underestimate peak temperatures. With an inference time of approximately 1 ms per field, the proposed approach enables real- time virtual sensing and provides a scalable alternative to dense sensor deployment. The framework offers a robust foundation for digital twin applications and continuous thermal monitoring in operational data centers.

Keywords: Data Center Cooling, Neural Networks (PINN), Virtual Sensing, Sparse Data Reconstruction, Thermal Digital Twin

1. Introduction

Modern data centers require continuous thermal monitoring to ensure safe and efficient operation. However, high-resolution temperature measurements are difficult to obtain due to limitations in sensor density, installation cost, and system complexity. As a result, thermal management often relies on sparse and indirect measurements, which are insufficient to capture localized hotspots and spatial gradients.

This challenge is further amplified by the growing energy demand driven by cloud computing, artificial intelligence, and large-scale digital infrastructure. Cooling systems account for nearly 30–40% of total operational power consumption in data centers [1, 9]. Zhang et al. [1] highlighted the importance of efficient cooling systems for sustainable operation, while Zhao et al. [2] identified temperature gradients and hotspot formation as key contributors to energy inefficiency and thermal risk.

This limitation defines an inverse problem: reconstructing the full thermal field from incomplete observations. Classical approaches rely on interpolation techniques, which lack physical grounding, or computational fluid dynamics (CFD), which is computationally expensive for real-time applications. Although CFD-based studies have shown that airflow management can improve thermal performance [3, 10], their cost limits their use in real-time monitoring and control.

Dense sensor deployment further increases system complexity and instrumentation requirements, making high-resolution monitoring impractical [4]. Consequently, sparse sensing strategies have gained attention for reconstructing full thermal fields from limited data. Wang et al. [5] proposed an analytical-solution-embedded

neural network for 3D temperature reconstruction, while Wang et al. [11] demonstrated that optimized sensor placement can reduce hardware requirements while maintaining accuracy.

Recent advances in physics-informed machine learning provide a promising alternative by embedding physical laws into data-driven models. Physics-informed neural networks (PINNs), introduced by Raissi et al. [7], incorporate governing equations such as Navier–Stokes, continuity, and energy conservation into the loss function, improving physical consistency while reducing data requirements. Karniadakis et al. [8] further demonstrated their robustness compared to purely data-driven models. PINNs have also been successfully applied to reconstruct flow fields from sparse and noisy measurements [4], highlighting their potential for thermal field reconstruction.

Despite these developments, the application of physics-constrained learning to sparse thermal field reconstruction in air-cooled data centers remains limited.

The present work proposes a physics-constrained deep learning framework for reconstructing temperature fields from sparse observations, focusing on physical consistency, robustness, and reliable hotspot detection. This study targets full-field reconstruction from limited measurements. By embedding physical constraints into the learning process, the model enables stable and physically consistent predictions in unobserved regions. This approach addresses the ill-posed nature of sparse sensing and provides a foundation for virtual sensing, real-time monitoring, and digital twin applications in data centers.

2. Methodology

2.1. CFD Model and Computational Domain

The CFD dataset used in this study represents a standard server rack cooling configuration and includes variations in inlet velocity and temperature and provides spatial temperature fields for supervised learning. For brevity, detailed geometric and numerical descriptions are not repeated.

2.2. Neural Network Model

Our previous study [13] introduced a physics-constrained neural network (PCNN) framework for forward prediction and optimization of data center cooling performance. In that work, the model was trained to predict temperature fields given operating conditions and was coupled with optimization algorithms to improve cooling efficiency. The network architecture combined Fourier feature encoding residual neural networks to capture multi-scale spatial variations. The present study adopts the same architectural framework but addresses a fundamentally different problem: reconstruction of full thermal fields from sparse measurements. Figure 1 illustrates the architecture of the proposed physics-constrained neural network (PCNN). In the figure

$$\mathcal{L} = \mathcal{L}_{data} + \lambda \mathcal{L}_{physics}$$

where the physics term enforces energy consistency and physically admissible temperature distributions.

The model takes spatial coordinates (x z)and flow velocity V as inputs, which are encoded using spatial and parametric Fourier features and processed through residual blocks. The network predicts the temperature difference ΔT, while training is guided by a combined data and physics-based loss.

The physics term, progressively enforced through a curriculum strategy, enables physically consistent predictions even in regions with sparse data.

2.3. Dataset Generation

A total of 15 CFD cases are generated using a full factorial design based on inlet velocity and temperature. The inlet velocity varies as:

$$V = 0.5, 0.75, 1.0, 1.25, 1.5 \text{ m/s}$$

while the inlet temperature is defined as:

$$T_{in} = 18, 22.5, 27°C$$

Temperature data are extracted from a horizontal plane

A uniform grid of 24×24points yield 576 spatial data points per case and a total of 8,640 data points across the dataset, which are used for training and validation.

2.4. Physical Interpretation of the Flow Field

Cold air enters the domain and is forced through narrow channels between server cards, enhancing convective heat transfer. As the flow progresses, it absorbs heat from GPU and PCB regions, leading to a temperature rise along the flow direction.

The confined geometry induces channeling behavior with localized velocity accelerations and strong thermal gradients. Hotspots occur near GPU locations, while the outlet flow removes accumulated thermal energy. These characteristics highlight the complexity of thermal field prediction and justify the use of physics-informed surrogate models.

2.5. Training Setup

The PCNN is trained using a six-stage curriculum learning strategy to ensure stable convergence and progressive enforcement of physical constraints. Training begins with a data-dominated warmup phase, followed by gradual increase of the constraint weight w_c, enabling the model to satisfy governing physical laws. The final stages emphasize strict physical consistency and refined accuracy.

2.6. Physics-Constrained Learning

The model incorporates physics-based constraints derived from heat transfer principles, conservation laws, and observed flow behavior. These constraints enforce physically consistent relationships, bounded temperature fields, and global energy balance.

In sparse reconstruction, they act as structural priors that regularize the inverse problem and prevent non-physical solutions in regions without measurements.

2.7. Training and Validation

The PCNN is trained on the CFD dataset using the described curriculum strategy and evaluated on unseen interpolation cases within the training parameter space.

Validation cases are designed to require interpolation in velocity, temperature, or both, allowing assessment of full-field reconstruction capability rather than simple data reproduction. The model achieves stable convergence

with sub-degree accuracy and no signs of overfitting.

Compared to an unconstrained neural network, the PCNN significantly improves reconstruction accuracy while maintaining physically consistent behavior across unseen cases.

3. Results and Discussion

The performance of the proposed physics- constrained neural network (PCNN) is evaluated in terms of reconstruction accuracy, physical consistency, and robustness under sparse data conditions. This indicates that the reconstruction is governed by physical constraints rather than interpolation between sparse measurements.

Figure 2 shows the PCNN-predicted temperature fields for all training cases across varying inlet velocities (V=0.5-1.5 m/s) and temperatures (T_{in}=18-27°C). A distinct hotspot consistently appears at the GPU location, with realistic gradients indicating accurate capture of conduction–convection behavior.

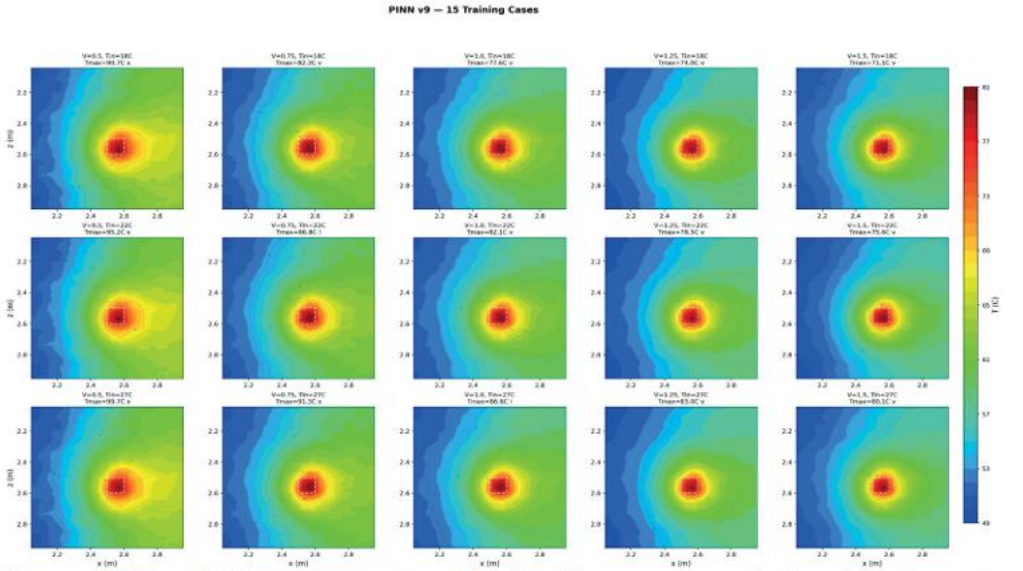


Figure 2: PCNN-predicted temperature contours for all training cases across velocity and inlet temperature variations.

Figure 2: PCNN-predicted temperature contours for all training cases across velocity and inlet temperature variations.

Higher inlet velocities reduce peak temperature and enhance the thermal wake, while higher inlet temperatures shift the field upward without altering its structure. The absence of spurious peaks confirms physical consistency.

Validation cases using unseen intermediate velocities (V=0.62, 0.85, 1.10 m/s) demonstrate that the PCNN accurately reconstructs temperature fields through interpolation, outperforming an unconstrained model.

Table 1 summarizes the reconstruction performance under sparse sensing conditions. The unconstrained neural network consistently underpredicts peak temperatures, with errors ranging from –3.60°C to –5.08°C, indicating a systematic bias that may lead to unsafe thermal assessments. In contrast, the PCNN achieves high accuracy across all cases, with small positive errors between +0.55°C and +0.94°C and a mean absolute error (MAE) of 0.75°C

Table 1: Reconstruction performance under sparse sensing. Note that these values correspond to reconstruction accuracy rather than forward prediction error

Case	V (m/s)	Tin (°C)	Fluent Tmax (°C)	PCNN Tmax (°C)	NN Tmax (°C)	PCNN Error (°C)	NN Error (°C)
1	0.62	20	87.40	87.98	83.80	+0.58	-3.60
2	0.62	25	92.43	92.98	88.80	+0.55	-3.63
3	0.85	20	81.72	82.66	76.64	+0.94	-5.08
4	0.85	27	88.72	89.66	83.64	+0.94	-5.08
5	1.10	22	79.62	80.37	75.24	+0.75	-4.38
MAE	–	–	–	–	–	0.75	4.35

4. Limitations

First, the study is limited to a single server rack within a 20 m × 5 m domain. Effects such as multi-rack interaction, airflow recirculation, and room-scale redistribution are not captured, making the trained PCNN configuration-specific and requiring retraining for different layouts.

Second, both CFD simulations and PCNN predictions are restricted to steady-state conditions, whereas real data centers exhibit transient behavior due to workload variability and environmental fluctuations.

Third, the model is trained on a single horizontal plane at y = 1.02 m, neglecting full three-dimensional effects such as buoyancy-driven stratification. Additionally, validation is performed only against CFD data, meaning any CFD inaccuracies are directly learned by the model. A formal grid independence study was not conducted, and discretization errors remain unquantified despite residual convergence ($<1\times10^{-3}$).

Finally, the dataset is limited to $V \in [0.5,1.5]$ m/s and $T_{in} \in [18,27°C]$, so performance outside this range has not been evaluated. The individual contribution of the 11 physics constraints was also not isolated, leaving the optimal constraint set unclear.

5. Conclusion

This study presents a physics-constrained deep learning framework for reconstructing temperature fields in air-cooled data centers from sparse sensor data. By embedding governing physical principles into the loss function, the PCNN achieves high accuracy while maintaining physical consistency. This confirms that the reconstruction problem is regularized by the imposed physical constraints, which restrict the solution space to physically admissible states.

The PCNN does not reconstruct the field through interpolation between sensor points, but by enforcing physically admissible solutions constrained by global energy behavior.

Compared to an unconstrained model, the PCNN significantly improves reconstruction accuracy and exhibits a slight conservative bias, which is beneficial for thermal safety.

The framework also offers a major computational advantage, predicting full temperature fields in approximately 1 ms compared to nearly 60 minutes for CFD. These results demonstrate that physics-constrained learning is an effective alternative to CFD, particularly for real-time monitoring and applications involving sparse data.

References

- Q. Zhang et al., "A survey on data center cooling systems: Technology, power consump- tion modeling and control strategy optimization," Journal of Systems Architecture, vol. 119, 2021.
- R. Zhao et al., "A critical review on the thermal management of data center for local hotspot elimination," Energy and Buildings, 2023.
- D. Al Kez et al., "AI-driven cooling technologies for high-performance data centres: state-of-the-art review and future directions," Sustainable Energy Technologies and Assessments, 2025.
- H. Eivazi, Y. Wang, and R. Vinuesa, "Physics-informed deep-learning applications to experimental fluid mechanics," Measurement Science and Technology, 2024.
- W. Wang, B. Yu, Q. Ai, M. Liu, Y. Shuai, X. Wang, and X. Zhang, "Reconstructing 3D temperature fields from sparse discrete data by analytical solution-embedded neural network," Applied Thermal Engineering, 2025.
- J. Moore, J. Chase, P. Ranganathan, and R. Sharma, "Making scheduling 'cool': Temperature-aware workload placement in data centers," in Proceedings of USENIX Annual Technical Conference, 2005.
- M. Raissi, P. Perdikaris, and G. E. Karniadakis, "Physics-informed neural networks: A deep learning framework for solving forward and inverse problems involving nonlinear partial differential equations," Journal of Computational Physics, vol. 378, pp. 686–707, 2019.
- G. E. Karniadakis, I. G. Kevrekidis, L. Lu, P. Perdikaris, S. Wang, and L. Yang, "Physics-informed machine learning," Nature Reviews Physics, vol. 3, pp. 422–440, 2021.
- A. Shehabi et al., "United States Data Center Energy Usage Report," Lawrence Berkeley National Laboratory, 2016.
- S. Hu, M. Liu, S. Zhang, S. Dong, and R. Zheng, "Physics-informed Neural Net- work Combined with Characteristic-Based Split for Solving Navier-Stokes Equations," arXiv:2304.10717, 2023.
- Y. Wang, H. Liu, and Z. Chen, "Sparse sensor placement and temperature field reconstruction for data center thermal monitoring," Sensors, vol. 25, no. 16, 2025.
- J. Moore, J. Chase, P. Ranganathan, and R. Sharma, "Temperature-aware workload placement for cooling optimization in data centers," in USENIX Annual Technical Conference, 2005.
- Ö. Y. Türkarslan, K. Ö. Saçlı, and S. Onbaşıoğlu, "Physics-Constrained Neural Networks for Data Center Cooling Optimization with Genetic Algorithms," Not Published, 2026.

ARTIFICIAL INTELLIGENCE ASSISTED ANALYSIS OF FAN TYPES FOR AIR HANDLING UNITS

Mete Özşen
Alarko Carrier Sanayi ve Ticaret A.Ş., Turkey
Corresponding email: mete.ozsen@alarko-carrier.com.tr

SUMMARY

Centrifugal and Electronically Commutated (EC) fan types were compared with using AI tool. Reference working points according to air handling unit sizes were determined to select fans. With using fan suppliers' software, a dataset that has 10651 data includes fan power and revolutions for 81 fan models was created. Dataset was used to train AI tool and then all analyses were made by AI tool giving suitable prompts.

Analyses were made for 1000 - 40000 m^3/h airflow range and 150, 450 and 900 Pa pressure differences. For 150 Pa, centrifugal fans consume less power than EC fans while for other pressure differences EC fans consume less power. At working point of 7500 m^3/h and 450 Pa, when considering cheapest centrifugal fan and EC fan with lowest power, return of investment (ROI) of EC fan is between 1 and 3 years for between 1500 and 4500 annual operating hours. ROI is less than 1 year for 900 Pa at any annual operating hour. It is concluded that EC fans get much more suitable when pressure difference and/or annual operating hours increase.

INTRODUCTION

Artificial intelligence (AI) is widely used for data analysis in HVAC control systems. In a building energy management system, by analyzing data from sensors, the system can be maintained at its optimal operating point with the lowest possible energy consumption. Yayla et al. [1] achieved 10% energy saving with using AI based control mechanism compared to traditional control systems. A systematic review was made by Aghili et al. [2] about AI usage in energy management systems. In addition to data analysis, AI usage in engineering calculations and analyses is also increasing. Chou & Bui [3] achieved to use AI approaches to predict heating and cooling loads of buildings below 4% mean absolute percentage error. Mazuroski et al. [4] reduced the computational time using AI for building performance simulations.

In this study, an AI tool was trained using a dataset containing a wide range of fan performance values. Comparisons and analyses were then carried out using appropriate prompts. The results were generated graphically by the AI. The results were interpreted and presented.

MATERIAL AND METHODS

Reference value analysis

To select a fan, airflow rate and pressure difference are required parameters. 6 different cross section velocities that are 0.5, 1, 1.5, 2, 2.5 and 3 m/s and 4 different air handling unit (AHU) cross sections that are 0.36, 1.54, 3.54 and 8 m2 were used to obtain different air flow rates. For pressure difference calculation, a supply AHU comprised dampers, filters, coils, electric heater, humidifier and silencer was taken as a reference unit as shown in Figure 1. For each cross section, components were selected and pressure difference were calculated for each cross-section velocities with using Airovision [5] AHU selection software. With this way 24 reference working points (air flow and pressure difference) were obtained.

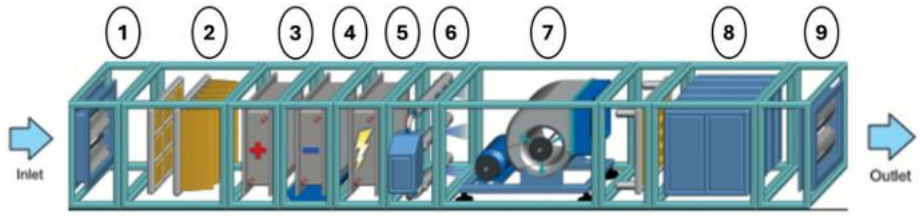


Figure 1. Reference air handling unit (AHU), 1. Inlet damper, 2. Panel and bag filters, 3. Heating coil, 4. Cooling coil, 5 Electric heater, 6. Humidifier, 7. Fan, 8. Silencer, 9 Outlet damper.

Using these 24 reference points, a method to calculate pressure difference depending on the cross-section area and cross section velocities were created to increase reference points. In this method 0.36 m2 was taken reference AHU cross section size. First pressure difference for reference AHU size was calculated depending on the cross-section velocity with using Equation 1. And then cross section correction applied to obtain pressure difference for other AHU size. Cross section correction is calculated using Equation 2. R is cross section ratio between reference AHU size and real AHU size. With this method pressure differences were obtained for all other AHU sizes dynamically. Total 54 reference points were calculated.

$$\Delta P_R = 78.05\, v^2 + 86.85\, v \qquad \text{Equation 1}$$

$$\Delta P = \Delta P_R\,(0.0002\, R^2 - 0.0115\, R + 1.0129) \qquad \text{Equation 2}$$

Fan dataset

For working points obtained from reference value analysis, suitable fans were selected with using supplier selection software. For centrifugal fan Comefri selection software [6] and for EC fan EBM selection software [7] were used. To increase working points, 6 additional pressure differences were added for each airflow rate. Pressure differences were increased up to 300 Pa with 50 Pa step for each air flow rate to get additional working points. As a result, total 324 working points were used to select fans.

For each point, suppliers' selection software can give a list of suitable fans. That means for each working point there is more than one fan that has different performance values. To get fan models and their performance values a small software was developed. Thanks to run this software, dataset includes fans and their performance values was obtained. In this dataset there are 5726 data for 40 different centrifugal fan models and 4925 data for 41 different EC fan models. Each data has fan shaft power and rpm values for working points.

AI tool

This study's aim is to make comprehensive analysis using AI tool. For that reason, fan datasets which AI tool need were created. ChatGPT [8] was used as AI tool in this study. To train AI tool, centrifugal fan dataset and EC fan dataset loaded separately. Then to test AI, random working points that have not included dataset, was given AI and asked for selection of suitable fans. In test stage, AI decided to use interpolation instead of any machine learning models since dataset includes enough data to predict fan performance for any working point request. One strict condition has determined that is requested working point has to be inside dataset's minimum and maximum points. If any points are outside of dataset, AI doesn't suggest any fan.

After training AI tool, comparison analyses were made with directing AI with suitable prompt. Results shown in graphical were created by AI tool.

RESULTS and DISCUSSION

To compare centrifugal and EC fan types, air flow range between 1000 and 40000 m³/h was used since most reference working points are in this range. In comparisons, fans that have minimum absorbed power were selected by AI tool for each fan type at any working point. For centrifugal fan type 2 parallel fan option and for EC fan type up to 5 parallel fan options were considered when selecting suitable fans.

Figure 2. shows absorbed power comparison for 150 Pa pressure difference. Absorbed power for EC fans is taken from dataset. For centrifugal fans, absorbed power is calculated with taking into account of fan shaft power, motor efficiency and belt-pullet system efficiency. Fan shaft power is taken from dataset. Motor efficiency and belt-pulley system efficiency assume as 0.9 and 0.92 respectively. Figure 2. also shows EC fan advantage percentage. Negative percentage means that EC fan absorbed power is bigger than centrifugal fan. It can be seen that all points except 5000 m³/h centrifugal fan have smaller power than EC fan. There is no any trend between power advantage and airflow rate. Result in point at 5000 m³/h is different than other points. Probably there is no enough data to select smaller power in centrifugal fan model. Dataset should be expanded considering these results.

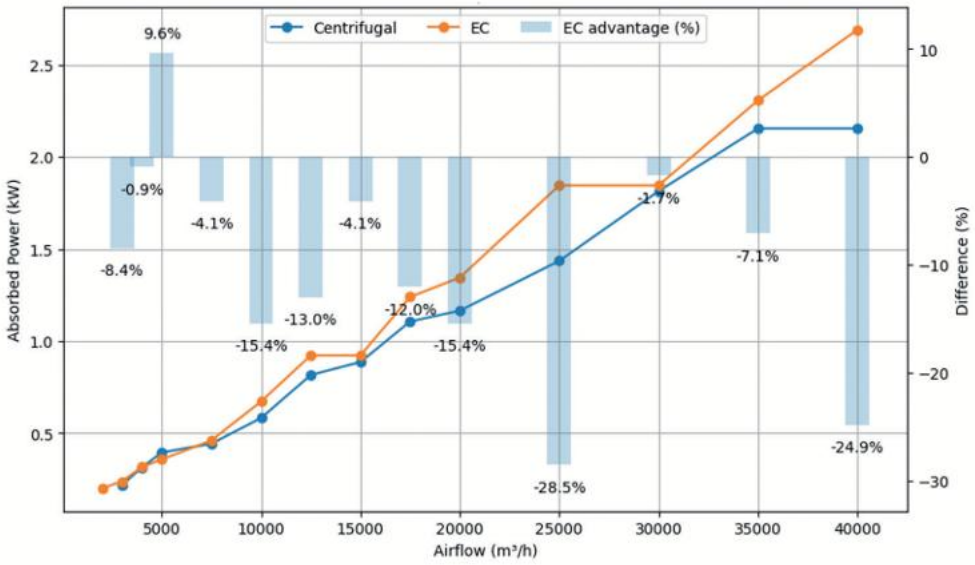


Figure 2. Absorbed power comparison at 150 Pa.

Figure 3 shows EC advantage in different pressure differences. It can be seen that EC fans have smaller power than centrifugal fans for 450 and 900 Pa. When pressure difference increases, EC fan type is suggested for almost all airflow rates. EC fan advantage percentage is not related to airflow rate or pressure difference. Advantage percentage has no similar trend.

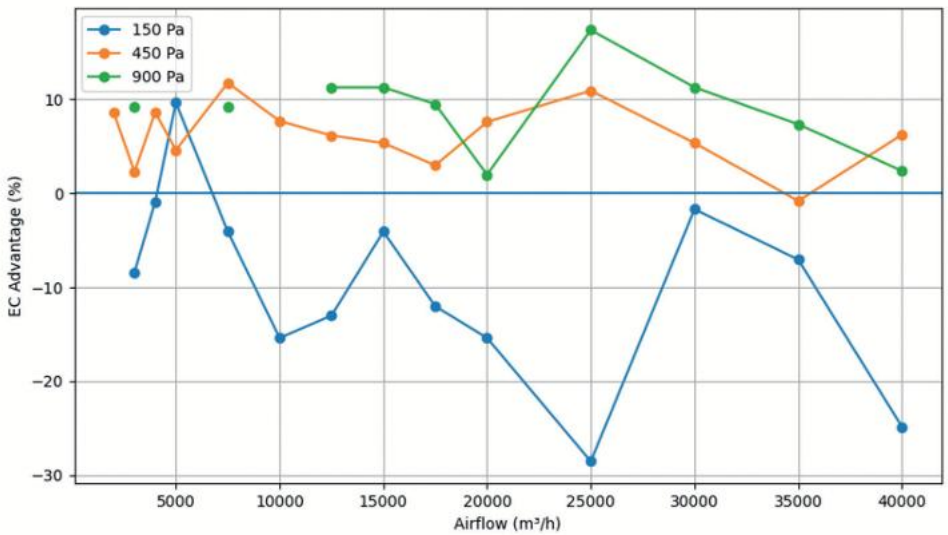


Figure 3. EC fan advantage percentage between fan types with lowest power

Initial cost differences between EC fan and centrifugal fan are shown in Figure 4 for selections at 450 Pa. Cost of centrifugal fans include motor and belt pulley prices. All points except two of them EC fan is much expensive. Maximum difference is 71.1% at 7500 m³/h. Figure 4 also shows EC fan annual energy savings. Except one point EC fans save energy compared to centrifugal fans. Saving of the EC fan is broken at 35000 m³/h. This point should be examined in deep to be sure that AI is working correctly.

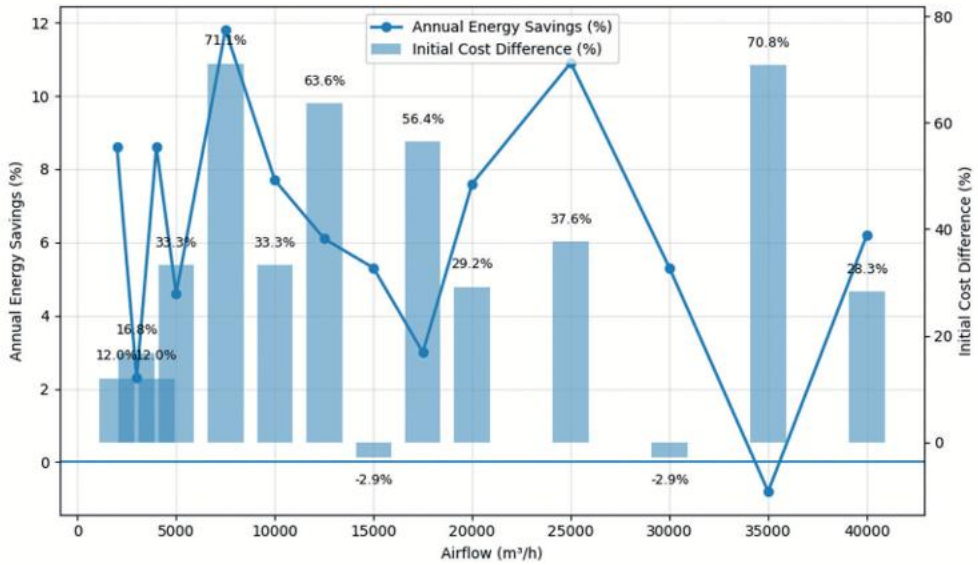


Figure 4. Initial cost and annual saving comparison at 450 Pa.

Generally EC fans consume less annual energy than centrifugal fans however EC fans are more expensive than centrifugal ones. For that reason, usage of EC fan should be evaluated with annual energy saving cost. To consider both initial cost and energy saving cost, return of investment (ROI) should be calculated. To do this, annual operating hours should be determined. Figure 5 shows ROI values for 7500 m³/h that is most cost difference case. It can be seen that ROI decreases with increasing annual operating hours. In addition, ROI is also decreasing when pressure difference is increasing for an air flow rate. It can be suggested that for 900 Pa pressure difference EC fan should be chosen for any annual operating hours for 7500 m³/h.

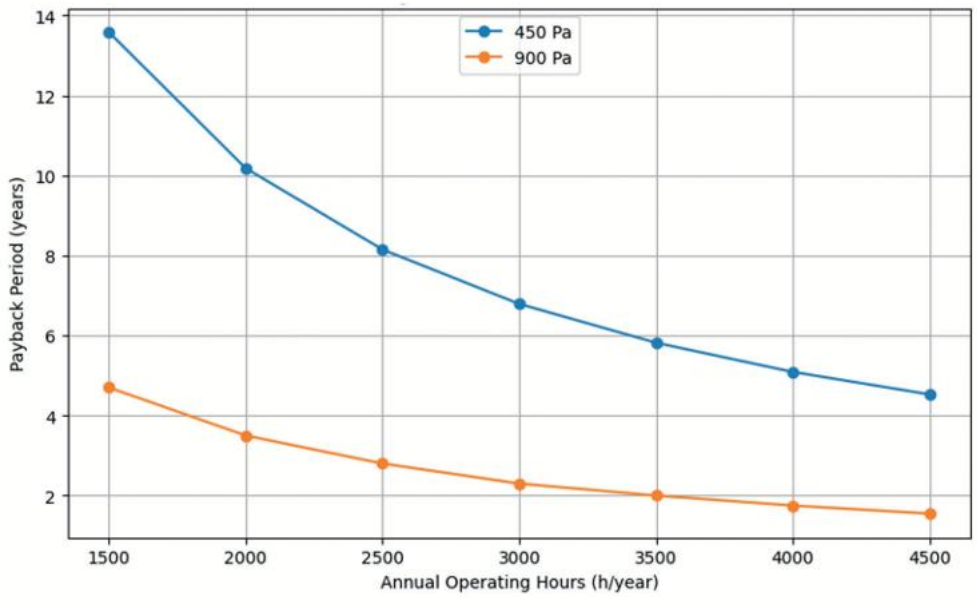


Figure 5. Return of investment period of EC fan compared to centrifugal fan with lowest power for 7500 m³/h and 450 Pa.

Generally, cheapest fan is selected for a required working point among suitable fans. For that reason a comparison was made between cheapest fan and the fan with the lowest absorbed power. Figure 6 shows ROI values for fans with lowest absorbed power according to cheapest fan at 7500 m³/h. For among centrifugal fans, selecting fan with lowest power is highly suggested for any annual operating hours and any pressure difference. For among EC fans, selecting fan with lowest power can be recommended for annual hours bigger than 2000 h for 900 Pa and 3500 for 450 Pa. Additionally when considering all fans together, it is strongly recommended that EC fans with lowest power should be selected for any working point and any operating hours.

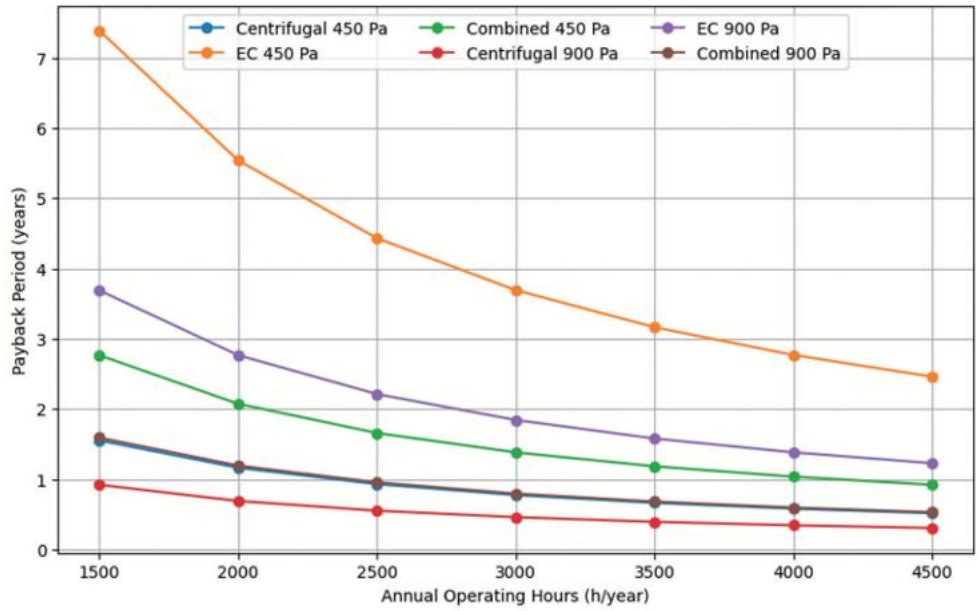


Figure 6. Return of investment period for fans with lowest power compared to fan with cheapest cost for 7500 m³/h and 450 Pa.

CONCLUSION

To compare EC and centrifugal fans with assisting AI tool, a comprehensive dataset was created. Giving dataset, some restricts and directions to AI tool, results were obtained. All the graphs in this study were generated using an AI tool.

Comparisons were made for airflow range between 1000 - 40000 m^3/h and for 150, 450 and 900 Pa static pressure differences. Except 150 Pa, EC fans have lowest absorbed power almost all working points. There are few points that broken this trend. Those points should be examined in deep to be sure AI tool.

Generally EC fan solution is the expensive than centrifugal fan. However, EC fans have annual energy saving. To determine whether using EC fan has advantage or not, ROI was calculated for different annual operating hours. Except for the 150 Pa pressure difference, EC fan gets much more suitable when annual operating hours and/or pressure difference increases for 7500 m^3/h airflow rate.

Generally cheapest fan is selected among suitable fans for required working point in applications. When comparison between cheapest fan solution and the fan with lowest absorbed power, ROI is always smaller than 3 years and EC fan is always lowest power fan solution.

This study shows that AI tool can be trained via dataset created for related product. And giving suitable restrictions and directions, it is a powerful analysis tool. In design stage, AI tools help designers to select components or systems with suitable ROI. In future studies a ROI analysis method should be developed to obtain a vision for wide range of airflow rate.

ACKNOWLEDGEMENT

In this study, ChatGPT developed by OpenAI was used (30 March 2026).

REFERENCES

[1] Yayla, A., Świerczewska, K. S., Kaya, M., Karaca, B., Arayici, Y., Ayözen, Y. E., & Tokdemir, O. B. (2022). Artificial Intelligence (AI)-Based Occupant-Centric Heating Ventilation and Air Conditioning (HVAC) Control System for Multi-Zone Commercial Buildings. Sustainability, 14(23), 16107. https://doi.org/10.3390/su142316107

[2] Aghili, S. A., Haji Mohammad Rezaei, A., Tafazzoli, M., Khanzadi, M., & Rahbar, M. (2025). Artificial Intelligence Approaches to Energy Management in HVAC Systems: A Systematic Review. Buildings, 15(7), 1008. https://doi.org/10.3390/buildings15071008

[3] Chou, Jui-Sheng & Bui Dac-Khuong, (2014). Modeling Heating and Cooling Loads By Artificial Intelligence For Energy-Efficient Building Design. Energy and Buildings, 82, 437-446

[4] Mazuroski, W., Berger, J., Oliveira, R. C. L. F., Mendes, N (2018). An Artificial Intelligence-Based Method to Efficiently Bring CFD to Building Simulation. Journal of Building Performance Simulation. 11(5), 588-603.

[5] Alarko Carrier, "Airovision", E1.23 (24.03.2026)

[6] COMEFRI S.p.A., "Aeolus4Next", 2.0.24248.0 Sep 2024

[7] ebm-papst Mulfingen GmbH & Co. KG, "ebm-papst FanScout", v3.0.3.9824 collection: 39173/03.06.2025

[8] OpenAI. ChatGPT, 01.02 - 29.03.2026. ChatGPT, https://chat.openai.com/

Artificial Intelligence-Based Prediction Approaches for Reducing Building Energy Consumption Against the Urban Heat Island Effect: The Case of Balikesir Province

Mustafa Serhan Ünlütürk[1], Emre Yavuz1 and Türkan Göksal Özbalta[2] (12 pt normal, style: Author)
[1]Balikesir University, Faculty of Architecture, Department of Architecture, Turkiye
[2]Ege University, Engineering Faculty, Civil Engineering Department, Turkiye
Corresponding email: serhan.unluturk@balikesir.edu.tr

SUMMARY

The urban heat island (UHI) effect increases building cooling loads, particularly during summer months, leading to higher energy consumption and greenhouse gas emissions. In this context, accurately predicting building energy performance is crucial for climate-sensitive planning and developing energy efficiency strategies. Artificial intelligence (AI)-based prediction models utilise meteorological data (air temperature, relative humidity, wind speed), remote sensing-based land surface temperature (LST), land use/cover data, building morphology and historical energy consumption data. The study focused on a residential property in a densely populated area of Balıkesir and used Ladybug to calculate the building's energy consumption.For calibration, air temperature and relative humidity measurements were taken using Hobo Onset data loggers over a period of 7 days. The residential unit (apartment) in the multi-storey building was modelled parametrically in the Grasshopper, and the simulation of the urban heat island effect in the area was carried out using the Dragonfly. The simulations utilised climate data for the year 2050, generated taking into account the effects of the rise in temperature resulting from the climate crisis. Based on the predicted temperature increase, the temperature of the area was reduced by balancing the height of the buildings, surface albedo values, and green space ratio parameters using the Dragonfly urban optimisation. The thermal performance and energy consumption value of the building were simulated using Ladybug by integrating the residential structure into the optimised city model. The energy performance of the residential building in its current state was compared with the optimisation results and analysed.

INTRODUCTION

The rapid growth of urbanisation, high-density development, and the increase in the proportion of impervious surfaces are adversely affecting microclimate conditions in urban areas, leading to higher temperatures than in rural areas. This phenomenon is known as the Urban Heat Island (UHI) effect [1]. Rising temperatures increase cooling loads within buildings and drive up energy consumption. Furthermore, increased energy consumption leads to increased greenhouse gas emissions [2]. The link between rising energy demand and climate change has made energy-efficient solutions in cities a critical area of research. The United Nations' Sustainable Development Goals (SDG 7: Affordable and Clean Energy; SDG 11: Sustainable Cities and Communities) aim to develop energy-efficient design proposals for cities and ensure optimal energy performance in residential buildings [3, 4]. Reducing energy consumption in homes, where individuals spend most of their day, impacts environmental sustainability and economic efficiency [5].

The UHI effect is a significant environmental challenge that must be addressed today, given rising energy consumption and adverse climatic conditions [6]. The literature contains studies aimed at mitigating the UHI effect. However, these studies largely adopt simulation-based approaches. Table 1 analyses the effects of the UHI on building energy performance, taking into account studies conducted in the literature from 2020 to the

present, meteorological data, methodology, region, and the use of artificial intelligence. A study conducted in the United States [7] investigated the effects of the UHI on energy consumption in buildings. To achieve the study's objective, simulation and sensitivity analysis methods were employed. Rhino/Grasshopper was used to model the study area parametrically, and UHI simulations were carried out using the UMI. EnergyPlus was used to perform the energy simulations for the buildings in the area. The results of the study indicate that the UHI reduces the annual heating load in buildings by 7.5% whilst increasing the cooling load by 21.2% [7]. A study conducted in Diyarbakır in 2022 aimed to identify areas potentially affected by the UHI and produced surface temperature maps (LST) of these areas using Landsat 7. The study found that temperatures in areas where the UHI effect could be observed were approximately 14% higher than in rural areas [8]. In a 2023 study conducted in Abdi Tebriz, a parametric urban model was created in Rhino/Grasshopper to investigate the intensity of the UHI effect of urban forms, and a UHI simulation was performed using Dragonfly. The study found that UHI effects from different urban forms vary with the seasons. UHI intensity is highest in rectangular forms during warm periods, whilst it is highest in L-shaped forms during cold periods [9]. A 2024 study examining skyscrapers in Istanbul investigates their impact on surface temperatures in these areas. The study utilised Geographic Information Systems (GIS) as a method and generated Land Surface Temperature (LST) maps of the areas. The results indicate that, despite the shading effect of skyscrapers, their unplanned development has increased surface temperatures by approximately 10% [10].

Table 1. Previous Works about UHI.

Paper, Year	Region	Method	Tool(s)	AI	Future Weather Projection
This paper, 2026	Balikesir, Türkiye	Machine Learning, Simulation, Optimisation	Rhino/Grasshopper, Dragonfly, Ladybug	+	2050
[11], 2020	Duran, Ekvador	Simulation	UWG, TRNSYS, ArcGIS,	N/A	N/A
[13], 2020	Austin, Texas, ABD	Simulation	Artificial Neural Network	+	N/A
[7], 2021	Des Moines, Iowa, ABD	Simulation and Sensitivity Analysis	Rhinoceros,Grasshopper, UMI,EnergyPlus	N/A	N/A
[8], 2022	Diyarbakir, Turkiye	Remote Sensing, GIS	Landsat TM 7, Landsat TM 8, Arc-GIS 10.2	N/A	N/A
[14], 2022	Adana, Turkiye	Remote Sensing, Data Analysis	LANDSAT 8 OLI/TIRS	N/A	N/A
[9], 2023	Tabriz, Iran	Simulation	Rhino Grasshopper, Ladybug, Honeybee, Dragonfly, UWG	N/A	N/A
[12], 2023	Wuhan, China	Observation, Fieldwork, Numerical Simulation	ArcMap, ANSYS Fluent CFD	N/A	N/A
[10], 2024	Istanbul, Turkiye	Remote Sensing, GIS	ARCGIS, Landsat TM 5 (1990, 2009) Landsat 8 (OLI-TIRS) (2021)	N/A	N/A

In recent years, advances in artificial intelligence (AI) and data-driven methods have increased the likelihood of obtaining highly accurate predictions. AI-supported approaches enable an integrated assessment of the UHI

effect on building energy performance [15]. Although some simulation and data-driven studies in recent years have utilised AI applications, the vast majority of these approaches do not integrate future climate projections into their analyses [16]. This situation makes it difficult to develop an urban model that will ensure long-term accuracy. Within this scope, the study aims to develop an AI-based optimisation framework sensitive to future climate projections in UHI simulations, with the objective of developing an optimal urban model for at least 30 years. Furthermore, the study investigates the effects of design decisions made at the urban level on energy consumption at the building scale.

MATERIAL and METHOD

This study investigates the impact of optimising the UHI effect on energy consumption in residential buildings in Balıkesir, which has a Mediterranean (CSA) climate type according to the Köppen-Geiger classification. For the purposes of the study, the 2nd Oruçgazi Neighbourhood in Balıkesir, characterised by dense urban development, was selected. Furthermore, to demonstrate the UHI effect in the region, the study has defined a reference area located near the study area but with lower levels of urbanisation. The reference area, which differs from the 2nd Oruçgazi Neighbourhood—the subject of the field study—in terms of urbanisation and green space density, aims to reveal the spatial variation of the UHI effect. Figure 1 shows the study areas using satellite maps.



Figure 1. Satellite maps of 2nd Oruçgazi Neighbourhood (left) and the reference area (right).

The study examined a residential property in the 2nd Oruçgazi Neighbourhood to investigate the energy performance of the proposed urban model, developed through optimisations aimed at reducing the UHI effect. The residential unit under study is situated on the 4th floor of a 7-storey building and is representative of the typical building character in the area. The unit was physically surveyed using a Hobo device, and its geometric and physical characteristics were defined within a parametric modelling environment, enabling a detailed analysis of the UHI effect's impact on the energy performance of the building. Figure 2 shows the location of the residential unit.



Figure 2. Location of case building.

Rhinoceros/Grasshopper has parametrically modelled Oruçgazi Mahallesi in Balıkesir Province and the selected reference area to represent their urban morphology and surface characteristics. To determine the impact of UHI in the region, Dragonfly conducted microclimate simulations for a 3-month cooling period using current climate data.

The study generated climate data for Balıkesir in 2050 under the RCP 4.5 scenario using Meteonorm v8 to assess the long-term effects of climate change. Dragonfly Urban Opt utilised the climate data to optimise the UHI effect at the urban scale. Using a Genetic Algorithm, it developed alternative urban scenarios by balancing building heights and surface albedo parameters.

The HOBO Onset Data Logger measured indoor temperature and relative humidity data in the case building. Grasshopper modelled the case building parametrically. Ladybug conducted energy simulations for both the existing urban fabric and the optimised urban model. Within this scope, the study comparatively assessed the effects of urban design interventions aimed at reducing the UHI effect on building energy consumption. Figure 3 summarises workflow of the study.

FINDINGS

The first phase of the study involves creating a parametric model of the urban morphology and surface characteristics of the 2nd Oruçgazi neighbourhood and the reference area. The parametric models developed in Rhino/Grasshopper digitally reflect urban characteristics, including building density, building heights, and the distribution of open and green spaces. Figure 4 presents the parametric models of the 2nd Oruçgazi Neighbourhood and the reference area. The figure shows that the 2nd Oruçgazi Neighbourhood is denser and has more storeys than the reference area.

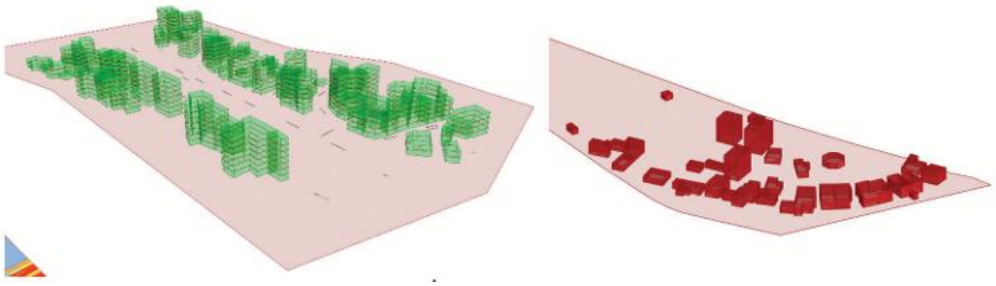


Figure 4. Parametric model of 2nd Oruçgazi Neighbourhood and reference area.

The UHI simulations conducted by Dragonfly using parametric models span a three-month cooling period. These simulations highlight the effects of building density and surface albedo values in the neighbourhood on the UHI. Dragonfly's UHI simulations indicate that, compared to the reference area, the average temperature in the study area is 1.25°C higher during the three-month cooling period. This temperature difference negatively affects both outdoor and indoor thermal comfort during the summer.

The next stage of the study involved identifying the optimised parameters. The number of storeys and surface albedo values were optimised to reduce the UHI effect in the region. The study aimed to reduce the UHI effect by developing 1,050 different combinations of these urban design parameters. Table 1 specifies the parameter value ranges.

Table 1. Optimised parameters.

Parameters	Explanation	Unit	Boundary
x1	Number of Storeys	Number	[1-10]
x2	Albedo effect	%	[0.10-0.99]

Figure 5 presents a visual representation of the proposed urban model resulting from the optimisation. In the current situation, the buildings in the area have 5-8 storeys, whereas the proposed model resulting from the optimisation has 2–3 storeys. The optimisation has improved surface reflectivity by increasing surface albedo values. These spatial and physical improvements have reduced the UHI effect from around 2.82 to 0.86, resulting in a reduction of approximately 69.5%.

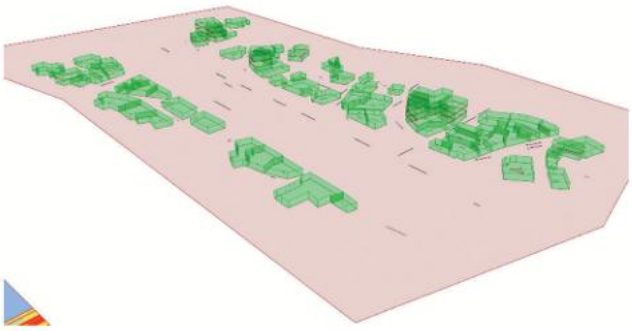


Figure 5. Optimised model of 2nd Oruçgazi Neighbourhood.

In another section of the study, temperature and relative humidity measurements were taken over a two-week period during the heating season at a residential property in the region to calibrate the Hobo Onset Datalogger model. A parametric model of the property was created in Rhino/Grasshopper, and an energy simulation was performed with Ladybug. The study continued to conduct energy simulations for both the current state and the optimised urban model.

In another section of the study, temperature and relative humidity measurements were taken over a two-week period during the heating season at a residential property in the region to calibrate the Hobo Onset Datalogger. The study created a digital twin of the 3x3 m room in the residential property using the Rhino/Grasshopper interface and conducted an energy simulation with Ladybug. The study continued the energy simulations for both the current state and the optimised urban model. Ladybug performed the simulation using current climate data and tested its reliability with an MBE of 6% and a CV RMSE of 11%.

The rise in temperatures due to the climate crisis will increase the cooling load, particularly during the summer months. The study, which optimised UHI based on Balıkesir's 2050 climate projections, has also integrated these projections into the Ladybug model. Whilst the average energy consumption per square metre during the summer period was 4.88 kWh in the current urban model, this consumption has fallen to 4.32 kWh in the optimised model. It was observed that cooling energy was reduced by 11% through changes in urban interventions, whilst building design parameters remained unchanged.

CONCLUSION

The study examined the reduction of the UHI effect through the balancing of urban design parameters and surface characteristics, whilst also considering building energy performance in an integrated manner. Using parametric modelling and microclimate simulations conducted in the 2nd Oruçgazi Neighbourhood of Balıkesir, which exhibits the characteristics of the Mediterranean (CSA) climate type—a warm climate type—the study found that temperatures in this area are higher than in the reference area, particularly during the cooling season. Dragonfly's UHI optimisation resulted in an average temperature 1.25°C higher than the reference area during the three-month cooling period, clearly demonstrating the UHI effect.

Dragonfly UrbanOpt balanced the number of floors and surface albedo values, and by simulating the UHI for 1,050 different urban models, it played a significant role in reducing the UHI effect in the region. The UHI value, currently 2.82, was reduced to 0.86 in the proposed model obtained through optimisation. These findings highlight the impact of lower-rise development and high-albedo surfaces on the microclimate.

Analyses at the building scale in the region demonstrate that improvements at the urban scale are reflected in indoor environmental performance. The results of Ladybug energy simulations show that urban design decisions directly influence not only outdoor comfort but also building energy performance.

The study has certain limitations. It restricted UHI simulations to a three-month cooling period and did not conduct an annual assessment. Furthermore, the study has accounted for only the parameters of storey height and surface albedo, whilst excluding other important variables such as wind flows, vegetation types, water surfaces, and material thermal properties. The energy simulation for residential buildings was conducted using a single building model, thereby limiting the generalisability to different building typologies.

Future studies could examine more comprehensive urban models that integrate wind effects, shading strategies, green infrastructure and water bodies to mitigate the urban heat island effect. Furthermore, incorporating different building typologies and usage scenarios into energy analyses will provide a more comprehensive understanding of the building-scale impacts of urban decisions.

REFERENCES

[1] I. D. Stewart and T. R. Oke, "Local climate zones for urban temperature studies," Bull. Amer. Meteorol. Soc., vol. 93, no. 12, pp. 1879–1900, 2012.

[2] IEA Paris, The Future of Cooling: Opportunities for Energy-Efficient Air Conditioning, Paris, 2018.

[3] United Nations, "Sustainable Development Goal 7: Affordable and Clean Energy," [Online]. Available: https://sdgs.un.org/goals/goal7

[4] United Nations, "Sustainable Development Goal 11: Sustainable Cities and Communities," [Online]. Available: https://sdgs.un.org/goals/goal11

[5] Global Alliance for Buildings and Construction, Global Status Report for Buildings and Construction, 10, 2020.

[6] M. Santamouris, "Regulating the damaged thermostat of the cities—Status, impacts and mitigation challenges," Energy Buildings, vol. 91, pp. 43–56, 2015.

[7] S. Ghiasi, U. Passe, Y. Zhou, and J. R. Thompson, "A sensitivity analysis to investigate urban heat island impact on building energy consumption," in Proc. 17th IBPSA Conf., Bruges, Belgium, 2021.

[8] A. Koç, A. Caf, C. Koç, and D. T. Kejanli, "Examining the temporal and spatial distribution of potential urban heat island formations," Environ. Sci. Pollut. Res. Int., vol. 29, no. 8, 2022.

[9] Z. Abdi, H. Alizadeh Hooshmand, S. Mohammadi Saleh, and M. Sabouri Saber, "Analysis of urban form typology using urban heat island indicators: Case study of Ferdous neighborhood of Tabriz," Front. Ecol. Evol., vol. 10, 2023.

[10] Ö. Ünsal, P. Aksak, and Ş. Kartum, "Investigation of Surface Urban Heat Island by High-Rise Buildings: Istanbul Levent Region," Papers Appl. Geogr., pp. 1–17, 2024.

[11] J. Litardo, M. Palme, M. Borbor-Cordova, R. Caiza, J. Macias, R. Hidalgo-Leon, and G. Soriano, "Urban heat island intensity and buildings' energy needs in Duran, Ecuador: Simulation studies and proposal of mitigation strategies," Sustain. Cities Soc., vol. 62, 102387, 2020.

[12] M. Makvandi, W. Li, X. Ou, H. Chai, Z. Khodabakhshi, J. Fu, P. F. Yuan, and E. d. l. J. Horimbere, "Urban heat mitigation towards climate change adaptation: An eco-sustainable design strategy to improve environmental performance under rapid urbanization," Atmosphere, vol. 14, no. 4, 638, 2023.

[13] A. Asadi, H. Arefi, and H. Fathipoor, "Simulation of green roofs and their potential mitigating effects on the urban heat island using an artificial neural network: A case study in Austin, Texas," Adv. Space Res., vol. 66, no. 8, pp. 1846–1862, 2020.

[14] M. Ünal, "Kentsel Yüzey Isı Adalarının Belirlenmesinde Yer Yüzey Sıcaklık Verilerinin Kullanımı," Avrupa Bilim Ve Teknoloji Dergisi, no. 33, pp. 213–222, 2022.

[15] A. Jafarian, R. Z. Farahani, T. A. Granberg, and K. Steins, "Technology-Driven Emergency Mass Evacuation: An Operations and Engineering Management Perspective," IEEE Trans. Eng. Manage., 2026.

[16] S. Legg, "IPCC, 2021: Climate change 2021-the physical science basis," Interaction, vol. 49, no. 4, pp. 44–45, 2021.

TTMD
Turkish Society of HVAC & Sanitary Engineers
XVII TTMD INTERNATIONAL HVAC&R TECHNOLOGIES SYMPOSIUM
ARTIFICIAL INTELLIGENCE IN BUILDINGS
14-15 MAY 2026

Artificial Intelligence for Data Center Thermal Management: Methods, Integration, and Practical Guidelines

Ömer Yiğit Türkarslan, Koray Ömercan Saçlı, Seyhan Onbaşıoğlu
Istanbul Technical University, Faculty of Mechanical Engineering
turkarslano23@itu.edu.tr, sacli24@itu.edu.tr, onbasiogl1@itu.edu.tr

SUMMARY

Data centers consume a rapidly growing share of global electricity, with cooling systems accounting for up to 38% of total facility energy. Traditional approaches such as CFD simulations and experimental measurements are too slow and costly for real-time optimization. This paper provides a tutorial-style guide for mechanical engineers and data center operators seeking to integrate AI methods into thermal management workflows. We review data-driven surrogates, physics-informed neural networks (PINNs), and physics-constrained neural networks (PCNNs), comparing them in terms of data requirements, accuracy, physical consistency, and implementation complexity. Practical strategies for incorporating physics knowledge—including soft and hard constraints, curriculum learning, and adaptive loss weighting—are discussed. Application areas covering rack-level temperature prediction, cooling system optimization, and emerging directions such as liquid cooling and reinforcement learning-based control are examined. Finally, practical guidelines for data generation, model selection, training, and validation are provided.

Keywords: data center, thermal management, machine learning, physics-informed neural networks, surrogate modeling

1. INTRODUCTION

Data centers have become the backbone of modern digital infrastructure. However, this growth comes with a substantial energy cost. A comprehensive review of 100 data centers by Ni and Bai [1] found that cooling accounts for an average of 38% of total energy consumption, reaching up to 61% in poorly optimized facilities. The same study reported a mean Power Usage Effectiveness (PUE) of 2.13, with values ranging from 1.33 to 3.85, indicating that more than half of the total energy is lost to non-IT overhead.

Conventional approaches rely primarily on CFD simulations and physical experiments. While CFD provides detailed spatial resolution, a single steady-state simulation can require up to an hour on multi-core processors [3]. Running parametric studies quickly becomes impractical. Experimental approaches are costly, difficult to scale, and limited by sensor placement.

Machine learning offers a pathway to overcome these limitations. ML surrogates can produce thermal predictions in milliseconds rather than hours [3, 4]. However, purely data-driven models may violate fundamental physical laws. Physics-informed and physics-constrained approaches combine ML speed with physical reliability [2, 5].

Despite the growing body of research, a gap remains between academic literature and practical implementation. This paper addresses that gap by providing a structured tutorial. The main contribution of this work is a structured comparison framework and practical implementation guidelines that bridge the gap between theoretical ML research and data center engineering practice. Section 2 reviews the main AI methods. Section 3 discusses strategies for integrating physics knowledge. Section 4 examines application areas. Section 5 provides practical guidelines. Section 6 concludes with an outlook.

2. AI METHODS FOR DATA CENTER THERMAL MANAGEMENT

2.1 Data-driven surrogates

Data-driven surrogate models learn input-output mappings directly from training data without incorporating governing equations. The most common architecture is the multi-layer perceptron (MLP). Zhang et al. [3] demonstrated that MLP surrogates trained on CFD data achieve inference times of approximately 9 ms—five orders of magnitude faster than direct simulation. Magdy et al. [4] compared ANNs, random forests, and CNNs for indoor thermal prediction, finding that ANNs achieved MAE of 0.12 K with $R^2 = 0.98$. CNNs are well suited for spatial patterns in temperature fields, while LSTM networks capture temporal dependencies for transient prediction. The primary limitation is the lack of physical guarantees: outside the training distribution, these models may produce non-physical results.

2.2 Physics-informed neural networks (PINNs)

Physics-informed neural networks, introduced by Raissi et al. [5], embed governing partial differential equations (PDEs) directly into the training loss function. The total loss takes the form L = MSEdata + MSEPDE, where the second term penalizes deviations from the governing equations evaluated at collocation points throughout the domain. This formulation enables training with sparse data, as the PDE constraints provide additional supervision across the entire computational domain. Raissi et al. demonstrated that with only 2000 data points, unknown parameters in the Burgers equation could be recovered with errors below 1% [5].

Cai et al. [6, 7] applied PINNs to 3D flow and heat transfer problems, achieving L2 errors of 1–2%. PINNs can use CNN/RNN architectures, and L-BFGS optimization often converges faster than Adam for moderate-sized datasets [8]. Frameworks such as NVIDIA Modulus and DeepXDE have accelerated adoption [8]. Lawal et al. [17] categorized variants into extended PINNs, hybrid PINNs, and minimized-loss formulations. Key challenges include spectral bias [18] and gradient pathology [9]. Ren et al. [9] showed that dynamic loss weighting based on NTK theory improves accuracy by up to 83%. Domain decomposition [9], one-hot encoding [15], and noise-robust formulations [16] further address these issues.

2.3 Physics-constrained neural networks (PCNNs)

Physics-constrained neural networks enforce behavioral constraints derived from physical principles rather than embedding PDE residuals. Following Karniadakis et al. [2], PCNNs use learning biases to guide predictions toward physical consistency. Soft constraints add penalty terms for known behaviors (e.g., positive temperature rise, monotonic forced convection response), while hard constraints modify the architecture itself. Liu and Wang [14] achieved a ten-fold MSE reduction using multi-fidelity PCNNs. Chen et al. [11] developed an adaptive PCNN with Softplus activations guaranteeing positive physical coefficients, achieving 79.2% MAE reduction while maintaining energy conservation over 7-day horizons. A key practical advantage of PCNNs is that they do not require explicit PDE formulation or evaluation at collocation points, making them more accessible for complex turbulent flow applications.

2.4 Hybrid and other approaches

Hybrid methods combine physical models with neural networks. Li et al. [10] used a first-principles baseline with ANN residual correction, reducing cooling energy prediction error from 278.4 W (physics only) to 91.5 W (combined), with $R^2 = 0.9969$. Reinforcement learning (RL) takes a different approach: agents learn control policies through environment interaction. Zhan et al. [19] proposed physics-informed offline RL using graph neural networks for DC cooling optimization, addressing safety concerns with limited historical data.

2.5 Comparison of approaches

Table 1 provides a systematic comparison of the main AI approaches discussed in this section, considering key factors relevant to practical implementation.

Table 1. Comparison of AI approaches for data center thermal management

Method	Data Need	Physics Guarantee	Complexity	Inference Speed	Best Use Case
Data-driven (MLP, CNN)	High (50-500 cases)	None	Low	~ms	Abundant data, interpolation
PINN	Low-Medium	Strong (PDE)	High	~ms	Sparse data, known PDEs
PCNN	Medium	Moderate (behavioral)	Medium	~ms	Complex systems, partial physics
Hybrid (physics+ANN)	Medium	Moderate (structural)	Medium-High	~ms	Residual correction
RL-based control	High (episodes)	Optional (reward)	High	Real-time	Active control, dynamic loads

3. INTEGRATING PHYSICS KNOWLEDGE INTO MACHINE LEARNING

3.1 Why pure ML fails

As noted in Section 2.1, purely data-driven models lack physical guarantees and may fail to generalize beyond the training distribution. When extrapolating, they may predict non-physical behaviors such as non-monotonic temperature-velocity relationships that contradict forced convection physics, or energy balances that do not close. Such violations are dangerous in data center applications as they may lead to underestimation of hot spot temperatures, causing hardware damage. Standard neural networks have no intrinsic mechanism to enforce physical laws—they only learn statistical patterns from training data.

3.2 Sources of physics knowledge

Physics knowledge applicable to thermal management can be derived from several sources [2]. First-principles constraints come from governing equations: Navier-Stokes for fluid flow, the energy equation for heat transfer, and constitutive relations such as Fourier's law. PDE-level theorems include maximum principles and conservation laws. Empirical correlations, such as expected heat transfer coefficient ranges and temperature trends across server racks, provide additional supervision. Dimensional analysis and scaling laws further constrain predictions within physically meaningful ranges.

3.3 Implementation strategies

Soft constraints add penalty terms to the loss function: $L = L_{data} + \lambda \cdot L_{constraint}$. Patel et al. [13] found that optimal values around $\lambda \approx 3$ provided the best trade-off between data fidelity and physical consistency. Soft constraints are flexible and can encode any differentiable physical condition, but only penalize violations rather than preventing them.

Hard constraints modify the network architecture to guarantee physical properties by construction. Examples include Softplus activations for non-negative outputs [11], skip connections embedding known relationships, and output layers satisfying conservation equations. Liu and Wang [14] demonstrated that multi-fidelity architectures with hard constraints achieve approximately 10× improvement in accuracy. Hard constraints provide stronger guarantees but require careful architectural design.

3.4 Training strategies

Effective training requires specialized strategies. Curriculum learning presents data in structured sequences—starting with simpler cases and progressively introducing complexity—improving convergence [9]. For instance, a curriculum may begin with operating conditions producing smooth thermal fields and progressively introduce cases with sharper gradients near heat sources. Adaptive loss weighting (GradNorm, NTK-based methods) dynamically adjusts loss component importance, preventing gradient pathology; Ren et al. [9] demonstrated that such methods can substantially improve accuracy over fixed-weight alternatives. Fourier feature encoding [18] addresses spectral bias by enabling networks to learn high-frequency functions, which is critical for capturing sharp temperature gradients near rack inlets and outlets.

3.5 General framework

Figure 1 describes the general framework for physics-integrated ML in data center thermal management. The workflow consists of four stages: (1) Data Generation via CFD or experiments across multiple operating conditions; (2) Physics Integration through constraint formulation and architectural choices; (3) Model Training using combined data-driven and physics-informed objectives; and (4) Deployment, where the trained surrogate is coupled with an optimization algorithm for real-time cooling control or design exploration.

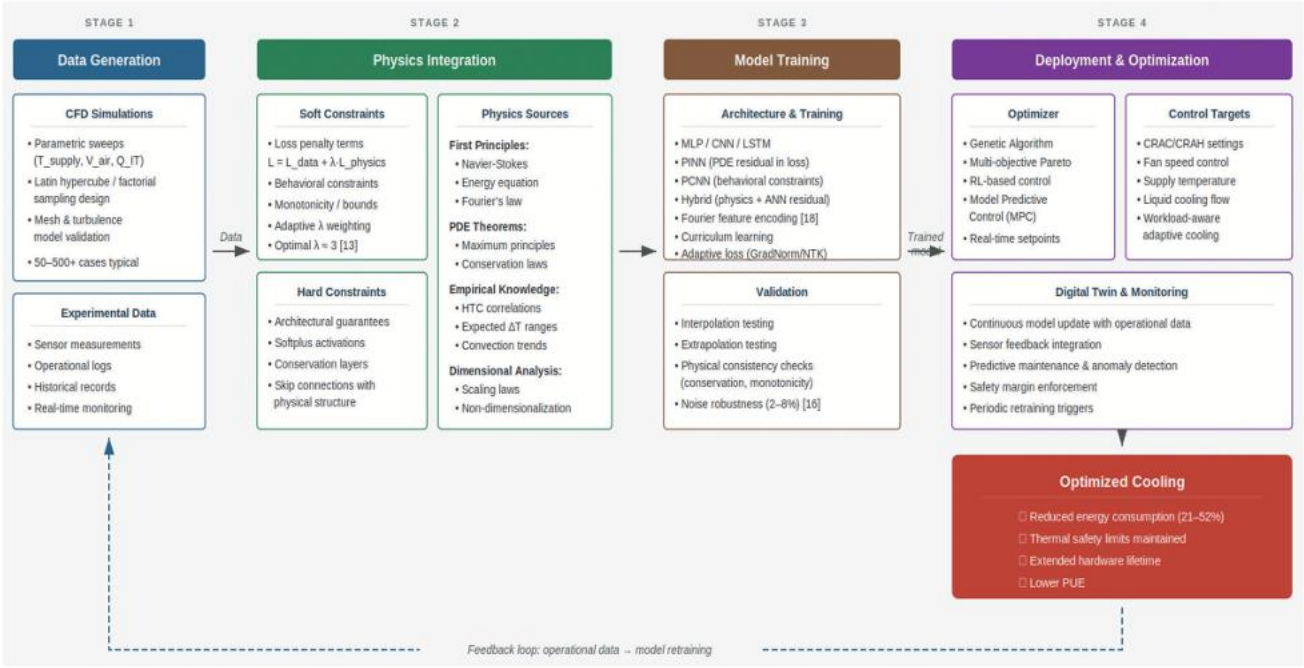


Figure 1. General framework for physics-integrated ML in data center thermal management.

4. APPLICATION AREAS AND CURRENT STATE

4.1 Rack-level temperature prediction

Predicting rack-level temperature distributions is the most common ML application in data center thermal management. Chen et al. [11] applied an adaptive PCNN that maintained energy conservation over extended prediction horizons while significantly improving accuracy over conventional approaches. These surrogates can be queried thousands of times within optimization loops, enabling real-time decision making impossible with direct CFD.

4.2 Cooling system optimization

Thermal surrogates can be coupled with optimization algorithms. Athavale et al. [12] used genetic algorithms to optimize CRAC settings with cabinet-level control, achieving 21–52% cooling energy savings. RL-based approaches offer continuous adaptation: Zhan et al. [19] demonstrated physics-informed offline RL using graph neural networks for safe DC cooling optimization with limited historical data.

4.3 Emerging directions

Liquid cooling (direct-to-chip and immersion) is becoming essential as rack densities reach higher energy levels in AI facilities [20], introducing new optimization variables such as coolant flow rates and hybrid air-liquid configurations. Digital twin technology and model predictive control combined with ML surrogates have been proposed as promising directions for proactive cooling adjustments under variable AI workloads.

5. PRACTICAL GUIDELINES

5.1 Data generation

The quality of training data is among the most critical factors in ML model performance. Zhang et al. [3] showed that 50 CFD cases capture general trends while 500 cases are needed for high-accuracy surrogates. A factorial or Latin hypercube sampling strategy across key parameters (supply temperature, airflow velocity, heat load) ensures representative coverage. Validation data should be reserved for both interpolation and extrapolation testing. Mesh resolution and turbulence model settings must be validated before generating the training dataset.

5.2 Model selection guide

The choice of ML approach depends on several factors. If abundant high-quality data is available and the application is purely interpolative, a data-driven surrogate (MLP or CNN) is the simplest and fastest option. If data is sparse but the governing equations are well known, PINNs provide additional supervision through PDE constraints. If the full PDE formulation is impractical but qualitative physical behaviors are understood, PCNNs offer a practical middle ground. If a first-principles model already exists, a hybrid approach that corrects residual errors with an ANN often achieves the best accuracy. For real-time control applications requiring continuous adaptation, RL-based methods are most appropriate.

5.3 Training best practices

Several training practices have been shown to improve model performance consistently across applications. Fourier feature encoding should be applied when the target function contains sharp spatial gradients [18]. Activation function selection matters: GELU and Swish have been observed to outperform ReLU for smooth regression tasks in the authors' experience, while Softplus is preferred when non-negative outputs are required [11]. Curriculum learning, where simpler training cases are presented before complex ones, improves convergence for physics-constrained models. Adaptive loss weighting using GradNorm or similar methods should be applied when multiple loss terms are present. Learning rate scheduling with warm-up and cosine annealing is generally recommended over fixed learning rates for improved convergence stability.

5.4 Validation and deployment

Validation must go beyond aggregate error metrics. Models should be tested for physical consistency and correct trend behavior. Interpolation and extrapolation capability should be evaluated separately. Eivazi et al. [16] demonstrated that PINNs can handle 2–8% noise while maintaining accuracy. For deployment, safety margins should be applied to critical predictions. Periodic retraining with new operational data ensures models remain accurate as configurations evolve.

6. CONCLUSION AND OUTLOOK

This paper has presented a structured overview of AI methods for data center thermal management. Data-driven surrogates offer speed but risk non-physical predictions. PINNs and PCNNs mitigate this through physics integration at different levels of complexity. Hybrid methods combining physical models with neural network correction often achieve the best accuracy. The choice should be guided by data availability, physics knowledge, and application requirements.

This tutorial has several limitations. The comparison in Table 1 is qualitative and based on reported results from different studies rather than a unified benchmark. The discussion focuses primarily on air-cooled configurations; liquid cooling systems involve fundamentally different physics that warrant separate treatment. Additionally, the practical guidelines in Section 5 reflect general best practices rather than application-specific optimization.

Looking forward, the transition to liquid cooling, digital twin platforms, and multi-objective optimization balancing energy efficiency with hardware reliability will define the next generation of AI-driven thermal management. The continued development of physics-constrained architectures will make these tools accessible to a wider range of practitioners. For practitioners beginning to adopt these methods, we recommend starting with a data-driven baseline, validating it against physical consistency checks, and progressively incorporating physics constraints as domain knowledge becomes available.

REFERENCES

[1] Ni, J., & Bai, X. (2017). A review of air conditioning energy performance in data centers. Renewable and Sustainable Energy Reviews, 67, 625–640.

[2] Karniadakis, G. E., Kevrekidis, I. G., Lu, L., Perdikaris, P., Wang, S., & Yang, L. (2021). Physics-informed machine learning. Nature Reviews Physics, 3(6), 422–440.

[3] Zhang, T., Dey, B., Veeraraghavan, K., Kulkarni, H., & Chakraborty, A. (2022). Demystifying the data need of ML-surrogates for CFD simulations. arXiv:2205.08355.

[4] Magdy, M., Metry, P., & Mekhael, S. (2025). Developing a machine learning model to predict CFD simulations. In EinB2025 Conference.

[5] Raissi, M., Perdikaris, P., & Karniadakis, G. E. (2019). Physics-informed neural networks: A deep learning framework for solving forward and inverse problems. Journal of Computational Physics, 378, 686–707.

[6] Cai, S., Wang, Z., Wang, S., Perdikaris, P., & Karniadakis, G. E. (2021). Physics-informed neural networks for heat transfer problems. Journal of Heat Transfer, 143(6), 060801.

[7] Cai, S., Mao, Z., Wang, Z., Yin, M., & Karniadakis, G. E. (2021). Physics-informed neural networks (PINNs) for fluid mechanics: A review. Acta Mechanica Sinica, 37(12), 1727–1738.

[8] Cuomo, S., Di Cola, V. S., Giampaolo, F., Rozza, G., Raissi, M., & Piccialli, F. (2022). Scientific machine learning through physics-informed neural networks: Where we are and what's next. Journal of Scientific Computing, 92, 88.

[9] Ren, Z., Zhou, S., Liu, D., & Liu, Q. (2025). Physics-informed neural networks: Review of methodological evolution. Applied Sciences, 15(14), 8092.

[10] Li, X., Wang, X., He, Z., Chen, X., & Li, Z. (2024). Combining physical laws and artificial neural networks for data center cooling energy prediction. Energy & Buildings, 311, 114170.

[11] Chen, D., Chui, C. K., & Lee, P. S. (2025). Adaptive physically consistent neural networks for data center thermal dynamics. Applied Energy, 377, 124637.

[12] Athavale, J., Yoda, M., & Joshi, Y. (2021). Genetic algorithm-based cooling energy optimization of data centers. International Journal of Numerical Methods for Heat & Fluid Flow, 31(10), 3148–3168.

[13] Patel, R. S., Bhartiya, S., & Gudi, R. D. (2022). Physics constrained learning in neural network modeling. IFAC-PapersOnLine, 55(7), 79–85.

[14] Liu, D., & Wang, Y. (2019). Multi-fidelity physics-constrained neural network and its application in materials modeling. Journal of Mechanical Design, 141(12), 121403.

[15] Yang, Y., & Mesri, Y. (2022). Learning by neural networks under physical constraints for simulation data. Computers & Fluids, 248, 105632.

[16] Eivazi, H., Wang, Y., & Vinuesa, R. (2024). Physics-informed deep learning for experimental fluid mechanics. Measurement Science and Technology, 35, 075303.

[17] Lawal, Z. K., Yassin, H., Lai, D. T. C., & Che Idris, A. (2022). Physics-informed neural network (PINN) evolution and beyond: A systematic literature review. Big Data and Cognitive Computing, 6(4), 140.

[18] Tancik, M., Srinivasan, P. P., Mildenhall, B., Fridovich-Keil, S., Raghavan, N., Singhal, U., ... & Ng, R. (2020). Fourier features let networks learn high frequency functions in low dimensional domains. NeurIPS 33, 7537–7547.

[19] Zhan, X., Zhu, X., Cheng, P., et al. (2025). Data center cooling system optimization using offline reinforcement learning. In The Thirteenth International Conference on Learning Representations (ICLR 2025).

[20] Zhou, D., Du, L., Xu, R., et al. (2025). Accelerating liquid cooling adoption in data centers: Necessity, challenges and solutions. Technology Review for Carbon Neutrality, 1, 9550014.

TTMD
Turkish Society of HVAC & Sanitary Engineers
XVII TTMD INTERNATIONAL HVAC&R TECHNOLOGIES SYMPOSIUM
ARTIFICIAL INTELLIGENCE IN BUILDINGS
14-15 MAY 2026

Machine Learning Based Solar PV Forecasting for Sustainable Buildings

Safiullah Shirzad[1], Tuğba Gürler[2]
[1,2] Hitit University, Türkiye
Corresponding email: tugbagurlerdr@gmail.com

SUMMARY

Accurate forecasting of solar photovoltaic (PV) energy production is a critical component for optimizing system performance, supporting intelligent energy management, and ensuring the economic viability of rooftop installations, particularly in energy-scarce and data-limited regions. Unsustainable buildings, reliable PV energy forecasting plays a key role in enabling energy aware operation of electricity intensive systems such as heat pumps and HVAC+R, where heating and cooling loads must be dynamically aligned with on site renewable energy generation. This study presents an artificial neural network (ANN)–based energy forecasting framework of a 4 kW grid-connected rooftop solar PV system using real-time operational data from Kabul, Afghanistan. Hourly energy generation data collected over a one-year period were used to train and validate a feed-forward ANN model with a 6–64–64–1architecture. Model performance was evaluated using standard statistical indicators, including root mean squared error (RMSE), mean absolute error (MAE), mean absolute scaled error (MASE), and the coefficient of determination (R^2). The ANN model demonstrated high predictive accuracy, achieving an R^2 exceeding 0.95 and substantially lower error values compared to simulation-based estimates from the Global Solar Atlas (GSA), which exhibited higher deviations from measured data. From a building energy perspective, such improvements are valuable for supporting the planning of electricity intensive systems such as HVAC, as accurate forecasts of on site PV generation improve understanding of local energy availability and peak generation periods. The proposed framework offers a practical and scalable solution for strengthening rooftop PV deployment in Afghanistan and other energy vulnerable, data scarce regions, contributing to low carbon and resilient building energy systems. While the present study focuses on PV forecasting, the results provide an important basis for future energy aware building applications.

Keywords: Artificial neural network; Solar photovoltaic systems; Energy forecasting; Energy Management; Real operational data, Sustainable buildings

INTRODUCTION

Solar photovoltaic (PV) systems are increasingly recognized as a key technology for sustainable energy generation in buildings, particularly in regions facing energy shortages and grid instability [1]. Accurate forecasting of PV energy output plays a critical role in optimizing building energy management systems, improving HVAC scheduling, and reducing peak electricity demand in smart and conventional buildings. The building sector plays a vital role in sustainability discussions due to its high levels of resource consumption and greenhouse gas (GHG) emissions. Buildings are responsible for approximately 40% of global resource use, 30% of total energy consumption, and around 30% of global carbon emissions [2-7], making them a key focus area for implementing sustainable strategies. As a result, adopting a comprehensive approach to sustainable development in building design has become essential. Sustainable architecture, which emerged as a major trend in the early 21st century [8], seeks to integrate economic, social, and environmental dimensions within construction projects simultaneously [9-10]. The building sector accounts for a significant share of global energy consumption and greenhouse gas emissions

due to the high energy demand associated with space heating, space cooling, and domestic hot water (DHW) requirements. The operations of buildings account for approximately 30% of global final energy consumption and 26% of energy-related CO_2 emissions [11].In this context, the electrification of building systems and their integration with renewable energy sources have emerged as key strategies for achieving climate goals.

Photovoltaic (PV)-integrated HVAC systems have gained increasing attention in recent years, and numerous studies in the literature focus on their design, performance analysis, and operational strategies. Most existing research investigates PV-assisted or PV-driven HVAC systems through simulation-based or experimental case studies, generally emphasizing energy savings and system efficiency [12-13]. Among these hybrid approaches, solar assisted heat pump (SAHP) systems have been extensively investigated. Early research mainly focused on single applications such as space heating or DHW production, whereas later studies examined dual-function systems combining heating and cooling or heating and hot water production [14].

However, in many developing regions such as Afghanistan, the application of advanced forecasting models remains limited due to data scarcity, lack of real-time monitoring systems, and reliance on satellite-based simulation tools such as the Global Solar Atlas (GSA). These simulation tools often rely on long-term averaged meteorological datasets, which may not accurately reflect real operational performance under local environmental conditions.

Despite these advances, there remains a gap in applying ANN-based forecasting frameworks using real one-year operational rooftop PV data in Afghanistan, combined with techno-economic evaluation under local tariff structures. This study addresses this gap by developing and validating an ANN model for PV energy forecasting and assessing its economic implications for rooftop solar systems in Kabul.

Bibliographic Analysis

The bibliographic analysis was conducted using VOS viewer software. This timeframe was selected to capture the most recent advances in renewable energy forecasting, machine learning applications, and building energy management systems. Figure 2 provides an overlay visualization, where node colors indicate the average publication year of related research.

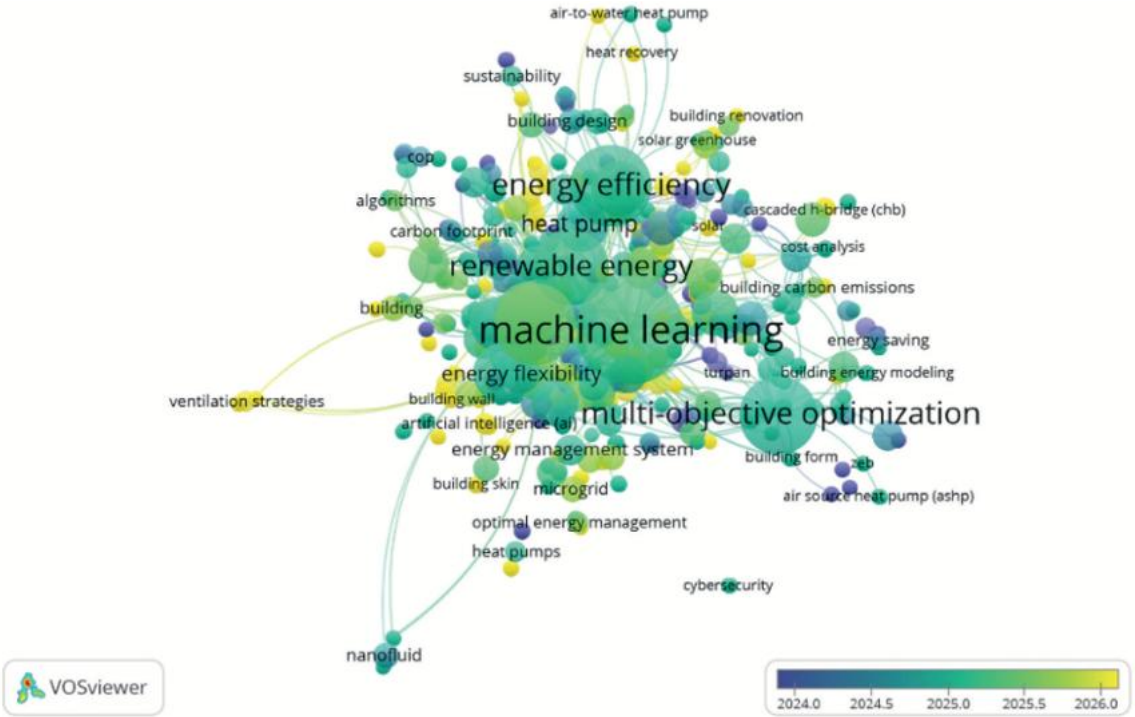


Fig. 1 Overlay visualization of keyword co-occurrence over time.

Novelty and Contribution:

- First ANN-based solar forecasting study using real operational data from Afghanistan – a data-scarce, energy-vulnerable region not represented in existing bibliographic networks.
- Machine learning significantly outperforms conventional simulation tools – achieving R^2>0.95 compared to Global Solar Atlas estimates.
- First explicit integration of PV forecasting with HVAC energy management – bridging renewable energy and building system clusters identified in the bibliographic analysis.

METHODOLOGY

Site selection

The system is installed on the roof of a residential building in the Arzan Qemat area of Kabul city, Afghanistan, at latitude 34.55° N and longitude 69.20° E, as shown in Figure 3.



Fig.2. the study site location

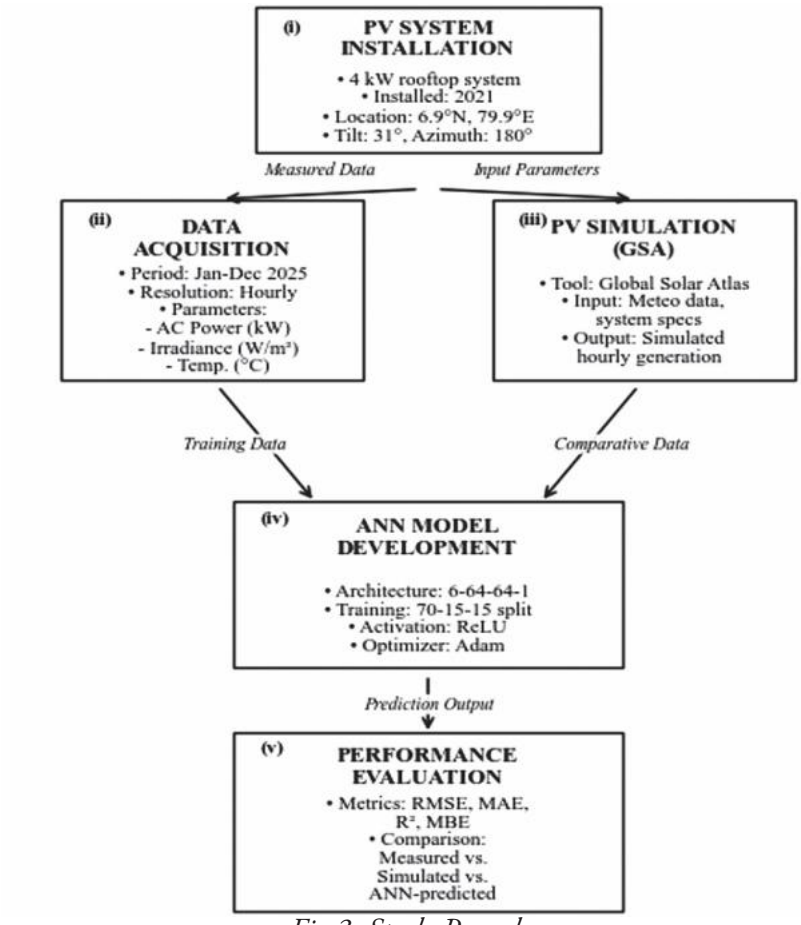


Fig.3. Study Procedure

Performance indicators

Root Mean Squared Error (RMSE) measures the standard deviation of prediction errors and penalizes larger deviations more strongly [15]:

$$RMSE = \sqrt{\frac{1}{n}\sum_{i=1}^{n}(y_i - \hat{y}_i)^2} \quad (1)$$

Mean Absolute Error (MAE) represents the average magnitude of the absolute differences between the predicted and measured values:

$$MAE = \frac{1}{n}\sum_{i=1}^{n} | y_i - \hat{y}_i | \quad (2)$$

Mean Absolute Scaled Error (MASE) evaluates forecasting accuracy relative to a naive baseline model and allows scale-independent comparison:

$$MASE = \frac{1}{n}\sum_{i=1}^{n}\frac{| y_i - \hat{y}_i |}{MAE_{naive}} \quad (3)$$

Coefficient of Determination (R^2) implies the fraction of variance in the studied data described by the following mathematic model:

$$R^2 = 1 - \frac{\sum_{i=1}^{n}(y_i - \hat{y}_i)^2}{\sum_{i=1}^{n}(y_i - \bar{y})^2} \quad (4)$$

where $\hat{y}_i$ is the measured energy output, $\hat{y}_i$ is the predicted value, $\bar{y}$ is the mean of the measured values, and n is the number of samples.

RESULTS AND DISCUSSIONS

Energy production forecasting

Hourly solar PV energy generation data were collected directly from the inverter using the WatchPower software. The acquired dataset was preprocessed to remove missing and corrupted values. The cleaned dataset was then divided into training, validation, and testing subsets. An Artificial Neural Network (ANN) model was implemented to forecast solar energy production using real-time measured data and corresponding meteorological parameters. To enhance the robustness of the analysis, simulation results obtained from the GSA were also considered and compared with the measured and predicted outputs. The performance of the ANN model was evaluated using standard statistical indicators, including root mean squared error (RMSE), mean absolute error (MAE), mean absolute scaled error (MASE), and the coefficient of determination (R^2). The following sections describe the dataset, the ANN model architecture, and the evaluation criteria adopted in this study. Figure 4 shows the energy output of the model, simulation and real data.

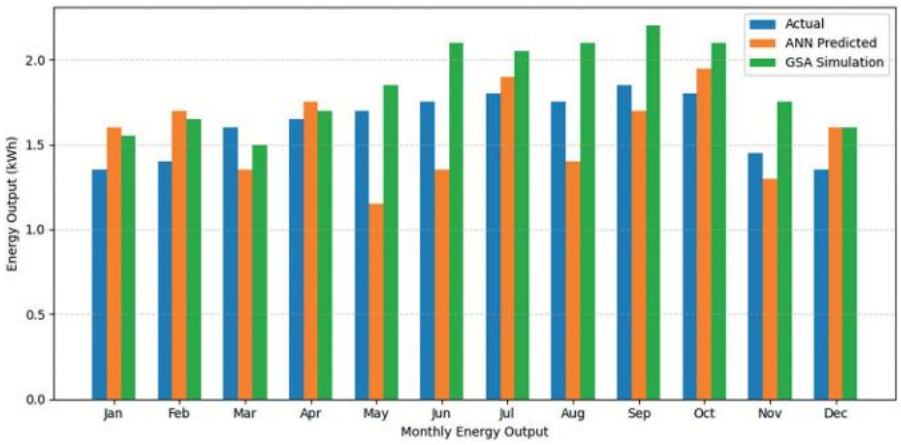


Fig 4 The energy output of the model, simulation and real data

Performance Comparison with GSA

To benchmark the prediction accuracy of the proposed artificial neural network (ANN) model, its results were compared with simulation-based energy estimates obtained from the GSA. Table 1, figure 5 presents the comparative performance indicators between the ANN predictions and GSA simulation results using standard statistical metrics.

Table 1. ANN predictions and GSA simulation

Model	RMSE (kWh)	MAE (kWh)	MBE (kWh)	R^2
ANN	0.116	0.097	0.048	0.975
GSA	1.157	0.926	0.300	–1.447

The ANN model demonstrates substantially higher predictive accuracy than the GSA simulation, as reflected by significantly lower RMSE and MAE values and a markedly higher coefficient of determination (R^2). This discrepancy can be attributed to the fact that GSA relies on long-term averaged satellite data and generalized loss assumptions, whereas the ANN model is trained using real-time, site-specific operational data, allowing it to better capture temporal variability and actual system behavior. Both values are significantly lower than unity, indicating superior performance compared to a naïve benchmark. The lower validation error further demonstrates the robustness and strong generalization capability of the ANN model.

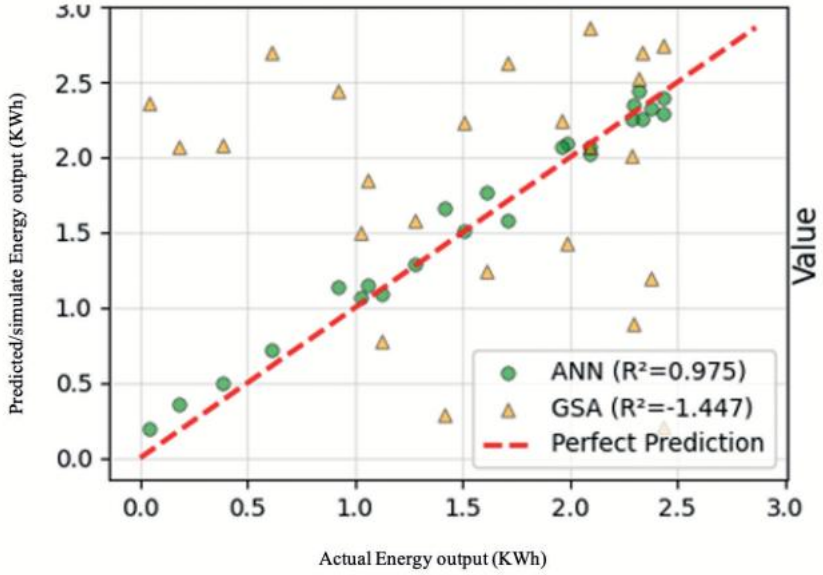


Fig 5. Actual versus ANN energy output

Figure 5 presents the scatter plot between actual and ANN-predicted energy outputs. The strong linear alignment along the 45° reference line and a high coefficient of determination (R^2 = 0.975) confirm the excellent predictive accuracy of the ANN model.

CONCLUSION AND FUTURE WORKS

This study demonstrated the potential of artificial neural network (ANN) based photovoltaic power forecasting to support the predictive operation of HVAC and building energy systems in PV integrated buildings. Using site specific weather and operational data, the ANN model achieved good accuracy in short term PV power prediction. This capability is important for enabling proactive HVAC control, supporting load shifting, and improving the use of onsite renewable energy.

However, the ANN model was trained using a limited set of meteorological and operational inputs available at the study site. Forecast accuracy could be further improved by using higher resolution weather data or by including additional factors such as PV soiling effects and variations in inverter efficiency.

Future research could expand this work by using long term, multiyear datasets to examine the robustness and adaptability of ANN based forecasting models under different climatic conditions. Furthermore, applying advanced or hybrid machine-learning methods such as deep learning, ensemble techniques, or ANN based optimization approaches may further improve prediction accuracy and enhance the role of data-driven forecasting in energy efficient buildings.

REFERENCE:

1. Shirzad, S. (2025). The Impact of Net Metering Policies on Solar Rooftop Adoption in Afghanistan. Energy RESEARCH LETTERS, 7(Early View).
2. Shen J, Krietemeyer B, Bartosh A et al (2021) Green Design Studio: a modular-based approach for high-performance build ing design. Build Simul 14:241–268. https://doi.org/10.1007/ s12273-020-0728-9 2. 3. 4. 5. 6. 7. 8. 9.

3. Khakian R, Karimimoshaver M, Aram F et al (2020) Modeling nearly zero energy buildings for sustainable development in rural areas. Energies 13. https://doi.org/10.3390/en13102593
4. Sameer H, Bringezu S (2019) Life cycle input indicators of mate rial resource use for enhancing sustainability assessment schemes of buildings. J Build Eng 21:230–242. https://doi.org/10.1016/j. jobe.2018.10.010
5. Invidiata A, Lavagna M, Ghisi E (2018) Selecting design strat egies using multi-criteria decision making to improve the sustainability of buildings. Build Environ 139:58–68. https://doi. org/10.1016/j.buildenv.2018.04.041
6. Saadatian O, Haw LC, Sopian K, Sulaiman MY (2012) Review of windcatcher technologies. Renew Sustain Energy Rev 16:1477 1495. https://doi.org/10.1016/j.rser.2011.11.037
7. Harish VSKV, Kumar A (2016) A review on modeling and simu lation of building energy systems. Renew Sustain Energy Rev 56:1272–1292
8. Mousavi L, Mahdavinejhad M (2013) Search for sustainability in Contemporary Architecture of Iran. Am J Civ Eng Archit 1:129 142. https://doi.org/10.12691/ajcea-1-6-3
9. Williams DE (2007) Sustainable urban and community design
10. Damirchi Loo L, Mahdavinejad M (2018) Analysis of design indicators of sustainable buildings with an emphasis on efficiency of Energy Consumption (Energy Efficiency). Civ Eng J 4:897. https://doi.org/10.28991/cej-0309142
11. International Energy Agency. (2023). Buildings – Energy system. International Energy Agency. https://www.iea.org/energy-system/buildings
12. Ahmed, B., Ahmed, A., Mujeeb, A., Zhang, H.-N., Li, X.-B., Qu, K.-Y., & Li, F.-C. (2026).Dynamic occupancy-aware HVAC control in large office building using enhanced soft actor-critic with PV and thermal energy storage integration. Applied Thermal Engineering, https://doi.org/10.1016/j.applthermaleng.2026.129937
13. Bashir, F. M., Almatared, M., Sulaiman, M., Nasrallah, E., Rassas, N. H., & Dodo, Y. A. (2026). An operational digital twin for co-optimizing HVAC, PV/battery, and wall shading under time-of-use tariffs: A real-world online whole-home study with economic model predictive control. Journal of Building Engineering, 121, 115705. https://doi.org/10.1016/j.jobe.2026.115705
14. Wu, W., & Skye, H. M. (2018).Net-zero nation: HVAC and PV systems for residential net-zero energy buildings across the United States. Energy Conversion and Management, 177, 605–628.https://doi.org/10.1016/j.enconman.2018.09.084
15. Mulani, S., 2020. RMSE - root mean square error in python - AskPython. Section: Python Programming Examples.


TTMD
Turkish Society of HVAC & Sanitary Engineers
AI